



Synthesis of Concrete Bridge Piles Prestressed with CFRP Systems

Final Report

University of Houston

Abdeldjelil Belarbi
Mina Dawood
Matthias Bowman

The University of Texas at Tyler

Amir Mirmiran

Technical Report Documentation Page

1. Report No. FHWA/TX-17/0-6917-1	2. Government Accession No.	3. Recipient's Catalog No.	
4. Title and Subtitle Synthesis of Concrete Bridge Piles Prestressed with CFRP Systems: Final Report		5. Report Date June 2017	
		6. Performing Organization Code	
7. Author(s) A. Belarbi, M. Dawood, A. Mirmiran, and M. Bowman		8. Performing Organization Report No. FHWA/TX-17/0-6917	
9. Performing Organization Name and Address Civil & Environmental Engineering Department The University of Houston 4800 Calhoun Rd Houston, TX 77004		10. Work Unit No. (TR AIS)	
		11. Contract or Grant No. PS 16-350	
12. Sponsoring Agency Name and Address Texas Department of Transportation Research and Technology Implementation Office P.O. Box 5080 Austin, TX 78763-5080		13. Type of Report and Period Covered Final Report January 2016 – December 2016	
		14. Sponsoring Agency Code	
15. Supplementary Notes Project performed in cooperation with the Texas Department of Transportation and the Federal Highway Administration.			
16. Abstract The Texas Department of Transportation frequently constructs prestressed concrete piles for use in bridge foundations. Such prestressed concrete piles are typically built with steel strands that are highly susceptible to environmental degradation and corrosion in harsh marine environments. The department currently employs many techniques to combat these structural degradation, but these measures address only the symptom- not the root cause. It would therefore be advantageous to the Agency to adopt a corrosion-resistant reinforcing material. It was then the aim of this research to assess the feasibility of employing carbon fiber-reinforced polymers (CFRP's) into TxDOT infrastructure through comprehensive literature synthesis, investigations in the field and interviews with design professionals, and a comparative analysis of mechanics and economics. The findings of these studies illustrated the feasibility of CFRP adoption when considered over the entire lifespan of a bridge structure, relying on CFRP's excellent environmental durability to mitigate the more expensive upfront costs. Incorporating CFRP prestressing strands into bridge piles, especially in aggressive, corrosive environments, has the potential to not only increase the overall lifespan of the structure, but requires far less departmental maintenance, saving a large sum of repair costs and design time. It is therefore the opinion of the Research Team that some important issues must be better understood and quantified, such as additional drivability concerns and splicing information, before the large-scale implementation of CFRP-prestressed piles is undertaken by the Department.			
17. Key Words Prestressed, CFRP, CFRP-Prestressed Piles		18. Distribution Statement No restrictions.	
19. Security Classif. (of report) Unclassified	20. Security Classif. (of this page) Unclassified	21. No. of pages 84	22. Price

TxDOT Project 0-6917
**Synthesis of Concrete Bridge Piles Prestressed with CFRP
Systems**

Final Report

Prepared by:

**Dr. Abdeldjelil Belarbi, Dr. Mina Dawood, Dr. Amir Mirmiran,
and Matthias Bowman**

Submitted to:



June 2017

DISCLAIMER

Author's Disclaimer — The contents of this report reflect the views of the author(s), who is (are) responsible for the facts and the accuracy of the data presented herein. The contents do not necessarily reflect the official view or policies of the Federal Highway Administration (FHWA) or the Texas Department of Transportation (TxDOT). This report does not constitute a standard, specification, or regulation.

Engineering Disclaimer — This report is not intended for construction, bidding, or permit purposes.

Executive Summary

The Texas Department of Transportation frequently constructs prestressed concrete piles for use in bridge foundations. Such prestressed concrete piles are typically built with steel strands that are highly susceptible to environmental degradation and corrosion in harsh and marine environments. The department currently employs many techniques to combat these structural degradation by strengthening and rehabilitation methods, but these measures address only the symptom-not the root cause. It would therefore be advantageous to the Agency to adopt a corrosion-resistant reinforcing material. It was then the aim of this research to assess the feasibility of employing carbon fiber-reinforced polymers (CFRP's) into TxDOT infrastructure through comprehensive literature synthesis, investigations in the field and interviews with design professionals, and a comparative analysis of mechanics and economics.

Chapter 1 gives a brief problem statement and research objectives. Chapter 2 of this report addresses the State-of-State and State-of-the-Art of CFRP reinforcement in substructure infrastructure both domestically and abroad, encompassing the material properties of CFRP's in a comprehensive literature synthesis. This portion also includes a review of the current state of piles within TxDOT jurisdiction, containing numerous site visits, interviews of design professionals and local contractors, and an analysis of current repair procedures.

Chapters 3 of the report constitutes a comparative analysis of the mechanics and economics of conventional steel reinforcement and CFRP's, citing a parametric cross sectional interaction analysis and a model life-cycle cost analysis. The findings of these studies illustrated the feasibility of CFRP adoption when considered over the entire lifespan of a bridge structure, relying on CFRP's excellent environmental durability to mitigate the more expensive upfront costs.

Incorporating CFRP prestressing strands into bridge piles, especially in aggressive, corrosive environments, has the potential to not only increase the overall lifespan of the structure, but requires far less departmental maintenance, saving a large sum of repair costs and design time. While there is a significant amount of literature and case study that speak to the benefits of CFRP implementation, it was also the goal of the Research Team to investigate any potential gaps in knowledge with the technology in Chapter 4. Chapters 5 provides some concluding remarks and recommendations for further research needs. It is therefore the opinion of the Research Team that some important issues must be better understood and quantified, such as additional drivability concerns and splicing information, before the large-scale implementation of CFRP-prestressed piles is undertaken by the Department.

Table of Contents

Chapter 1: Introduction	1
1.1 Problem Statement	1
1.2 Research Objectives	1
Chapter 2: Literature Review	2
2.1 Assessment of Conditions of Existing Piles in TX	2
2.2 Rate of Occurrence of Deficiencies Associated with Reinforcement Corrosion	2
2.3 Locations and Structures Susceptible to Pile Reinforcement Corrosion	8
2.4 Reviewing State-of-the-Art, and State of Practice	9
2.4.1 Current Methods of Repair and Associated Costs	9
2.4.2 Pile Inspections	12
2.4.3 Costs Associated with Maintenance	14
2.4.4 Frequency of Pile Replacements.....	14
2.4.5 Condition of Piles Summary	15
2.5 CFRP Material Properties	15
2.6 CFRP Strength	17
2.7 CFRP Durability	19
2.8 Detailing Requirements for Splices and Embedments	20
2.9 Current and Proposed Design and Detailing Specifications	21
2.10 Internal Transverse Reinforcement -- Ties and Spirals	22
2.11 Performance of FRP Transverse Reinforcement in Piles	23
2.12 External FRP Stay-in-Place Forms and Jackets	25
2.13 Drivability of CFRP-Prestressed Concrete Piles	26
Chapter 3: Comparative Analysis	27
3.1 Mechanical Behavioral Comparison for Steel and CFRP	27
3.2 Development of P-M Interaction Diagrams for (i) Steel and (ii) CFRP	28
3.2.1 Prestressed Steel.....	31
3.2.2 Prestressed CFRP	34
3.3 Comparison of Findings with Previous Literature	41
3.4 Assessment of Transverse Reinforcement	42
3.5 Mechanical Behavior Summary	44
3.6 Comparative Cost Analysis	44

3.7 Relevant Costs	47
3.8 Life Cycle Cost Analysis	47
3.8.1 Construction and Maintenance Costs	48
3.8.2 Increased Service Life	51
3.8.3 Design Costs	52
3.8.4 User Cost Savings	53
3.8.5 Rehabilitation Cost	55
3.8.6 Salvage Value	55
3.8.7 Comparative Cost Summary	55
Chapter 4: Additional Gaps in Knowledge	57
4.1 Introduction	57
4.2 Further Drivability Concerns & Reduction of Concrete Cover	57
4.3 Deterioration of CFRP in Saltwater and Ultra Violet Light	59
4.4 Embedment Length and Splicing Configurations	61
4.5 Prestress Loss Effects for CFRP Strands	62
4.6 Statistical Reliability Analyses of CFRP's	63
4.7 Circular, Octagonal, and Square-Reinforcement Patterns in Piles	64
Chapter 5: Summary and Recommendations for Further Study	66
5.1 Summary	66
5.2 Recommendations for Further Study and Implementation	67
References	68

List of Figures

Figure 1. Deteriorated pile- cracked and spalling, TxDOT Beaumont District b. 1978.	3
Figure 2. Bridge Located on IH 610 EB CONN & 18TH St. b. 1975, (a) Substructure View, (b) US 290 EB to IH EB Elevation View, (c) Concrete Spalling in Pile; Bridge Located in Brazoria County b. 2003, (d) Substructure Close View; Bridge Located on White Oak BYU Yale- Heights, (e) Substructure, (f) Concrete Spalling on Pile.....	5
Figure 3. (a) Bridge View from 59 b. 1975, (b) Close View of Deficits; Bridge Located Basson Dr. & BNSF RR, (c) Concrete Delamination and Spalling; Bridge Located on IH 610 FR'S, (d) elevation view, (e) Concrete Spalling, Reinforcement Exposure, and Vertical Cracks on pile	6
Figure 4. Bridge Located on IH 610 b. 1975, (a) Elevation View, (b) Concrete Spalling and Reinforcement Exposure; Bridge Located Goodyear RR & Dr., (c) Bridge Elevation View, and (d) Concrete Spalling with Exposed and Deteriorated Reinforcement; Bridge Located on Normandy St., (e) Concrete Spalling and Reinforcement Exposure; Bridge Located on Hardy Toll Rd & UPRR, (f) Concrete Spalling and Exposed Reinforcement.	7
Figure 5. FRP Wrapping Retrofit (left), Plastic Pile Jacket (right).....	10
Figure 6. Cracked Collars Used to Repair Previous Spalling, TxDOT Beaumont District b. 1978.....	11
Figure 7. Spalling of Concrete Collar, Seawolf Parkway, TxDOT Houston District.....	11
Figure 8. Inspection of Deteriorated Pile Collar, TxDOT Houston District.....	13
Figure 9. Acoustic Mapping of Submerged Substructure, TxDOT Houston District.	13
Figure 10. Numerous Configurations of CFCC Strands, Tokyo Rope 2012.....	16
Figure 11. CFRP Specimens Exposed to Alkali Solution, adapted from Arockiasamy and Amer (1998).....	19
Figure 12. CFRP Specimens Exposed to Alkali Baths at Elevated Temperatures, Benmokrane (2015).....	20
Figure 13. Anchorage System for CFCC Coupled with Steel Strands, Grace et al. (2012).....	22
Figure 14. Arching Action for Hooped Circular Reinforced Concrete (RC) Columns, adapted from Afifi et al. (2014)	24
Figure 15. Stress-Strain Curves of CFRP and Steel.....	27
Figure 16. Standard Section for Prestressed 18" x 18" pile, adapted from TxDOT Bridge Division Specification.....	29
Figure 17. Strains and forces found in cross section due to prestressing.	31
Figure 18. Influence of $f'c$ iteration on strength interactions; $f_{tu}=270$ ksi, $f_{fe}=230$ ksi, $E_{ps}=29,000$ ksi, $A_{ps}=2.26in^2$	33
Figure 19. Influence of reinforcement ratio iteration on strength interactions; $f_{tu} =270$ ksi, $f_{fe}=230$ ksi, $E_{ps}=29,000ksi$	34
Figure 20. Strains and forces found in cross section due to prestressing.	35

Figure 21. Influence of f'_c iteration on strength interactions; $f_{fu} = 360$ ksi, $f_{fe} = 216$ ksi, $E_{pf} = 20,000$ ksi, $A_{pf} = 2.26$ in ²	37
Figure 22. Influence of reinforcement ratio iteration on strength interactions; $f_{fu} = 360$ ksi, $f_{fe} = 216$ ksi, $E_{pf} = 20,000$ ksi.	38
Figure 23. Non-Dimensionalized P-M Diagram of Equivalent PC & FRP PC Section, 5 ksi f'_c . (Steel: 270 ksi, $f_{fe} = 230$ ksi, $E_{ps} = 29,000$ ksi; CFRP: 360 ksi, $f_{fe} = 216$ ksi, $E_{fs} = 20,000$ ksi).	39
Figure 24. Strength Interaction Diagram of FRP RC; 250 ksi, $f'_c = 5$ ksi, $E_{pf} = 20,000$ ksi, $\rho = 4\%$ (Benmokrane et al. 2015).	41
Figure 25. Strength Interaction Diagram, Steel PC; 250 ksi, $f'_c = 6$ ksi, $E_{ps} = 29,000$ ksi (Nawy 1998).	42
Figure 26. Life-Cycle Cost Analysis Steps, adapted from Grace et al. (2012).	46
Figure 27. TxDOT Specification for Prestressed Concrete Piles, (a) Typical Section Thru Piles, and (b) Pile Build Up Detail	48
Figure 28. Yearly Increase of TxDOT Repair and Replacements; TxDOT Yearly Bridge Facts).....	51
Figure 29. Cash Flow Diagram Illustrating Costs Occurred per Reinforcement Type.....	53
Figure 30. Successfully Driven Prestressed-CFRP Piles, Ozyildirim and Sharp (2013).	58
Figure 31. Current TxDOT Transverse Reinforcement Spec. for Prestressed Piling	59
Figure 32. Spool of CFCC Transverse Reinforcement with Yarn Covering	60
Figure 33. FDOT Design Aid for Prestressed Concrete Pile Splices.	61
Figure 34. FDOT Prestressing Casting Bed (Roddenberry et al. 2016).....	63
Figure 35. A Realization of Underlying Poisson Process (Der Kiureghian et al. 2005).....	64
Figure 36. Circular and Rectangular Cross Sections for Prestressed Concrete.....	64

List of Tables

Table 1. Adapted from Tokyo Rope USA Product Specifications (Tokyo Rope, 2012)..... 17

Table 2. Material Properties of Prestressing CFRP. 17

Table 3. TxDOT Splicing Details for Uncoated Steel Bars, TxDOT Bridge Detailing Guide 2014. 21

Table 4. Various Material Properties of Differing Concrete Strengths, adapted from Collins and Mitchell 1991. 30

Table 5. Stress-Block Factors for Parabolic Stress-Strain Curves, adapted from Collins and Mitchell 1991. 30

Table 6. Stress-Block Factors for Non-Parabolic Stress-Strain Relationships, adapted from Collins and Mitchell 1991. 30

Table 7. Cost of pile replacement in coastal regions, State of Texas..... 49

Table 8. Initial Construction Costs to Annual Maintenance. 50

Table 9. User Delay Assumptions for Bridge Rehabilitation. 54

Chapter 1: Introduction

1.1 Problem Statement

Transportation infrastructure is aging and deteriorating mostly due to corrosion problems related to the prestressing steel strands. A corrosion-free material for prestressing will create alternatives for bridge engineers to design long-lasting and safer bridges. Otherwise, corrosion may create significant additional maintenance and replacement costs to TxDOT. Furthermore, the loss of area of the prestressing steel may result in lower load-carrying capacity of bridge members, which may eventually lead to structural failure, hence a major concern for public safety.

Prestressed concrete piles are exposed to aggressive environmental affects that cause corrosion of their internal prestressing steel. The loss of functionality due to corrosion of the prestressing reinforcement may cause service interruptions or replacements, and in most cases, may require expensive interventions. A promising alternative to prestressing steel is corrosion-resistant carbon fiber reinforced polymer (CFRP) prestressing strands. The behavior of CFRP prestressed concrete piles should be investigated as a possible component of bridges with much longer target design lives, potentially exceeding 100 years.

Current investigations indicate that some DOTs are including pilot studies using CFRP in their design of prestressed piles. Most of these studies have limited laboratory tests. Furthermore, there is a lack of comprehensive design specifications and construction procedures to enable transportation engineers to adopt this innovative technology.

1.2 Research Objectives

The objective of the project was to conduct a synthesis of the use of CFRP reinforcement in prestressed concrete piles with a focus on assessing the following features:

- 1) Current and historic use;
- 2) Existing specifications;
- 3) Current standards adopted by Departments of Transportation and others;
- 4) Construction requirements including assessment of the need for CFRP transverse reinforcements;
- 5) Design and detailing requirements;
- 6) Cost comparison to steel prestressed piles;
- 7) Installation requirements for various soil conditions (including drivability); and
- 8) Limitations of CFRP prestressed piles.

Chapter 2: Literature Review

2.1 Assessment of Conditions of Existing Piles in TX

In order to evaluate the potential for adoption of CFRP strands as reinforcement for prestressed concrete piles by the Agency, practicality and economic benefit must be quantified. The structural capabilities and material properties of CFRP-reinforcement have been provided in the subsequent portions of the Literature Review. The over-arching question this project must satisfy is what potential for economic benefit to the Agency this technology could provide. While this issue will be more quantitatively expressed in the Cost Analysis portion of research, the qualitative component of this answer will be expressed here. In Chapter 2 of this Report, the Research Team quantifies the actual need for CFRP-reinforcement in the State, namely, where the Agency stands to benefit financially from the implementation of this technology.

The Research Team interviewed TxDOT district engineers and bridge engineers, and private consultants who practice geotechnical engineering for marine environments. Collectively, the team received feedback from the Beaumont, Corpus Christi, Houston, Pharr, and Yoakum TxDOT districts as well as from private firms across the State.

2.2 Rate of Occurrence of Deficiencies Associated with Reinforcement Corrosion

The team attempted to quantify the state of typical reinforcement in piles around Texas by asking various design professionals and TxDOT authorities about their experiences with their maintenance. According to these sources, as far as serious degradation or necessary replacement goes, traditional prestressed concrete piles are not typically replaced before the life-cycle of the bridge has been reached (Costley, R., 2016, April - May. Email correspondence; Lee, A., 2016, April – May; Stephens, D., 2016, April. Email correspondence and personal interview). TxDOT bridge engineers in the districts where interviews were conducted indicated that a typical bridge pile's lifespan is concurrent with the overall lifespan of approximately 75 years. This lifespan, while being used to design structures today, was not in place 20 years ago, where it was more common to design structures for 50 year lifespans (Coward, D. 2016, May 2. Phone interview). It is in this respect that while newly constructed bridges within the State should require less maintenance over their respective life-cycles due to improved design practices, with nearly 40,000 bridges in Texas older than 20 years according to the National Bridge Inventory. Figure 1 shows a severely deteriorating bridge structure in the Beaumont district, exemplifying the continual challenges the Department faces in their bridges.



Figure 1. Deteriorated pile- cracked and spalling, TxDOT Beaumont District b. 1978.

While total replacement of bridge piles is uncommon within some TxDOT districts such as Beaumont, Houston, and Yoakum, district engineers Rex Costley and Andrew Lee indicated that remediation efforts are very often implemented on piles to prevent further section loss before full pile replacement is needed (Costley, R. (2016, April - May). Email correspondence). Cast-in-place piling, according to the source, tended to show more rapid deterioration than pre-stressed concrete piling (Costley 2016). This suggests that the typical steel prestressed piles are resilient to begin with. Beaumont and Houston districts have indicated that while piles are often repaired in their districts, this deterioration issue is not critical and the methods available to their design engineers are sufficient to tackle the issue. The Corpus Christi and Pharr districts, however, have indicated that the corrosion of steel reinforcement is in fact a significant issue in their jurisdictions. The issue of pile deterioration is one that is faced in all the districts where information was gathered. In Districts where more funds were spent to mitigate cracking and spalling more frequently, be it with concrete collars or FRP wraps, there were little or no reports of complete pile replacement. While full replacement of piles is uncommon, the maintenance of these structures is a constant undertaking.

Prestressed concrete piles will experience deterioration and spalling of their concrete cover more severely as the steel reinforcement is corroded. There is a greater chance for corrosion of steel strands in the vicinity of marine environment especially when water level fluctuates, i.e., tidal zone. Continuous wetting and drying expedites the corrosion process significantly. The structures in those areas have experienced higher deterioration rates due to infiltration of salt water. Among factors that may affect deterioration of steel-reinforced structures, corrosion is the largest factor which may produce cracking and spalling in the surrounding concrete, a loss of bond between the two materials, and a loss of overall steel cross section. The deterioration process of reinforced concrete due to corrosion can be described by six steps (Thoft-Christensen 2003; Gulikers 2005). The degradation process begins with chloride

penetration in the concrete, leading to initiation of corrosion to the reinforcing steel, a significant increase of corrosion to the reinforcement, in turn leading to initial cracking of the concrete, a worsening of cracks propagating within the concrete, and finally, concrete spalling. After initial corrosion of the steel reinforcement, the rate of further degradation depends primarily on the availability of moisture and oxygen at the cathode (Bentur et al. 1997; ACI Committee 2002).

While prestressed concrete piles in coastal regions predominantly suffer from deterioration issues, there are several incidences of deficits in piles in urban areas. The Research Team has also carried out an investigation on existing piles in the south Texas area. Figures 2 to 4 present some of the existing piles which exhibit different types of deterioration such as cracks in concrete, and concrete spalling which eventually resulted in the exposure and corrosion of reinforcement. This information has been taken from TxDOT database along with the research team's visits of existing bridges. The lack of documented instances suggests that the overall trend for reinforcement degradation within bridge piles due to environmental corrosion is relatively insignificant compared to other issues facing bridges. Upon numerous conversations with professionals familiar with the issue, this was confirmed by design professionals around the State. Therefore the Research Team changed its research focus from infrastructure replacement, to new construction, eliminating the degradation issue (however minor it has been reported) entirely.

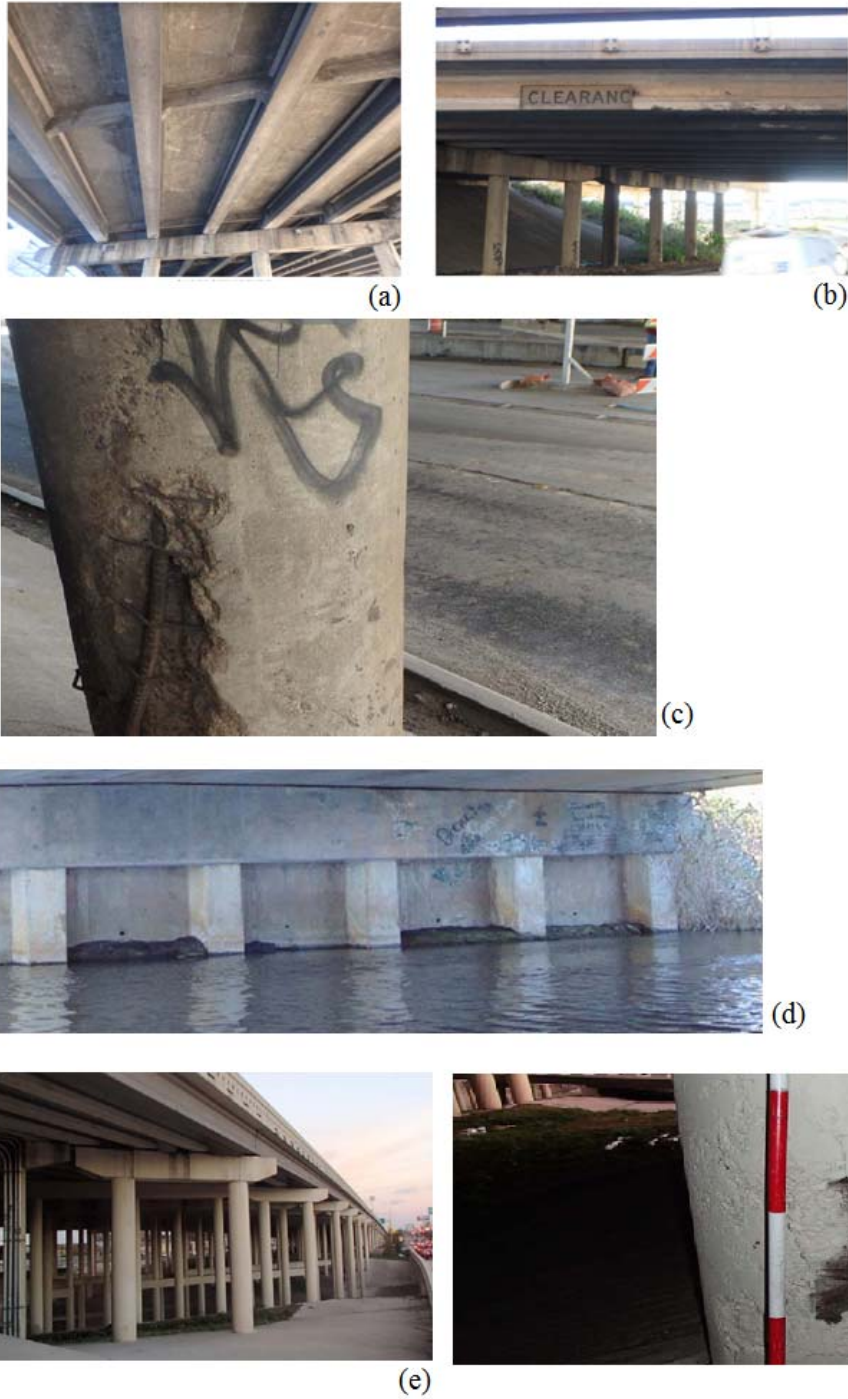


Figure 2. Bridge Located on IH 610 EB CONN & 18TH St. b. 1975, (a) Substructure View, (b) US 290 EB to IH EB Elevation View, (c) Concrete Spalling in Pile; Bridge Located in Brazoria County b. 2003, (d) Substructure Close View; Bridge Located on White Oak BYU Yale-Heights, (e) Substructure, (f) Concrete Spalling on Pile.



(a)



(b)



(c)



(d)



(e)

Figure 3. (a) Bridge View from 59 b. 1975, (b) Close View of Deficits; Bridge Located Basson Dr. & BNSF RR, (c) Concrete Delamination and Spalling; Bridge Located on IH 610 FR'S, (d) elevation view, (e) Concrete Spalling, Reinforcement Exposure, and Vertical Cracks on pile



(a)



(b)



(c)



(d)



(e)



(f)

Figure 4. Bridge Located on IH 610 b. 1975, (a) Elevation View, (b) Concrete Spalling and Reinforcement Exposure; Bridge Located Goodyear RR & Dr., (c) Bridge Elevation View, and (d) Concrete Spalling with Exposed and Deteriorated Reinforcement; Bridge Located on Normandy St., (e) Concrete Spalling and Reinforcement Exposure; Bridge Located on Hardy Toll Rd & UPRR, (f) Concrete Spalling and Exposed Reinforcement.

2.3 Locations and Structures Susceptible to Pile Reinforcement Corrosion

The typical section for a bridge pile is a 16in. by 24in. square, as specified by district engineers. Most piles are in trestle bent configurations and have prestressed reinforcement (Caron, C. (2016, April-June). Email correspondence). The Research Team used this information to create a comparative model between different types of reinforcement to develop the most accurate economic representation of potential implementation later in the Report.

As the Research Team has limited the scope study to the coastal regions of Texas (strictly limiting site visits and database inquiries to these Districts) at the suggestion of the Research and Technology Implementation Division (RTI), the potential application, as it applies to this project, is well beyond these coastal regions, potentially being implemented throughout the State. It was concluded that the most degenerative environment to bridge piles is the saline waters of the coasts, and therefore the team limited its studies to this. When reinforcing steel is exposed to this environment, as it would be at some point in its typical lifespan, it corrodes significantly faster. Structures directly exposed to wave action or constant inundation from corrosive salt waters experience higher deterioration rates due to infiltration (Caron, C. (2016, April-June). Email correspondence).

When referencing the bridge maintenance database to study various inspection records across the state, it was found that there different contractors used differing inspection nomenclature to report findings to the Department within the last 5-year window we analyzed the most prevalent organizational method to categorize inspected bridge elements was a ranking system from 1-10, where 10 was used to describe a structural element in perfect condition, and a 5 indicated rapid repairs need to be implemented. The second most used categorization of bridge elements was itemization from CS1-CS5, where CS1 indicated no loss of functionality and CS5 was used to describe significantly deficient structural elements. In this regard, of 22 bridges that were randomly selected for review, the average state of submerged piles in the district was an 8, with the most severe rating, a 7, given to a 6-span bridge crossing Taylor Bayou. These structures were selected based on several criteria including their high volumes of traffic, saline environmental conditions, and critical locations (the inability to reroute traffic through a close alternate route). While there are thousands of bridges in the State, these were singled-out as a high likelihood to benefit from CFRP-reinforcement.

This bridge crossing Taylor Bayou, last inspected in 2014, had eight of its driven reinforced-concrete piles thoroughly cataloged in the latest inspection. From the report performed and drafted by an independent engineering contractor, it was found that a significant amount of minor vertical cracks had begun to propagate along several of the piles. While not an issue that required significant attention, this study suggests a possibility of occurrences elsewhere. Structures may not be subjected to pressing issues of repair, but have sustained minor to moderate deterioration and scour.

The Research Team also reviewed inspection reports of the Seawolf Parkway, a large bridge structure part of the Pelican Island causeway in Galveston. This aging structure had a mixture of both timber and concrete piles in various states of degradation. The structure included a total of 173 submerged piles or drilled shafts. With 2 feet of water visibility, inspection divers were able to collect many pictures of spalling and cracking inherent in the old structure as will be evidenced later in this document. According to the maintenance records, many piles had been previously repaired with grout patches and fiberglass jackets with several of these jackets having exposed reinforcing steel below the waterline as the jackets themselves were deteriorating. There existed numerous vertical cracks on several reinforced concrete piles up to 1/16th wide within the tidal zone and spalling of concrete with reinforcing

steel exposed most likely due to vessel impacts. It was the opinion of the inspection contractors that repairs be done on the structure before the next inspection would be undertaken.

While some officials from the Department have raised concern over the limited scope CFRP-reinforced piles might have, many were forthcoming with other potential areas of benefit. According to these sources, hollow piles, fender systems, friction piles, sheet piling, and ferry landing piles might all be future applications in which CFRP-reinforced piling might one day be used to improve their durability. While the issue of corrosion does not affect the embedded steel reinforcement in the substructure as heavily as in components of the superstructure, according to the literature and numerous design professionals, this phenomenon is still a relevant issue and, if not addressed appropriately, can lead to significant deterioration of structural members of the lifespan of the member as evidenced in numerous site visits.

2.4 Reviewing State-of-the-Art, and State of Practice

In this section of the Report, the Research Team has composed a synthesis of relevant literature pertaining to the fields of general pile maintenance within the state of Texas and carbon fiber-reinforced polymers (CFRPs). The maintenance and strengthening of reinforced concrete (RC) and prestressed concrete (PC) structures employing polymeric composites are now well established procedures and exist as a viable procedure currently utilized by departments throughout the state. Embedding prestressed CFRP cables is still a burgeoning endeavor however, and still awaits significant implementation by state agencies. It is the purpose of this section to discuss and analyze previous lines of inquiry into this technology and how the state might stand to benefit from its adoption.

2.4.1 Current Methods of Repair and Associated Costs

To more accurately quantify the current maintenance and associated costs of managing the state's numerous bridge piles, the Research Team referred to the standard operating procedures laid forth by the Department. In the substructure of bridges where cracking and minor spalling are concerned, TxDOT spall repair guideline calls for bagged cementitious repair material with coarse aggregate to significantly reduce any potential for shrinkage and cracking when used to shore-up pile damage. When feasible, the manual instructs that contractors should use a pre-extended repair material or add coarse aggregate (typically pea gravel) for the patchwork. Using extended material is often not practical when using trowel-applied materials in vertical and overhead applications. Installing concrete patches, in the case of bridge pile remediation, should not always employ higher compressive strength concrete mix in the attempt to create a better patch. Realistically, very high compressive strength can lead to early failure as a result of excessive loads being transferred into the patch material (Concrete Repair Manual, 2015). The repair should typically require materials that have only enough strength for the structures original design loads. Intermediate spall repairs should be considered non-structural in nature and therefore compatible or lower compressive strengths are beneficial to successful integration. The Repair Manual goes on to instruct how the pile substrate must be prepared for additional patches of other repairs of this nature. It states that contractors must ensure that the substrate is clean and sound, typically done by sandblasting. Any contaminants, including laitance, oil, dust, debris, or other foreign particles should be removed and the surface should be clean and saturated.

Fiber-reinforced polymer wraps, in addition to concrete collars, are another tool used across the state to mitigate the effects of deteriorating infrastructure and to shore-up the load-carrying capacity of members. From interviews conducted at the Beaumont and Houston TxDOT branches, both districts have been regularly implementing this technology in their maintenance work. FRP wraps are closely related to

FRP prestressed cables in their material properties, but have been more readily adopted by DOT's due to their varied usage and relatively quick application times.

Another important technique used to counteract the deterioration of bridge piles is encapsulation. Encapsulation is a common method of pile repair that has been used across various coastal districts to remedy the deteriorating effects of corrosion. Contractors, after adequately preparing the substrate surface as laid forth by the Concrete Repair Manual, will increase the amount of concrete around a deteriorated surface by means of encapsulation. Encapsulating jackets can be manufactured to be translucent, allowing the impregnation of grout within the jacket to be monitored during installation. This process allows for precisely molded jackets that conform to the structure and come prefabricated with grout injection ports and overlapping seams. The inside surface of the encapsulating jackets need to be lightly grit-blasted to remove any dirt or residual mold release compounds. Individual pile encapsulation repairs should be completed in as short a time as possible to avoid any buildup of marine bio-films that can weaken the bond between pile and grout (Cowart, D. 2016, May 2. Phone interview). To achieve the optimal bond with repair grouts in any marine application, local water conditions must be considered. These encapsulation forms require temporary bracing during the grout injection sequence. Upon completion of the installation, the actual jacket form is left in place to provide long-term protection to the structural system to mitigate damages from any potential future impacts as shown in Figure 5.



Figure 5. FRP Wrapping Retrofit (left), Plastic Pile Jacket (right).

Yet another commonly used technique to repair deteriorating bridge piles is the implementation of concrete bridge collars. Pile collars essentially increase the amount of concrete around a pre-existing pile, filling-in spalled material in deteriorated locations and increasing the overall pile cross section. This reintroduces the spalled-off concrete barrier to the corrosion-susceptible steel reinforcement for the cost of the additional concrete, securing and erecting formwork, and the variable labor and maintenance costs associated with the construction. While this method can oftentimes be the most cost-efficient, the original pile is still susceptible to the same mechanisms that induced spalling in the first place, only addressing the symptoms of the problem- not correcting the issue of deterioration. Figures 6 and 7 illustrate an aging collar repair and the ensuing deterioration that takes place years after its original implementation.



Figure 6. Cracked Collars Used to Repair Previous Spalling, TxDOT Beaumont District b. 1978.



Figure 7. Spalling of Concrete Collar, Seawolf Parkway, TxDOT Houston District.

In addition to the maintenance provisions, previously, a preventative coat of epoxy would be painted onto at-risk bridge piles as an extra barrier to the elements. What was found in the field, however, was that this protective coat was likely to chip and would thereby focus the weathering of the reinforcement into a single, concentrated point. It was this shortcoming that has prevented districts such as Houston to continue its use. In its place, according to design professionals at TxDOT and several private entities, high-performance concrete (HPC) has become more prevalent in their use for special requirement projects. This material is currently employed by TxDOT to mitigate corrosion in highly susceptible environments, namely structural members exposed to the splash zone down to the mudline.

From interviews conducted by the Research Team with the design professionals at the TxDOT Beaumont and Houston offices, phone interviews with representatives from various midstream

infrastructure specialists for the energy sector, and contractors specializing in the construction of bridge piles, the overwhelming majority of simple pile repairs are completed utilizing concrete patches. Unless the damage to the substructure is critical and time is of the essence, a rather simple concrete patch will suffice for most purposes. If the spalling is more severe and significantly reduces the overall cross section of the pile, a concrete collar may then be considered. If the member must be reinforced immediately, FRP wraps can be implemented quickly. The costs of maintenance increases the more involved the repair process and material in use. Concrete patches and concrete collars are relatively cheap to employ (an average of \$25/SF of materials and labor according to TxDOT Low Bid Prices) and FRP wraps and fiberglass pile jackets more expensive (highly dependent on the type of application). Districts across the State must make the most economical decision in this respect, a question that might be avoided if the reinforcing material used in the pile would not corrode, a solution that would effectively eliminate the entire discussion thus far set forth by the removal of reinforcement degradation.

2.4.2 Pile Inspections

According to both Beaumont and Houston Districts, routine biennial inspections are the standard interval for bridge inspection as per FHWA mandate for bridge structures older than 10 years (Lee, A. (2016, April – May). Email correspondence and personal interview; Stephens, D. (2016, April). Email correspondence). As this figure is subject to the pre-existing conditions of the bridge in question, inspections can occur more often if needed. That is to say annual inspections for 20 year-old bridges are common practice in the field, whereas new bridges are just not routinely inspected. Underwater inspections on structures with submerged portions greater than 4 feet in depth are performed every 5 years regardless of the structure's age, usually executed by diving professionals (Stephens, D. (2016, April). Email correspondence). These dives, depending on the intricacy of the bridge inspected, are almost exclusively contracted-out to private engineering services, and can typically cost several thousands of dollars depending on the size of the structure and its accessibility (Coward, D., phone interview, May 2, 2016). For the purposes of this study, the research team contacted private engineering firms that are frequently contracted to inspect marine structures such as docks, wharfs, and marine terminals with significant piling systems in harsh environments. In this respect, inspections occur every 5 years for structures with less than 10 years of age, and a minimum of every 2 years for older structures, consistent with the precautions taken by TxDOT (Coward, D., phone interview, May 2, 2016).

It is typical on sizeable bridges for a team of 4 diving professionals to spend several days inspecting the entirety of the structure, carefully combing the submerged surfaces for any indication of cracking, spalling, marine build-up, or other deterioration. The most effective inspections involve taking photographs of piles for visual inspection by the design engineer as show in Figure 8. However, these can only be performed when local water conditions permit. Water conditions often prevent divers from capturing clear pictures of deterioration when the water is too dirty to offer adequate visibility. Not only does this slow down the inspection process it does not afford divers any visual indication of cracking, and they must then survey the structures by touch- a rather imprecise metric. These inspections can last anywhere from a few days to more than a week, involving several divers, boats, and scaffolding if the structure is too far above the water all costing Agencies across the State a significant chronic expense.

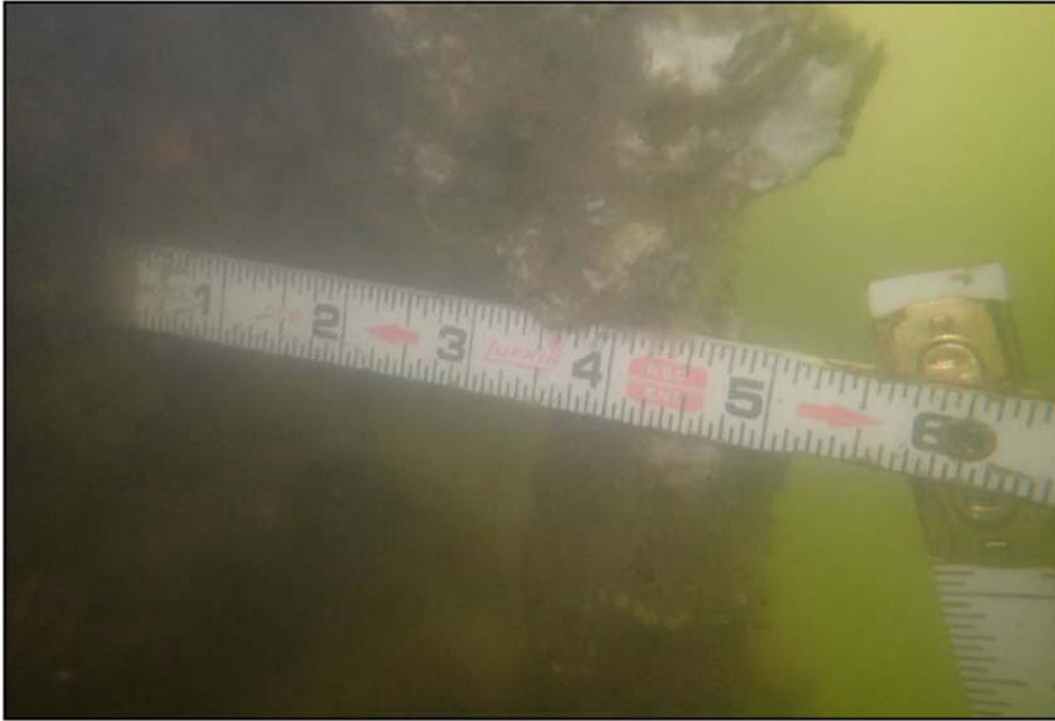


Figure 8. Inspection of Deteriorated Pile Collar, TxDOT Houston District.

In addition to lengthy dive inspections, a rather useful tool bridge inspectors have recently begun to employ in the field is acoustic imaging of subsurface structures, as can be seen in Figure 9. While still rather expensive and therefore relegated to only large-scale projects (identifying scour or impact damage as opposed to isolated spalling), acoustic imaging allows inspectors to accurately convey what is occurring below the waterline to the district engineers controlling the design of the remediation. The use of this technology requires not only costly imaging equipment, but also a significant amount of time on the part of the contractor to properly capture the data. As the technology matures, this process may find use in more bridge inspections across the State.

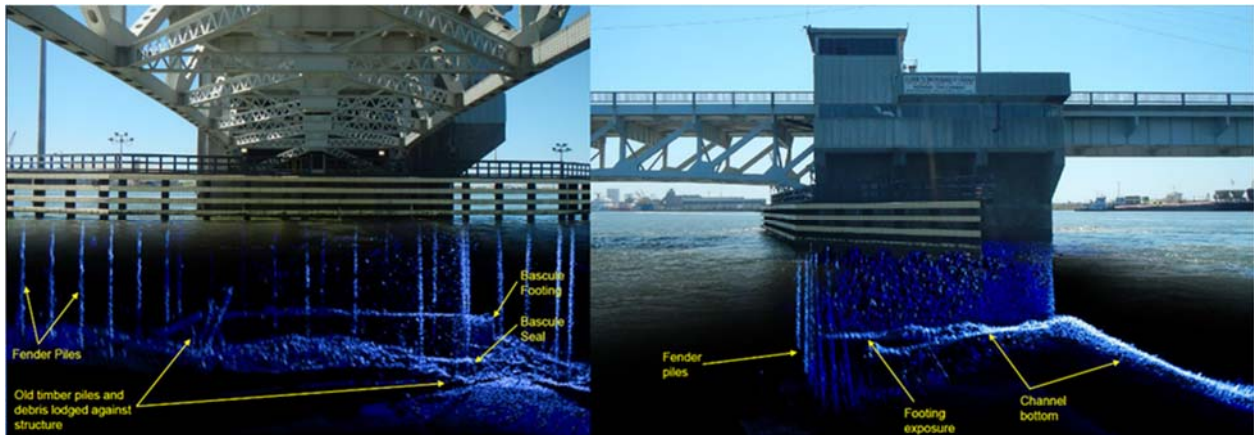


Figure 9. Acoustic Mapping of Submerged Substructure, TxDOT Houston District.

These inspections, performed by contracted engineering agencies or TxDOT, also vary significantly from site to site. Often times due to their embedment, bridge piles are only inspected visually for areas that contain cracks (Costley, R. 2016, April – May: Email correspondence; Cowart, D. 2016, May 2: Phone interview). Reinforcing steel is not included in these inspections unless there is indication of concrete spalling that might allow contact with the environment. Reinforcing bars and prestressing steel are assumed to be completely intact as long as there is no observable sign of concrete deterioration. This approach may conceal the early indications of reinforcement corrosion before expensive deterioration of the concrete is observed. As stated previously, there exists no single method that can comprehensively assess internal deficiencies. Visual inspection methods are often convenient for locating external symptoms, but results are qualitative and subjective (Dong and Ansari 2011). While visual inspection and localized load-testing are the most common methods of nondestructive testing for inspection, research has shown that such inspections have relatively limited accuracy and efficacy, with albeit a remote possibility, the ability to fail catastrophically between inspections (FHWA 2001).

2.4.3 Costs Associated with Maintenance

This method is typical in pile maintenance, and in general, the notion to address pile rehabilitation when it is convenient timing to replace another portion of the structure. As TxDOT's goal is minimal service interruption (as associated costs compound the longer a bridge is being serviced and the more traffic is affected), departments only perform partial closures whenever possible due to pile maintenance. Preventative maintenance such as crack repair, painting exposed surfaces, etc. becomes essential in this model to effectively extend the expected service life of a structural system. This is primarily done to avoid such costly associated costs, often implemented more frequently than essential maintenance for greater efficiency (Frangopol, 2011). In modern projects, it has become evident that life-cycle costs such as numerous inspections, maintenance repairs, design professional management, as well as associated costs can become more significant to the Agency than a structure's original cost. It is therefore advantageous to constrain lifecycle costs to a minimum to reduce such overall costs (Melchers, 2011).

Maintenance costs associated with substructure repair work for Corpus Christi District totaled close to \$75,000 according to sources from the Department and are expected to peak at \$350,000 next fiscal year as a large causeway structure requires crack injection and spall repair (Caron, C. (2016, April-June). Email correspondence). While this magnitude of maintenance is not typical, usually occurring every 8-10 years, it is significant enough to be of note in this study. This estimate is associated with a single bridge substructure, albeit a large one, in a single district. These large ticket repair projects are expected to occur elsewhere in the state in districts that have not been contacted by the Research Team in the scope of this synthesis study.

2.4.4 Frequency of Pile Replacements

Depending on the severity of cracking and spalling, the location of the piling, and the water elevation, departments across the state decide with what frequency bridge piles must be replaced. During the gathering of information in the interview process, it was found that bridge piles are very infrequently replaced- more often repaired by means of encapsulation jacket, fiber-wrapping, or concrete collar (Costley, R. (2016, April - May). Email correspondence; Lee, A. (2016, April - May). Email correspondence and personal interview; Stephens, D. (2016, April). Email correspondence). The Seawolf Bridge in Galveston for example, had at least 31 pile repairs at the time of the bridge inspection, with some of those repairs deteriorating themselves. The Hillebrandt Bayou Bridge (from the images provided by Beaumont District) had at least 23 pile repairs when the site visit was made, in large part due to its age. Overall, it is far more typical that a bridge pile be repaired by one of the aforementioned methods than a full

replacement, all repairs being highly correlated to the local environmental conditions and age of the structure.

2.4.5 Condition of Piles Summary

From the interviews conducted and information gathered regarding the state of piles in the coastal regions of Texas, it becomes apparent that prestressed CFRP-reinforcement would occupy a very small market in pile replacement. From the various industry professionals in these areas, it was stated that the need was not quite there as pile repair was far more probable than pile replacement- a use not conducive to the requirements of this technology.

Attention must be drawn away from clear-cut pile replacement to overall maintenance and life-cycle costs. It is apparent from our inquiries that the benefit of implementing CFRP-reinforced piles throughout the state's infrastructure lies not in existing pile replacement, but in new construction. The strength of the technology relies in its resilience to environmental degradation, thereby prolonging the numerous repairs that have been seen throughout this study to more conventional piles. If the CFRP-reinforced pre-stressed pile can allow a department to postpone expensive maintenance procedures numerous times over the span of the structure's life-cycle, this could be a significant boon to the Department economically and will be expanded upon in the Life-cycle Analysis in Chapter 3.

2.5 CFRP Material Properties

In regards to steel-reinforcement corrosion in the field, British Steel Corporation (BSC) has reported quantitative losses based on the environments in which they can be found. In industrial environments, BSC reported a loss of 0.007 in/year, 0.001 in/year in soil (gathered from piles extracted after 25 years), and 0.02 in/year in splash zones above high-tide. This is almost twice the rate of corrosion of a pile below low-tide levels where the structures remain submerged at all times (Flemming et al. 1992). Degradation begins as concrete degrades from a combination of several factors including high sulfate and chloride concentrations, low pH levels in soils and groundwater, or the occurrence of reactions between sulfate ions in groundwater and Portland cement. These actions result in chemical products of greater volume, causing cracking and spalling in the concrete which further exacerbates the problem of steel-reinforcement corrosion (Han et al. 2002).

CFRP consist of high-strength or high-modulus carbon fibers that have been impregnated with a resin matrix. Structural CFRP composites can be produced in different forms such as unidirectional plates and strips, sand coated reinforcing bars with circular cross-sections, multi-wire strands that are similar in geometry to prestressing steel, 2D grids, pre-formed stirrups and spirals, or bidirectional fabrics that are impregnated on site for strengthening or repair applications. Several types of CFRP materials are available for prestressing applications, one of which can be seen in Figure 10, below.

CFRP is manufactured by sending a precursor fiber (either polyacrylonitrile (PAN) or pitch fiber) through an air oven heated to 220°C which allows for the absorption of oxygen. The oxidized fibers sent to an inert atmospheric chamber ranging from 400 - 1600°C which then carbonizes the fibers. As these fibers emerge from the furnace, small surface charges are acquired from contact with guides and rollers, and the fibers are therefore given a protective coating. Several different polymeric solutions can be applied depending on the manufacturer, but typically a low molecular weight epoxy resin is employed. Next, a surface treatment is given to the fibers, improving adhesion to the matrix. This last step sanitizes the fiber surface, producing an etching on the fiber, and in addition, offers reactive oxide sites by chemical reaction (Hollaway 2011).

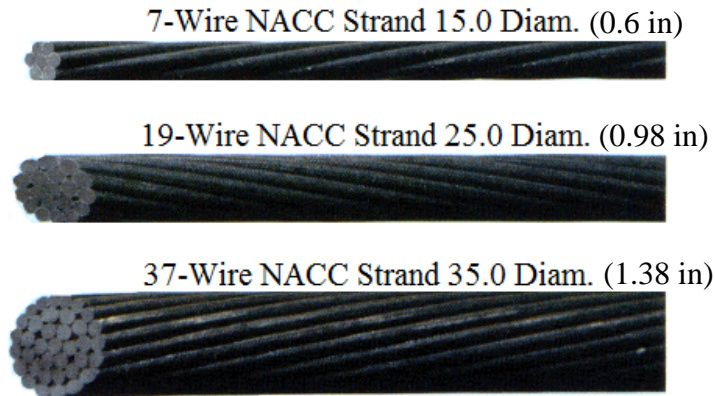






Figure 10. Numerous Configurations of CFCC Strands, Tokyo Rope 2012.

Among commercially available types of CFRP, twisted wire strands (similar to steel 7-wire strands) known as Tokyo Rope USA's carbon fiber composite cables (CFCC) are most commonly used for prestressing applications. Tokyo Rope USA's carbon fiber composite cables (CFCC) consist of polyacrylonitrile (PAN) continuous carbon fibers, created by carbonizing acrylic fibers at high temperatures (Enomoto et al. 2011). The coefficient of thermal expansion of the polymer is significantly higher than that of the fibers. Their hybridization stabilizes the composite to values similar to materials used in general civil engineering applications such as steel and concrete. Any differential thermal expansion of the FRP in conjunction with an RC member may generate additional stresses at bond lines during large temperature swings (Hamilton and Dolan 2000). The heat-treated epoxy resin and fibers, after carbonization, are then twisted together alongside other strands to form a single fiber core and then wrapped with protective synthetic yarn. This extra layer serves to mitigate the effects of mechanical abrasion and act as a protective coat against harmful UV light. The synthetic yarn also improves the CFRP's bond with surrounding concrete. The specific brand of CFRP mentioned above is indeed fabricated abroad, with the company recently opening a manufacturing plant in Michigan. Apart from this company, there exist many domestic producers of the material as well. Table 1 presents the basic geometries and mechanical properties of different types of multi-wire carbon fiber strands.

Continuous lengths of CFRP can be easily manufactured with less energy per kg to produce and transport compared to that of steel, and due to their low bending stiffness, are typically delivered to the construction site in bundled rolls. CFRP's exhibit resilient fatigue and creep properties, but also have the possibility of brittle failure, incur higher material costs and are susceptible to fire damage (Hollaway, 2011). Some of these negative properties of FRP's disappear when prestressed and embedded within concrete. While CFRP's, like their steel counterparts, must be fabricated in a plant, they must also be cut to size, bent to shape, and rolled in the same environment specially in the case of stirrups or spiral reinforcements. This inability to manipulate the material on site/external facility requires extensive planning and careful foresight from contractors during construction.

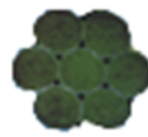
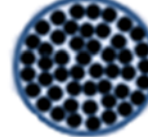

Table 1. Adapted from Tokyo Rope USA Product Specifications (Tokyo Rope, 2012).

Diameter Configuration		Diameter(in)	Effective cross-sectional area (in ²)	Guaranteed capacity (kips)	Nominal mass density (lb/ft)	Tensile elastic modulus (ksi)	
	1	5.0Φ	0.20	0.02	8.54	0.02	24220
	1 X 7	7.5Φ	0.30	0.05	13.49	0.04	22480
	1 X 7	10.5Φ	0.41	0.09	31.70	0.07	22480
	1 X 7	12.5Φ	0.49	0.12	41.37	0.09	22480
	1 X 7	15.2Φ	0.60	0.18	60.70	0.14	22480
	1 X 7	17.2Φ	0.68	0.23	78.69	0.19	22480
	1 X 19	20.5Φ	0.81	0.32	71.04	0.27	19869
	1 X 19	25.5Φ	1.00	0.47	104.99	0.4	19869
	1 X 19	28.5Φ	1.12	0.62	133.54	0.47	19869
	1 X 37	35.5Φ	1.40	0.92	189.07	0.79	18419
	1 X 37	40Φ	1.57	1.24	269.78	1.02	21030

2.6 CFRP Strength

Mechanical properties of CFRP directly correlate to the volume fraction of fibers and resin matrix inherent in the product. The unidirectional orientation of carbon fibers created during the manufacturing process gives the material a tensile strength equal or more than that of steel strand and has a much higher elastic modulus than Aramid FRP (a less expensive FRP alternative) (Han et al. 2002; Enomoto et al. 2011). CFRP has exceptionally high tensile strength-to-weight ratios (with densities 1/4th to 1/5th that of steel), a low coefficient of linear thermal expansion (around 0.2E-6 in/in/°C), and adequate corrosion resistance even in harsh chemical environments (based on ultimate strength tests performed on members submerged in alkaline solutions (Rizkalla et al. 2003; El-Salakawy 2003). This synthetic material’s resilience to alkaline-heavy environments, high specific strength and stiffness, thermal stability, and high specific damping capacity all speak to its significant potential as a possible answer to new infrastructure needs (Bakis et al. 2002; Sharp et al. 2014). This light-weight material, capable of displaying tensile strengths ranging from 286-464 ksi and a tensile modulus anywhere from 39160-74984 ksi, appears to be well-positioned to be used for pile reinforcement (Roddenberry et al. 2014). A snapshot of material properties (based on #4 nominal diameter provided by manufacturer) can be seen in the Table below.

Table 2. Material Properties of Prestressing CFRP.

	Cable A	Cable B	Bar
Cross-section			
	Twisted Wires	Straight Wires	Solid
Effective Cross-sectional Area, in²	0.118	0.126	0.196
Resin	Epoxy	Epoxy	Vinyl Ester
Fiber Volume Ratio	0.65	N/A*	N/A*
Longitudinal Tensile Strength, ksi	390	268	275.4
Longitudinal Modulus, ksi	22480	27000	20880
Maximum Longitudinal Strain, %	1.7	0.99	1.32

When considering the use of most FRP reinforcements, it is important to be aware that the material is linear and elastic up to failure and does not exhibit any plasticity or ductility, although it does have relative good strain capacity (typically up to 1.5% for CFRP depending on the fiber type). This lack of ductility should be properly accounted for when designing FRP-reinforced concrete structures. Further, since the elastic modulus of CFRP materials is typically around 75% that of structural steel, the design of CFRP reinforced and prestressed concrete elements may be governed by serviceability limit states such as deflection and cracking (Marco et al. 2012). However, for prestressed concrete piles, deflection and cracking are not expected to be the primary factors controlling the design, and typically will not enter consideration.

The vertical load-bearing capability of reinforced piles depends on a number of site conditions including the project's soil properties, the pile's material properties, and pile dimensions (Juran and Komornik 2006; FHWA 1998; Meyerhoff 1976). FRP structural piles exhibit anisotropic mechanical properties, have a low section stiffness, and a high elastic to shear modulus ratio- thereby giving shear deformation an important role in mechanical behavior. These properties, however, also yield a high creep rupture potential (Zhang et al. 2014). These visco-elastic properties, characteristic of the polymeric component of FRP's have such a tendency to creep, but the fiber portions of the composite, namely the carbon, glass, or aramid fibers have a stabilizing effect on the FRP. The effective creep behavior depends significantly on the overall fiber volume fraction and fiber orientation (Hollaway 2011).

Fiber tension during concrete curing (reinforcement prestressing) significantly benefits impact resistance, overall member tensile strength, elastic modulus, and increases the load carrying capacity for deflection levels corresponding to serviceability limit states (Triantafillou and Deskovic 1991; Zhu et al. 2015; Rezazadeh and Barros 2016). In the lab, relaxation rates were found (up to 33,000 hours) for prestressing level up to 80% of guaranteed strength which indicated that the relaxation values for Tokyo Rope USA CFCC was approximately half that of steel strands. This was based on a log time versus overall relaxation rate metric. Furthermore, several researchers (Arockiasamy and Sandepudi 1994; Arockiasamy and Amer 1998; Enomoto et al. 2011) also observed that the relaxation values of the CFRP tendons were insignificant. Above 80°C, however, relaxation of the reinforcing CFRP has been estimated to be relatively large and requires further investigation (Enomoto et al. 2009). That is to say, in typical pile environmental conditions general relaxation rates are equivalent to those found in prestressing steel.

As CFRP reinforcement in concrete piling is a relatively new frontier, there exists little literature regarding its failure mechanisms in the field. A similar structural use, column design, may point to such mechanisms, i.e. transverse tensile failure, fiber micro-buckling, and shear failure are the dominant modes of failure with FRP bars under compression (ACI 440.1R-06). Previous studies have shown that non-prestressed FRP is significantly stronger in tension than in compression, similar to conventional reinforcing steel under buckling scenarios (Wu 1990; Kobayashi and Fujisaki 1995).

With numerous beneficial material properties comes several downsides associated with CFRP. A high initial price of material (5 to 15 times that of steel depending on the material specifications), a low modulus of elasticity compared to steel, and low ultimate failure strain (again, compared to that of steel) are all characteristics of this material. More negative aspects include a high ratio of axial-to-lateral strength (which may cause concern to anchorages for prestressing), a high transverse thermal expansion coefficient compared to concrete. And also, because of the inherent susceptibility to creep rupture failure, CFRP's long-term strength can actually be lower than its initial strength. As stated before, CFRP exhibits an intolerance to UV light and has a low impact resistance (Roddenberry et al. 2014). These considerations can be abated with standard practices in place today, reflected in design equations associated with FRP's and manufacturing processes. What can be taken from this information is the distinct advantage CFRP's

have over conventional steel reinforcement in terms of strength, allowing for fewer strands of CFRP to support identical loads, potentially closing the significant gap in initial construction costs when comparing the two materials.

2.7 CFRP Durability

The environmental degradation of steel, according to a plethora of research over the course of decades, can be entirely eliminated through the implementation of CFRP tendons. Degradation has been observed to be more severe in GFRP better illustrating the capacity of CFRP to resist penetration from solutions with high alkalinity. Material degradation in reinforced concrete structures most typically manifests as the corrosion of internal steel reinforcement from prolonged chloride ingress or the carbonation of the concrete substrate (Hollaway 2011). Carbon fibers do not absorb environmental liquids are therefore subsequently resilient to ingress from alkalis or solvents (Balazs and Borosnyoi 2001). The resilience of CFRP's to this damaging process can be seen in the Figure below. Figure 11 illustrates the relatively small change in ultimate strength between specimens artificially degraded for 3 months versus those exposed to degradation for 9 months.

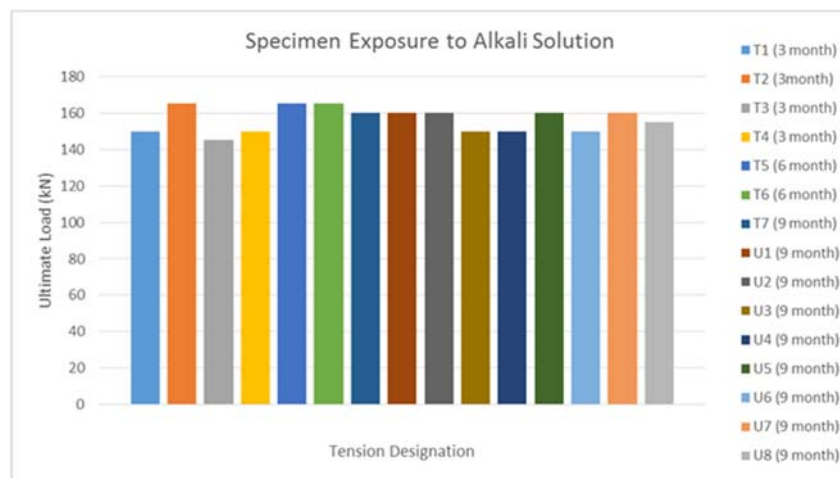


Figure 11. CFRP Specimens Exposed to Alkali Solution, adapted from Arockiasamy and Amer (1998).

From air, seawater, or alkali solutions, CFRP does not exhibit significant strength deterioration when exposed to these harmful solutions as can be seen from specimens ranging from 3-9 months of exposure (Katuski and Umoto 1995; Arockiasamy and Amer, 1998; Toumpanaki et al. 2014).

Because CFCC cables are produced in a controlled environment, they generally have higher fiber volume fractions (improving the creep-rupture-prone polymeric characteristics) and well-monitored temperature cures, resulting in far more consistent material properties, less varied than compared to wet lay-up FRP wraps (Hollaway, 2011). Numerous previous studies suggest that if properly designed and fabricated, polymer composite systems can provide longer lifetimes and lower maintenance costs than conventional reinforced concrete structures. In addition to the study published by Arockiasamy and Amer (1998), tests conducted by Benmokrane (2015) have yielded similar CFRP behavioral responses in harsh environments. Specimens exposed to elevated temperatures up to 60°C in alkali baths, at worst, experienced a 6% decrease in tensile strength as seen in Figure 12, below.

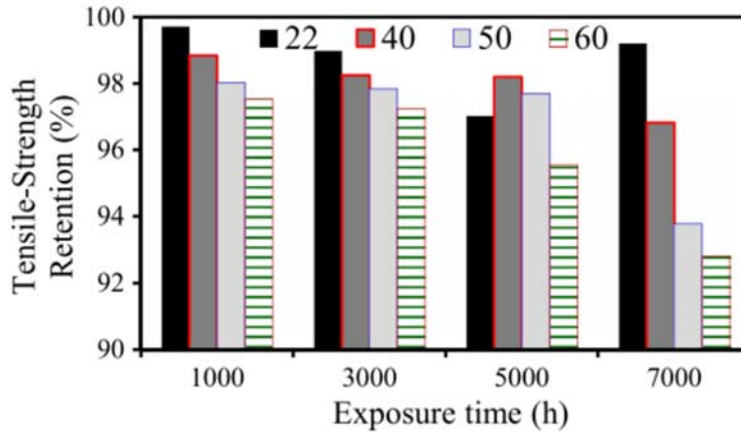


Figure 12. CFRP Specimens Exposed to Alkali Baths at Elevated Temperatures, Benmokrane (2015).

As a caveat to this line of reasoning however, a large majority of the current knowledge on durability is based on experimental accelerated laboratory testing of FRP materials. Design professionals must also be cognizant that the results based off FRP coupons that have been exposed to accelerated testing (typically in raised temperatures and in concentrated solutions) to analyze the long-term response of a site structural system need to be further investigated and verified to improve reliability modeling and its subsequent predictions, namely finding an accurate probability distribution than can quantify this phenomenon. It is in its excellent durability that CFRP reinforcement can compete with its relatively cheap counterpart, prestressed steel, allowing for uninterrupted use for more than a century. This, when paired with the need for fewer reinforcing strands to achieve equivalent capacities might allow the material to become economically equivalent, incentivizing the adoption of the highly-durable material.

2.8 Detailing Requirements for Splices and Embedments

When concrete piles attain significant lengths, cracking of long piles during handling, the cumbersome weight of these piles, and the costs associated in handling them lead engineers to splice lengths of shorter pile segments together to alleviate these problems (Bruce et al. 1974). These splices should be effective at doing this without reducing the structural capacity of the pile, extending the duration of construction, or significantly add to construction costs. Effective splicing of prestressed concrete piles can reduce or eliminate many problems associated with the installation of long piles. To date, there are no detailing requirements of splices or embedments applicable CFRP-prestressed concrete piles. In fact, there are no standard national guidelines on how conventional steel reinforcement is to be spliced together, a fact that has caused the adoption of numerous different methods across the US (Issa 1999). TxDOT classifies splice types based on the reinforcing material, tensile strength of reinforcement, and development length as seen in the Table 3.

Table 3. TxDOT Splicing Details for Uncoated Steel Bars, TxDOT Bridge Detailing Guide 2014.

Table 5-6: Class B Splices for uncoated bars (Class C Concrete, $f'_c = 3,600$ psi)

Size	A Ld		B 1.3 Ld	C 1.3 (1.4) Ld	D 1.3 (1.4) 0.8 Ld	E 1.3 (0.8) Ld
Grade 40 $f_y = 40,000$ psi	#3	(6.00") 1'-0"	1'-0"	1'-0"	1'-0"	1'-0"
	#4	(8.00") 1'-0"	1'-0"	1'-3"	1'-0"	1'-0"
	#5	(10.00") 1'-0"	1'-1"	1'-7"	1'-3"	1'-0"
	#6	(12.00") 1'-0"	1'-4"	1'-10"	1'-6"	1'-1"
	#7	(15.84") 1'-4"	1'-9"	2'-5"	2'-0"	1'-5"
	#8	(20.69") 1'-9"	2'-3"	3'-2"	2'-7"	1'-10"
	#9	(26.35") 2'-3"	2'-11"	4'-0"	3'-3"	2'-4"
	#10	(33.36") 2'-10"	3'-8"	5'-1"	4'-1"	2'-11"
	#11	(41.19") 3'-6"	4'-6"	6'-3"	5'-1"	3'-7"
	#14	(56.92") 4'-9"	-	-	-	-
#18	(73.79") 6'-2"	-	-	-	-	
Grade 60 $f_y = 60,000$ psi	#3	(9.00") 1'-0"	1'-0"	1'-5"	1'-2"	1'-0"
	#4	(12.00") 1'-0"	1'-4"	1'-10"	1'-6"	1'-1"
	#5	(15.00") 1'-3"	1'-8"	2'-4"	1'-11"	1'-4"
	#6	(18.00") 1'-6"	2'-0"	2'-9"	2'-3"	1'-7"
	#7	(23.76") 2'-0"	2'-7"	3'-8"	3'-0"	2'-1"
	#8	(31.03") 2'-8"	3'-5"	4'-9"	3'-10"	2'-9"
	#9	(39.53") 3'-4"	4'-4"	6'-0"	4'-10"	3'-6"
	#10	(50.04") 4'-3"	5'-6"	7'-8"	6'-2"	4'-5"
	#11	(61.78") 5'-2"	6'-9"	9'-5"	7'-7"	5'-5"
	#14	(85.384") 7'-2"	-	-	-	-
#18	(110.68") 9'-3"	-	-	-	-	

As CFRP cannot be significantly manipulated on site like conventional reinforcing steel without severely reducing its capacity, there must be much foresight on the part of the design engineer to account for the variable needs of the project. An alternative method of splicing these lengths together- namely by employing a dowel type of splice has been proposed. Steel dowels (as no current detailing requirements have been put forth for FRPs) are embedded within both ends of the to-be-spliced members and bonded with epoxy mortar, where the number of dowels needed is dependent on the cross-sectional area (Cook et al. 2003). The bottom pile will have a series of holes in its cross section to be inserted with rebars protruding from the upper pile, where precision of alignment is the most important aspect of the splice. An additional coating of epoxy or grout is also required as part of the installation.

Surface texture, embedment length, concrete cover, concrete compressive strength, and confinement provided by transverse reinforcement are all important factors when analyzing development length (Quayyum and Rteil 2012). According to some research, it was determined that CFRP (along with both AFRP and GFRP) had virtually identical development lengths when compared to the slightly longer development length of traditional reinforcing steel. That is to say, what was found for AFRP and GFRP, can be directly translated to CFRP. The development length of CFRP can be conservatively predicted by ACI design equations to ensure proper splicing locations, and transfer lengths of at least 50 times the tendon diameters are recommended (Lu et al. 2000).

This review of the state-of-practice, with regards to pile splicing indicates that there is a significant gap in existing knowledge. More comprehensive laboratory and field tests are needed to assess the performance of these measures for sets of data than can be used for structural reliability and quality assurance purposes.

2.9 Current and Proposed Design and Detailing Specifications

According to Arockiasamy and Amer (1998), design engineers cannot make the same design assumptions with CFRP as with steel reinforcements as ultimate conditions would no longer be valid due to the linear elasticity of CFRP cables up until failure (having no yield point). Unlike steel, this

fundamentally changes design approaches as there no longer exists a plastic deformation region to observe before failure. Alongside this, traditional wedge-type chuck anchors previously used for reinforcing steel strands cannot be used for CFRP due to the product's low transverse compressive strength and susceptibility to mechanical abrasion. Instead, a special wedge-type anchorage system was employed during fabrication, coupling steel strands to CFRP to act as sacrificial mediums to grasp while prestressing as seen in the Figure 13 below (Grace et al. 2012). Previous work on evaluation of the physical and mechanical characteristics of FRP systems mostly focuses on identification of material strength, stress-strain relationships, bond, development and transfer lengths, fatigue performance, anchorage systems, and losses due to creep, relaxation, and thermal effects. However, further research is needed to verify the efficiency of anchorage systems for FRP prestressing.

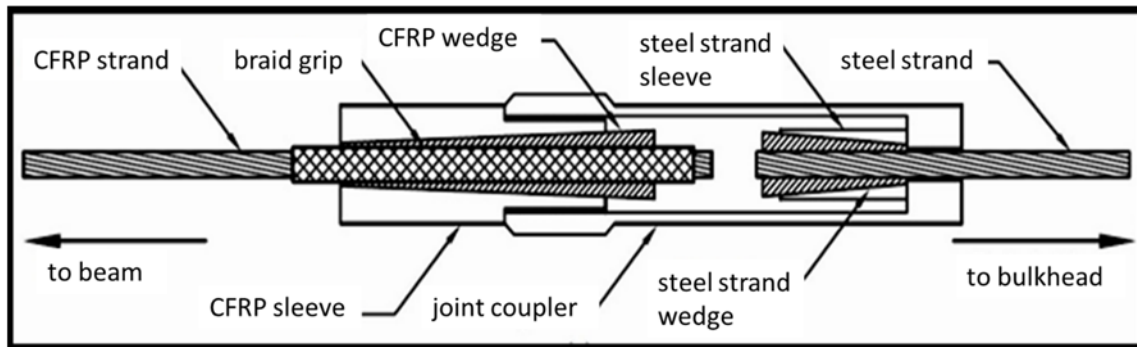


Figure 13. Anchorage System for CFCC Coupled with Steel Strands, Grace et al. (2012)

Han et al. (2002) describe several different design approaches to FRP-reinforced piles, indicating that it is possible that current design methods (such as ultimate load capacity or load-deflection response) can in fact be used to design FRP reinforced piles if adequate modifications to properties (such as interaction coefficient and ultimate creep coefficient) are considered. As sectional stiffness's are very similar to conventional piles, load-deformation response design is still valid in most applications, although pile deformation can be significantly underestimated with low stiffness FRP. Load-deflection response must be thoroughly revisited for use as traditional means to calculate values are not suitable due to FRP's anisotropic nature.

More recently, FDOT in conjunction with Florida State University, has published numerous specifications for CFRP implementation published in their Developmental D20600 series (CFRP prestressed only), Design Standard Index 20600 series (SS or CFRP strand), and the Fiber Reinforced Polymer Guidelines (FRPG) Vol.4, 2016. These standards together make a significant advancement to the widespread adoption of the material as technical specifications, namely, addressing design layout for prestressing strands, appropriate cable staggering, and pile pick up and storage details. However, these publications do not address many reservations design engineers would require as they do not detail splicing between piles for long pile configurations, do not address drivability concerns in differing soil types, or provide any guidance on transverse CFRP reinforcement in piles. If a pile is being constructed with prestressed CFRP strands so that its overall lifespan is to be increased, there cannot still be conventional steel transverse reinforcement present.

2. 10 Internal Transverse Reinforcement -- Ties and Spirals

According to standards published by TxDOT Bridge Division for prestressed piling, guidance was provided for a range of pile cross sections ranging from 16"x16" to 24"x24". According to the specification,

strands are to be located symmetrically about the axis of the pile with no more than one strand difference between any two adjacent sides. It is also standard for conventional prestressed steel strands to provide ½" 270 ksi low relaxation strands tensioned to 28.9 kips each.

Throughout the analytical comparison portion of this report, great care was taken to adhere to the specifications laid forth by TxDOT to present the use of CFRP exactly as conventional steel. The reinforcement pattern specified by TxDOT, was also used in the design of the CFRP member. From this document, it can be seen that a 2.5-inch clear cover is left around the transverse reinforcement when viewing the cross section, and 1-inch of space from the ends of the member in the profile view. After this initial space, TxDOT calls for transverse reinforcement to be spaced with a 1-inch pitch for the first 5 inches, a 3-inch pitch for the next 4 feet along the member, and 6-inch pitch for the remainder of the member to the center. This scheme is given for transverse spirals, and can be replicated with some additional labor with CFRP strands and ties. Currently, manufacturers can produce CFRP transverse reinforcement in a variety of different geometries that need be formed at the manufacturer's plant. The range of sizes offered are easily tailorable to current TxDOT needs, and it is in this spirit that care was taken to replace all conventional reinforcing steel in a one-for-one exchange for CFRP.

Another important decision affecting the implementation of CFRP prestressed strands is the Agency's willingness to strategically plan the delivery and constructability of the project. While this might hold true for conventional steel prestressing strands, manufacturers are far more comfortable with this standardized material, and are able to quite easily procure their strands at all times throughout construction. CFRP, on the other hand, is fabricated abroad, and is not readily-tailorable in the field. Workers cannot simply alter the shape of prefabricated CFRP transverse reinforcement to quickly adapt to the changing demands on the jobsite as this greatly decreases the material's effectiveness. This lack of flexibility in construction can only be mitigated by careful planning and scheduling deliveries of the material to coincide with their need. CFRP is also more labor-intensive, at least at this stage in its history, as workers must handle the material far more delicately, and as stated previously, cannot easily alter the shape of the strands to fit the exact needs on the jobsite.

2.11 Performance of FRP Transverse Reinforcement in Piles

While the behavior of FRP as primary reinforcement in concrete members has been significantly investigated, the behavior of FRP bars, spirals, and hoops embedded within reinforced concrete compressive members still requires additional information (Afifi et al. 2014). In regards to the use of GFRP bars as reinforcement, current design codes and specifications including CSA S806-02, SimTREC 2001, and ACI 440 have severe limitations for structural use- ignoring the compression strength of the reinforcing bar in the design (Almerich et al. 2012). It is rather apparent in the lack of literature on the subject, and it is therefore necessary to broaden the focus on CFRP tendons to FRP transverse reinforcement in general. Within columns undergoing compression (similar but apart from effects experienced in piles), it was found that CFRP transverse reinforcing (spirals) behaved similarly to steel up until experiencing peak loading (Afifi et al. 2013). CFRP reinforcing tendons have been found to be wholly effective at resisting the loading effects of compression until crushing of concrete substrate occurs. It was found that CFRP spiral spacing was more apparent on confinement efficiency and overall ductility than simple strength capacity, and that CFRP spirals and hoops utilized as transverse reinforcement (and in accordance with CSA S806-12 limitations) effectively confine the concrete core. Based on experimental results, GFRP embedded within columns as ties and spiral confinement were similar to steel in their capacity to do so (De Luca et al. 2011; Tobbi et al. 2012). The mechanism of CFRP reinforcement confinement is illustrated in Figure 14 below.

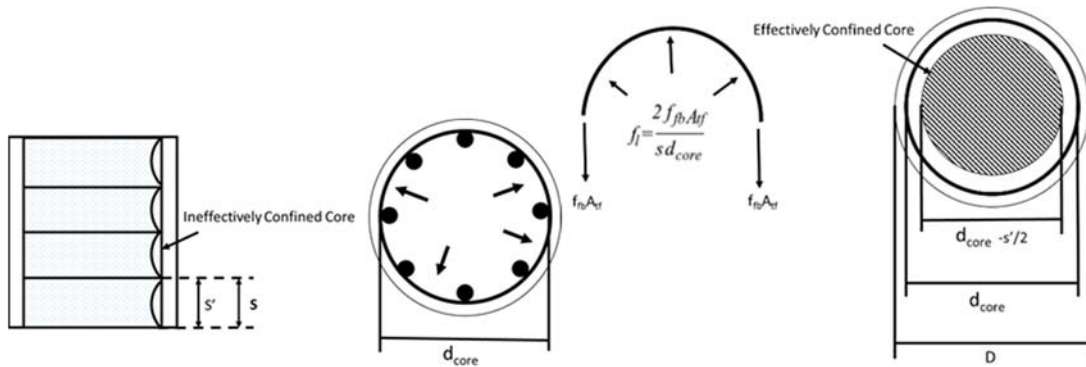


Figure 14. Arching Action for Hooped Circular Reinforced Concrete (RC) Columns, adapted from Afifi et al. (2014)

An experiment that did involve the use of CFRP as transverse reinforcement in piles yielded premature failure (in the pilot tests) due to the buckling of longitudinal CFRP reinforcement leading to ultimate failure of the column due to a hoop fracture (Arockiasamy and Amer 1998). This early failure helped in determining testing procedures to avoid such lateral failures, namely by drilling the ends of the CFRP tendons up to 1 inch to avoid directly contacting the loading plates used in the rig. This measure aided in eliminating buckling of longitudinal reinforcement in any of the following specimens and should therefore be considered to be implemented in the field. What was found from this research, however, was apparently less enhancement (due to CFRP confinement) than was reported in the literature at the time for similar steel lateral reinforcements.

In regards to the use of CFRP ties or spirals as transverse reinforcement, numerous studies have been conducted over the last two decades by researchers in the US, Canada, Europe, and Japan. It has been observed that many factors will ultimately affect the efficacy of internal ties and spirals such as the actual reinforcement configuration, longitudinal reinforcement ratio, volumetric ratio, and the size and spacing of hoops or spirals (Afifi et al. 2014). When these parameters are tailored to maximize their efficiency, experimental results (Alsayed et al. 1999; De Luca et al. 2010; Tobbi et al. 2012) have indicated that the overall performance of FRP ties and spirals acting as confinement for a concrete core behave similarly to traditional reinforcing steel. In addition, CFRP circular hoops were found to be as efficient as spirals in confining concrete as reported by Afifi et al. (2014), and according to their experimental results, GFRP and CFRP RC columns behaved similarly to steel RC columns and exhibited linear load-strain behavior up to 85% of their peak loads. These studies, however, did not specifically investigate the confinement effect in pile members, but pure axially loaded columns, a scenario that would realistically be experienced in these structures.

While different in application, these studies still prove useful to understand CFRP's confining effects as these two structural members act quite similarly. Mander et al. (1988) demonstrated that adequate confinement of a column's concrete core through transverse reinforcement enhances both strength and ductility thereby changing the material behavior significantly. As axial concrete strain develops under pure axial loading, the confining stress offered by FRP transverse reinforcement increases with concrete expansion until the FRP ruptures. This is due to the material's brittle characteristics, whereas the lateral confining stress given by conventional steel reinforcement remains virtually unchanged or increases marginally with concrete expansion after the steel has yielded, an idea that was touched upon in technical memo #1. However, confining concrete cores with transverse CFRP stirrups is a passive approach to increasing overall concrete strength and ductility. It has been observed that at low levels of axial strain, the confinement developed from transverse reinforcement is negligible as the

transverse strain is also negligible. For CFRP-confined concrete columns, as axial strain increases under some loading, passive confinement begins to play a significant role because confining stresses continue to increase as concrete expands due to the linear elastic properties of CFRP.

Afifi et al. (2014) proposed a modified Mander et al. (1988) confinement model for CFRP-RC concrete columns with modifications based on experimental findings and semi-empirical formulations. This equation illustrates the nonlinear relationship between the increase in concrete strength and the confinement ratio f'_1/f'_{co} , where f'_1 is the effective lateral confining pressure due to FRP stirrups. Afifi et al. (2014) results indicated that lateral FRP confinement was less effective at higher levels of confining pressure.

In a recently published article, Seliem et al. (2016) investigated the effectiveness of CFRP grid transverse reinforcement using pull-out specimen tests, and flexure testing a full-scale prestressed pile. In this CFRP grid configuration, testing results suggest using an embedment length of twice the grid spacing so that the CFRP can realize its full tensile strength. The same results also suggest that, except for short strands, the presence of transverse strands did not have significant impact on behavior. In Seliem's second test, results indicated that the CFRP grid was able to achieve the required confinement currently provided by steel spirals of equivalent size, and that full use of grid material was observed when inspecting the members upon failure, further illustrating its effectiveness. The capacity of piles reinforced by CFRP grid (and less prestressing force) was larger than that of control pile (reinforced with conventional prestressed steel). This slight increase in capacity can, according to Seliem et al. (2016), be attributed to enhanced confinement offered by the CFRP grid. Lastly, the use of grid reinforcement slightly increases flexural stiffness of prestressed pile due to presence of these longitudinal strands.

2.12 External FRP Stay-in-Place Forms and Jackets

CFRP-reinforced piles, it should be noted, can be maintained and reinforced as easily as any previous prestressed pile before, and therefore should not require additional resources from the Agency other than what is normally required. Confinement action exerted by the CFRP on the concrete core is of the passive type, and as previously stated, arises from lateral expansion of concrete under axial load. As axial stresses increase, corresponding lateral strains increases and the confining device develops a tensile hoop stress balanced by a uniform radial pressure which reacts against the concrete lateral expansion (ACI 440). When an FRP confined cylinder is subject to axial compression, the concrete expands laterally and this expansion is restrained by the FRP. Typical failure modes of CFRP jacket-confined columns are most often CFRP sheet fracture at the mid-height of the column followed by fracturing of lateral reinforcement and buckling of the longitudinal reinforcement. The amount of FRP layers present as well as their fiber orientation also heavily affect the overall ductility (if at any), confinement effectiveness, and ultimate load bearing capacity. Tests performed in the lab have indicated that FRP composite jackets can enhance the performance of eccentrically loaded concrete piers about 15% in terms of strength but especially in terms of ductility. The observed strength improvement was more relevant in the case of specimens loaded with smaller eccentricity, while the ductility improvement was more relevant in the case of bigger eccentricity.

As the number of layers of external FRP confinement increases, there is a diminished rate of returns on ductility and overall bearing capacity, yet a significant increase in stiffness can continue to occur (Issa et al. 2009). It was also noted that in that study, as column diameter increased, confinement effectiveness decreased.

2.13 Drivability of CFRP-Prestressed Concrete Piles

Of significant concern in this feasibility study was the capability of CFRP-reinforcement to withstand being driven into the earth without loss to its structural performance.

In one full-scale test, a GFRP-reinforced pile was successfully driven 25 feet into dense sands by a drop hammer with drop height of 6 feet (Sen et al. 1992) without significant impacts to structural capacity of the reinforcing tendons. While not the product of interest in this focus, GFRP is equally weak to mechanical abrasion, allowing this study to exemplify the feasibility of this type of reinforcement. In a series of tests involving CFRP, 25-foot-long piles were also driven into soil by a diesel hammer with a 6 foot drop height. No concrete spalling or damage of any kind was observed by the investigating team (who had aimed to simulate driving stresses employed by FDOT). From these results, the original prediction of the validity of the use of wave equation analysis was justified as its findings were in general agreement with the experimental data and therefore applicable to CFRP reinforcement (Arockiasamy and Amer 1998).

In a different FDOT investigation, along with the testing of numerous piles in a lab environment, two 100-ft long CFRP-prestressed concrete piles were driven at a bridge construction site adjacent to conventional steel-prestressed piles. From inspection, it was found that pile heads were locally damaged leading to concrete spalling. This was likely due to the intentional use of thin cushions and hard driving. Other than this minor damage to the pile heads, engineers recorded no damage to the integrity of the system. As noted by the research team, the pile's designed resistances were greater than the 900-kip suggested driving force as per FDOT's Structures Design Guidelines. This information was gathered employing both embedded data collectors (EDC) and pile driving analyzer (PDA) software (Roddenberry et al. 2014).

Chapter 3: Comparative Analysis

3.1 Mechanical Behavioral Comparison for Steel and CFRP

To better understand the relationship between conventional steel prestressing and prestressed FRP, it is necessary to look at their mechanical properties over the course of their use. Since CFRP exhibits a tensile strength equal or more than that of steel strands due to its unidirectional orientation of carbon fibers (Han et al. 2002, Enomoto et al. 2011), high corrosion resistance in harsh chemical environments (Rizkalla et al. 2003, El-Salakawy 2003, Afifi et al. 2014), and a tensile modulus typically from 39160-74984 ksi (Roddenberry et al. 2014), it is therefore well-positioned to be used for pile reinforcement. The stress-strain relationship of CFRP is compared to that of mild steel and prestressing steel, among other FRP's, can be seen in Figure 15, below.

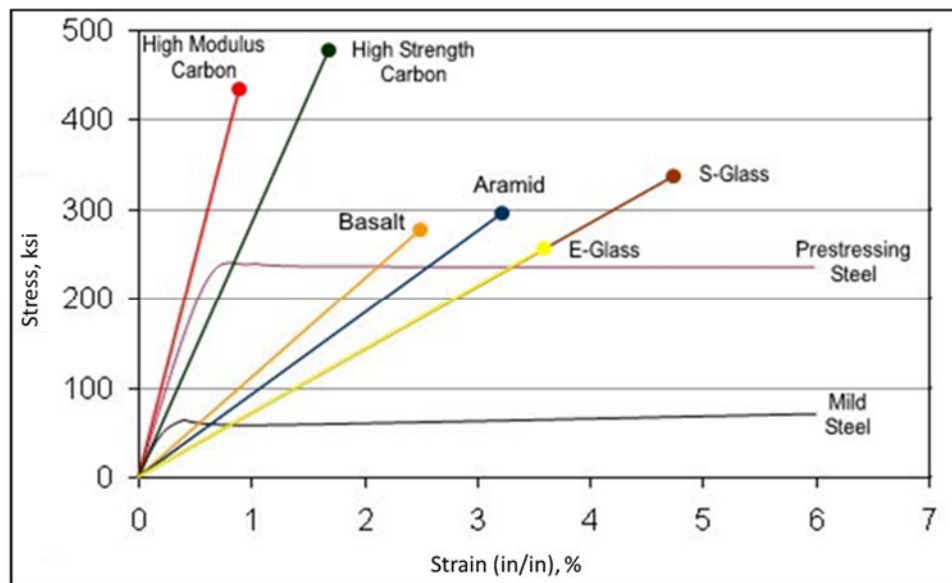


Figure 15. Stress-Strain Curves of CFRP and Steel.

As the material properties of CFRP do much to credit the adoption of this technology, it must then however, become a matter of economic judgement if the adoption of this material stands to benefit the Agency. As this specific cost analysis question will be addressed later in this Chapter, the task of equating these two materials into similar frames of reference will be done here.

In this portion of the discussion, work was done to quantify such material comparisons in the form of ultimate loadings these materials can sustain. Over the course of the following Chapter, materials will be presented side-by-side, employing the same reinforcement pattern, equivalent reinforcement ratios, and equivalent prestressed members. What became of this method was the eventual inclination to replace each prestressed steel strand one-for-one for prestressed CFRP strands. As previously stated, CFRP exhibits far more tensile strength than conventional prestressed steel and it was thought that in order to illustrate equivalent capacities, less CFRP strands would need to be employed. When FRP reinforcement is employed in non-prestressed concrete structures, designs are typically limited by serviceability requirements (ISIS). To ensure sufficient flexural stiffness for deflection control, a higher reinforcement ratio paired with a larger depth in member must be used. The advantages of high tensile strength by FRP's material properties are thereby only partially used. A more efficient use of the material in reinforcement can therefore be realized in prestressing applications.

Moving forward from this decision, prestressed piles using either steel or CFRP as reinforcement were modeled and developed into interaction diagrams to better facilitate comparison among different reinforcements. This was done parametrically in order to better illustrate a range of scenarios of reinforcement ratio and concrete compressive strengths that highlights the significant difference in performance between cracking moments and the capacity gained.

3.2 Development of P-M Interaction Diagrams for (i) Steel and (ii) CFRP

To formulate these mechanical properties, widely accepted and well-validated analysis approaches were used to develop axial load-bending moment interaction diagrams for steel and CFRP-prestressed concrete piles. These methods were taken directly from ACI and numerous other publications and are straight-forward and well-used means of analysis, namely, strain compatibility and force equilibrium. Design philosophy is rooted in the assumption that plane sections before bending remain plane, and after bending, lead to this linear strain distribution along the cross section. The concrete is subjected to strains only in the axial direction and the strain distribution in the concrete varies linearly over the depth of the cross section.

This allows for a fundamental comparative study, solely relying on the geometry of the pile's cross section in question, and inputting iterated values of f'_c and ρ as well as the various material properties of the reinforcement. The interaction diagram for a reinforced concrete section is given by the outer-most concrete fiber in compression reaching its ultimate strain while the outer-most steel layer in tension may or may not reach yield stress. The portion of the interaction diagram where steel in the outer-most tension layer is still in its elastic range is termed the compression controlled region, whereas the tension controlled region indicates where steel has yielded. At the meeting of the two portions of the interaction diagram is the balance point, defined as the outer-most concrete fiber reaching its ultimate in compression and the outer-most steel layer reaching the yielding strain concurrently.

For the purposes of the analysis, two reinforcement scenarios were considered: prestressed concrete (PC), and prestressed CFRP (FRP PC). The spreadsheet used to generate the interaction diagrams was first developed around RC and was later expanded to encompass the PC and FRP-PC by taking prestressing forces into account, namely the internal force inherent in each member before loading occurs during fabrication.

In Figure 16, the exact specifications laid forth by TxDOT Bridge Division were replicated in the construction of prestressed piles. As stated previously, this cross section remained the same throughout the course of each reinforcement scenario. This is to offer the most straight-forward comparison between the two materials, and might afford the Agency a more expedited path to CFRP's adoption if design standards can remain relatively unchanged. If design engineers can use familiar reinforcement patterns at equivalent strength values, CFRP might become that easier to implement upon its acceptance by TxDOT.

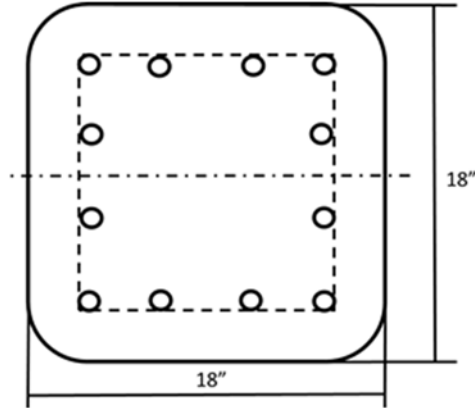


Figure 16. Standard Section for Prestressed 18'' x 18'' pile, adapted from TxDOT Bridge Division Specification.

The interaction diagram of a prestressed-column, either steel or CFRP, is comprised by the summation of forces of its constituents- the concrete section and the prestressing strands embedded within. The contribution of individual components can be computed separately and combined together to realize the entire sections capabilities.

For illustrative purposes, a standard 18 x 18-inch pile was considered for various reinforcement scenarios and reinforced according to current TxDOT specifications, as can be seen in Figure 16. Strands were located symmetrically about the axis of bending of the pile with no more than one strand difference between any two adjacent sides, as per specification callouts. With this in mind, the pile was designed with four layers of reinforcement, a clear-cover (cc) of 2.5 inches, and a 1 inch corner radius. To satisfy these requirements, the depths of reinforcement locations are given below:

$$d_1 = cc \quad (1)$$

$$d_2 = d_1 + \frac{(h-2(cc))}{3} \quad (2)$$

$$d_3 = d + \frac{2(h-2(cc))}{3} \quad (3)$$

$$d_4 = h - cc \quad (4)$$

Here, (d) represents the depth of the reinforcing member from the top of the cross section, (cc) represents the clear cover, and (h), the height of the cross section. With these dimensions in place, the strain compatibility was iterated along the depth of the member, incorporating geometric representations of prestressing and its effects on reinforcement strands. Using equilibrium conditions, the axial capacity for the cross section can be determined by summing all tension and compression values in the member. Employing parabolic stress-strain relationship for the concrete as described in Collins and Mitchell (1991), the following equations can be used when iteration of $f'c$ was factored into the generation of interaction diagrams.

$$\alpha\beta = \frac{\varepsilon_{cc}}{\varepsilon_{co}} - \frac{1}{3} \left(\frac{\varepsilon_{cc}}{\varepsilon_{co}} \right)^2 \quad (5)$$

$$(\alpha\beta) \left(1 - \frac{1}{2} \beta \right) = \frac{2}{3} \left(\frac{\varepsilon_{cc}}{\varepsilon_{co}} \right) - \frac{1}{4} \left(\frac{\varepsilon_{cc}}{\varepsilon_{co}} \right)^2 \quad (6)$$

The values generated by these relationships are derived entirely from the geometry of the stress-strain relationship of the concrete substrate, values of which can be found in Table 4, below. In this

equation, the relationship of the stress-strain diagram constitutes the relationship of α and β stress block factors. For these parametric studies, various values of f'_c were used to better characterize the mechanical properties at play within these cross-sections. For the 18" x 18" pile cross section, a typical f'_c value of 5,000 psi was selected. As can be seen below, the ϵ_{cc} value was taken to be 0.00203.

Table 4. Various Material Properties of Differing Concrete Strengths, adapted from Collins and Mitchell 1991.

f_c (psi)	3000	3500	4000	5000	6000	8000	10000	12000	16000
(Mpa)	20.7	24.1	27.6	34.5	41.4	55.2	69	82.7	110.3
E_c (ksi)	3191	3366	3530	3828	4098	4578	5000	5382	6060
(Mpa)	22000	23200	24300	26400	28300	31600	34500	37100	41800
ϵ_{co}	0.00188	0.00191	0.00194	0.00203	0.00213	0.00233	0.00253	0.00271	0.00307
n	2	2.2	2.4	2.8	3.2	4	4.8	5.6	7.2
k	1	1.06	1.11	1.23	1.34	1.56	1.78	2	2.45

For parabolic stress-strain relationships, a simple Table has been developed to tabulate the values of α and β from the $\epsilon_{cc}/\epsilon_{co}$ ratio, pictured below.

Table 5. Stress-Block Factors for Parabolic Stress-Strain Curves, adapted from Collins and Mitchell 1991.

$\epsilon_{cc}/\epsilon_{co}$	0.25	0.5	0.75	1	1.25	1.5	1.75	2
α	0.336	0.595	0.779	0.888	0.928	0.9	0.81	0.667
β	0.682	0.7	0.722	0.75	0.786	0.833	0.9	1

For less-parabolic relationships, interpolation of the following tabulated values is required to accurately develop α and β as the concrete strength was iterated from values in Table 6.

Table 6. Stress-Block Factors for Non-Parabolic Stress-Strain Relationships, adapted from Collins and Mitchell 1991.

f_c (psi)		$\epsilon_{cc}/\epsilon_{co}$							
		0.25	0.5	0.75	1	1.25	1.5	1.75	2
3000	α	0.359	0.641	0.818	0.91	0.945	0.947	0.93	0.904
	β	0.675	0.697	0.727	0.762	0.796	0.83	0.861	0.89
20.7	α	0.335	0.614	0.801	0.902	0.937	0.929	0.899	0.859
	β	0.672	0.689	0.717	0.75	0.788	0.827	0.864	0.9
3500	α	0.316	0.591	0.787	0.895	0.929	0.911	0.869	0.817
	β	0.67	0.684	0.709	0.741	0.781	0.825	0.869	0.911
27.6	α	0.29	0.556	0.762	0.884	0.912	0.871	0.801	0.724
	β	0.668	0.677	0.691	0.728	0.772	0.827	0.886	0.943
5000	α	0.272	0.53	0.742	0.874	0.896	0.83	0.735	0.641
	β	0.667	0.673	0.689	0.717	0.767	0.834	0.908	0.98
34.5	α	0.25	0.495	0.712	0.859	0.863	0.744	0.61	0.501
	β	0.667	0.669	0.679	0.704	0.763	0.859	0.963	1.061
6000	α	0.237	0.472	0.689	0.847	0.826	0.659	0.511	0.408
	β	0.667	0.668	0.674	0.695	0.767	0.893	1.022	1.132
41.4	α	0.228	0.456	0.672	0.838	0.786	0.585	0.441	0.35
	β	0.667	0.667	0.672	0.689	0.776	0.93	1.071	1.184
8000	α	0.218	0.435	0.648	0.824	0.702	0.484	0.363	0.29
	β	0.667	0.667	0.669	0.682	0.804	0.99	1.134	1.242
55.2	α								
	β								
10000	α								
	β								
69	α								
	β								
12000	α								
	β								
82.7	α								
	β								
16000	α								
	β								
110.3	α								
	β								

After the relevant α and β values have been determined for each iteration of 'c', equilibrium can be taken along the member cross section to determine the overall axial capacity. To generate the P-M diagram, locations of neutral axis to obtain the overall capacity of the cross-section were assumed.

3.2.1 Prestressed Steel

PC with Steel- Ultimate Moment Behavior

In order to better compare the various mechanical characteristics of these different types of prestressing reinforcement, some effort was given to offer similar-capacity interaction diagrams. The difference in the non-dimensional interaction diagram between conventional RC and prestressed concrete (PC) lies in the difference of strand diameter and the prestressing force applied to this. The same 18 x 18-inch cross section will be used to develop these relationships and the diameter of the reinforcing strand adheres to TxDOT specifications.

To begin the analysis, strain compatibility will be employed to describe the linear relationships between the different layers of reinforcement: ($d_{ps,i}$) refers to the depth of the strand layer i , (ϵ_{ce}) refers to the uniform strain in concrete brought on by prestressing, (c') represents the iterated depth of the neutral axis, (c) represents the actual depth of the neutral axis when the added strain in the concrete is considered, (ϵ_{cu}) refers to the ultimate concrete strain, ($\Delta\epsilon_{ps,i}$) represents the change in strain at layer i , (C_c) the contribution of concrete in compression, and finally ($F_{ps,i}$) the force in strand layer i .

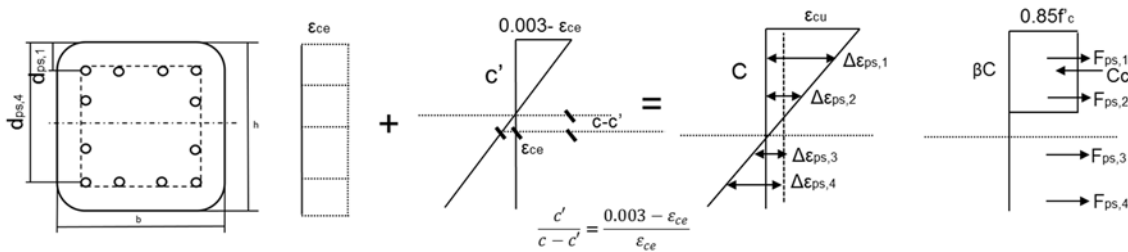


Figure 17. Strains and forces found in cross section due to prestressing.

As the interaction diagram is comprised of the strengths of its individual constituents, the concrete and prestressing reinforcement, the concrete compression force and its subsequent moment contribution equations are displayed below:

$$C_c = 0.85f'_c b(\beta c) \quad (7)$$

and

$$M_c = C_c(h/2 - \beta c/2) \quad (8)$$

Concrete's contribution to the interaction diagram does not change from that of RC, but what differs significantly however, is the inherent force within each prestressed member. As 0.5-inch diameter low relaxation strands with 270 ksi ultimate strength are implemented in this design, there will be a force present at each level of reinforcement before the application of load. The initial strain, a negative tensile value, in the prestressing strands can be found using the equation below:

$$\epsilon_{psi} = \frac{f_{pj}}{E_{ps}} \quad (9)$$

Where (ϵ_{psi}) is the corresponding initial strain in reinforcement utilizing Hooke's Law for linear-elastic stress-strain relationships.; (E_{ps}) is the Young's modulus of the prestressed steel, and (f_{pj})

represents the jacking prestress, shown below. Next, the strain from initial prestressing within concrete is found by the equation below.

$$\varepsilon_{ce} = \frac{A_{ps}f_{pj}}{(A_g - A_{ps})E_c} \quad (10)$$

Where (ε_{ce}) is the uniform strain in concrete; (A_{ps}) is the total area of prestressing strands; (A_g) is the gross area of the cross-section; (f_{pj}) is the jacking prestress, (E_c) is the Young's modulus of concrete.

Next, the strain change in the prestressing strands at layer i can be computed when the neutral axis is determined and using triangular strain compatibility, as can be seen in the following equation, below.

$$\Delta\varepsilon_{ps,i} = \varepsilon_{cu} \left(\frac{c' - d_{ps,i}}{c'} \right) + \varepsilon_{ce} \quad (11)$$

Here, (ε_{cu}) is the ultimate strain in concrete, and ($d_{ps,i}$) the location of the reinforcement layer. Next, the following equation illustrates the effective strain realized in each layer of reinforcement i , combining initial prestress and its change over loading, shown below:

$$\varepsilon_{ps,i} = \varepsilon_{psi} + \Delta\varepsilon_{ps,i}, \quad \varepsilon_{ps,i} < \varepsilon_{py} \quad (12)$$

else

$$\varepsilon_{ps,i} = \varepsilon_{py}$$

Where the initial strain is added to the strain change from loading ($\Delta\varepsilon_{ps,i}$). It should be noted that $\varepsilon_{ps,i}$ should be constrained to the stress-strain diagram for prestressing steel, transitioning from its linear elastic phase to its plateau yield strain up until strand rupture. This is noticeably different from the approach for CFRP, which will be addressed in the subsequent section.

From these relationships, solely based on the geometry of the reinforcement pattern, the force being developed in each strand was calculated. The equations used to quantify the forces are provided below. In the calculation of axial and bending capacity, tension was taken as negative and compression as positive. For the purposes of obtaining the ultimate axial and bending envelope, it is assumed the top concrete strain of the member reaches maximum at 0.003. What does change, however, is the proportion of force in each reinforcement layer, either a positive (compression) force, or a negative (tensile) one.

$$F_{ps,i} = A_{ps,i} E_{ps} \varepsilon_{ps,i} \quad (13)$$

Where ($F_{ps,i}$) is the axial force from prestressing strands in each layer i , ($\varepsilon_{ps,i}$) is the strain in the strand at layer, and ($A_{ps,i}$), the area of prestressing at each layer of reinforcement. These values can then be multiplied by their relative distance from the neutral axis of the pile cross section to determine a summation of moments. From this point, the magnitude of forces developed in each layer of reinforcement can be discerned for every iteration of the depth of neutral axis. This can be seen in the equation, below.

$$M_{ps,i} = F_{ps,i} \left(\frac{h}{2} - d_{ps,i} \right) \quad (14)$$

Where ($M_{ps,i}$) is the moment from prestressing strands at layer i , and ($d_{ps,i}$) the distance from the outermost compression side to the center of strand at the current layer. The resultant axial force and bending moment of the pile cross section are simply the summation of forces of the concrete contribution and that of the prestressing steel:

$$P = C_c + \sum_{i=1}^n F_{ps,i} \quad (15)$$

and

$$M = C_c \left(\frac{h}{2} - \beta \frac{c}{2} \right) + \sum_{i=1}^n F_{ps,i} \left(\frac{h}{2} - d_{ps,i} \right) \quad (16)$$

From this point, a non-dimensionalized interaction diagram for the ultimate capacity can be generated by graphing pairs of axial and bending capacities as 'c' is iterated along the depth of the cross section. The equations used to develop the interaction diagram for prestressed steel can be directly transferable to use in prestressed-CFRP.

The first quantity that was illustrated was how the profile of the ultimate capacity would alter as the compressive strength of concrete was iterated. The resulting P-M interaction diagram can be seen below in Figure 18.

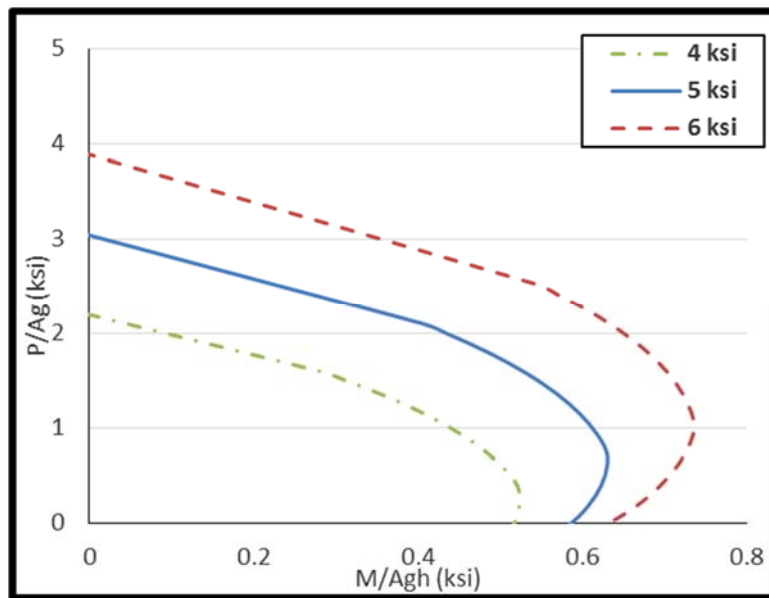


Figure 18. Influence of f'_c iteration on strength interactions; $f_{ru}=270$ ksi, $f_{re}=230$ ksi, $E_{ps}=29,000$ ksi, $A_{ps}=2.26\text{in}^2$.

The axial capacity of the PC pile increases proportionally with an increase in f'_c . As all curves in Figure 18 are created with the same reinforcement ratio and pattern, this implies that the cross-sectional member is not fully developed in lower values of f'_c . It is from Figure 18, the 6 ksi concrete offers the most complete view of the effects of prestressing. Increasing from 4 ksi to 6 ksi concrete strength, the bending moment capacity was increased 28%, a noticeable increase in bending capacity.

Figure 19 illustrates the iterative changing of the reinforcement ratio, ρ . this curve represents a diminished rate of returns when the more prestressing is used in a member if an increase in axial load resisting capacity is desired.

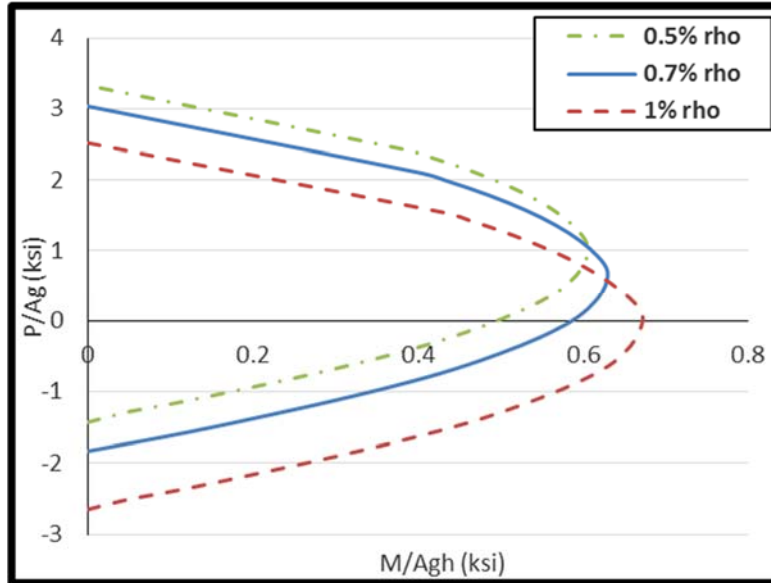


Figure 19. Influence of reinforcement ratio iteration on strength interactions; $f_{tu} = 270$ ksi, $f_{fe} = 230$ ksi, $E_{ps} = 29,000$ ksi.

As can be seen from the above Figure, concrete strength was kept uniform at 5 ksi throughout the three scenarios and the reinforcement ratio was increased slightly from case to case. Unlike conventional RC, strands used in PC are significantly smaller in diameter. While increasing the reinforcement ratio by around 0.25% there was a noticeable reduction in all P-M curves where axial and bending moments both interacted on the member and a significant increase in moment capacity. At higher levels of reinforcement ratio, the member could simply not withstand greater amounts of prestressing and its capacity waned in combined axial and bending moment configurations.

3.2.2 Prestressed CFRP

PC with CFRP- Ultimate Moment Behavior

To begin the analysis for a prestressed CFRP cross section, a similar strain compatibility figure is provided to illustrate nomenclature. As before, the linear relationships between the different layers of reinforcement ($dp_{f,i}$) refers to the depth of the CFRP strand layer i , (ϵ_{ce}) refers to the uniform strain in concrete brought on by prestressing, (cl) represents the iterated depth of the neutral-axis, (c) represents the actual depth of the neutral-axis when the added strain in the concrete is considered, (ϵ_{cu}) refers to the ultimate concrete strain, ($\Delta\epsilon_{pf,i}$) represents the change in strain at CFRP layer i , (C_c) the contribution of concrete in compression, and finally ($F_{pf,i}$) the force in strand layer i .

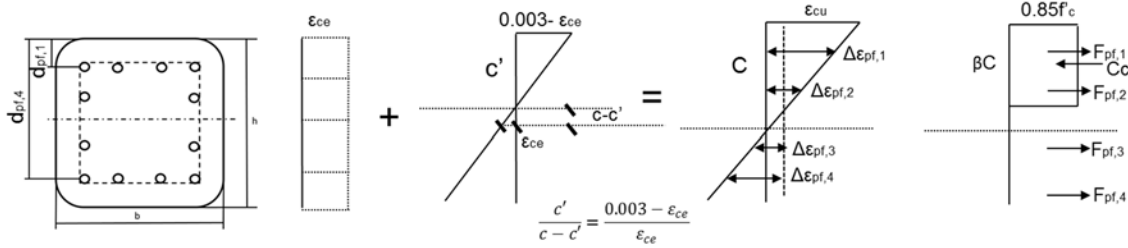


Figure 20. Strains and forces found in cross section due to prestressing.

As before, in calculating the relevant values found in the interaction diagram, the strengths of its individual constituents, the concrete and prestressing reinforcement are found separately. The concrete compression force and its subsequent moment contribution equations are displayed below, identical to the equations provided in the prestressed steel section.

$$C_c = 0.85f'_c b(\beta c) \quad (17)$$

and

$$M_c = C_c(h/2 - \beta c/2) \quad (18)$$

Concrete's contribution to the interaction diagram does not change from that of steel PC, and considerations for the initial force within each prestressed member are found below. As 0.5-inch diameter low relaxation strands with 360 ksi ultimate strength are implemented in portions in design, there will be a force present at each level of reinforcement before the application of load. The initial strain, a negative tensile value, in the prestressing strands can be found using the equation below:

$$\epsilon_{pfi} = \frac{f_{pj}}{E_{pf}} \quad (19)$$

Where (ϵ_{pfi}) is the corresponding initial strain in reinforcement utilizing Hooke's Law for linear-elastic stress-strain relationships; (E_{pf}) is the Young's modulus of the prestressed CFRP strands, and (f_{pj}) represents the jacking prestress, shown below. In the analysis, typical construction practices are followed, utilizing steel strands that are typically stressed to 85% of their yield stress. Allowable stresses propagating in CFRP strands are typically limited to 40 to 65% of their ultimate strength due to stress-rupture limitations (Hamilton and Dolan 2000). This is due to the brittle nature of the material, and the reduction of prestressing force is done in an effort to avoid this region. This lower range actually corresponds to strains between 1.5 to 2.5 times the typical prestressing strains used in steel tendons (ISIS). As opposed to continuing the inclusion of yielded prestressing strands to the ultimate capacity, it is assumed that CFRP strands rupture and discontinue their overall contribution. Therefore the calculation to develop the combined strain in each layer of reinforcement is modified slightly to account for this. Next, the strain from initial prestressing within concrete is found by the equation below.

$$\epsilon_{ce} = \frac{A_{pf}f_{pj}}{(A_g - A_{pf})E_c} \quad (20)$$

Where (ϵ_{ce}) is the uniform strain in concrete; (A_{pf}) is the total area of prestressing strands; (A_g) is the gross area of the cross-section; (f_j) is the jacking prestress, (E_c) is the Young's modulus of concrete. Next, the strain change in the prestressing strands at layer i can be computed when the neutral axis is determined and using triangular strain compatibility, as can be seen in the following equation, below.

$$\Delta\varepsilon_{pf,i} = \varepsilon_{cu} \left(\frac{c' - d_{pf,i}}{c'} \right) + \varepsilon_{ce} \quad (21)$$

Here, (ε_{cu}) is the ultimate strain in concrete, and ($d_{pf,i}$) the location of the reinforcement layer. Next, the following equation illustrates the effective strain realized in each layer of reinforcement i , combining initial prestress and its change over loading, shown below:

$$\varepsilon_{pf,i} = \varepsilon_{pfi} + \Delta\varepsilon_{pf,i} , \varepsilon_{pf,i} < \varepsilon_{pfi} \quad (22)$$

else

$$\varepsilon_{ps,i} = 0 \text{ as strand has ruptured}$$

Where the initial strain is added to the strain change from loading ($\Delta\varepsilon_{pf,i}$). It should be noted that $\varepsilon_{pf,i}$ should be constrained to the stress-strain diagram for prestressing CFRP, as the material express no yielding capacity. Unlike prestressing steel that experiences a yield plateau, CFRP simply ruptures and is no longer considered contributing to capacity. Balanced strain conditions for prestressed CFRP cross sections exist at a point when the reinforcement reaches its ultimate strain in tension, ε_{pfi} , just as the concrete in compression attains a maximum usable strain at ε_{cu} . At this point, the member will fail suddenly and without any indication as the strands rupture instead of reach yielding strains as in prestressed steel. This leads to the CFRP balance ratio to being an indicator of failure as opposed to any assurance of ductility. Rather than avoid compression failure, which occurs when the reinforcement ratio is greater than the balanced ratio, it should be encouraged in prestressed-CFRP applications. The failure mode is less violent and is similar to that of an over-reinforced concrete beam with internal steel reinforcement.

To counteract catastrophic brittle failure in these piles, it appears that concrete columns with prestressed CFRP can be safeguarded by providing a reinforcement ratio larger than a minimum ratio. ACI 318 limits of 1% on reinforcement ratios set for steel-reinforced concrete columns would therefore not be adequate for prestressed CFRP pile. On the other side of the argument, the maximum limit of 8% remains applicable as it is instituted to prevent rebar congestion during fabrication, a constructability issue.

Returning to finding internal forces from these geometric relationships, the force being developed in each strand was calculated. The equations used to quantify the forces are provided below. In the calculation of axial and bending capacity, tension was taken as negative and compression as positive. For the purposes of obtaining the ultimate axial and bending envelope, it is assumed the top concrete strain of the member reaches maximum at 0.003. What does change, however, is the proportion of force in each reinforcement layer, either a positive (compression) force, or a negative (tensile) one.

$$F_{pf,i} = A_{pf,i} E_{pf} \varepsilon_{pf,i} \quad (23)$$

Where ($F_{pf,i}$) is the axial force from prestressing strands in each layer i , ($\varepsilon_{pf,i}$) is the strain in the strand at layer, and ($A_{pf,i}$), the area of prestressing at each layer of reinforcement. These values can then be multiplied by their relative distance from the neutral axis of the pile cross section to determine a summation of moments. From this point, the magnitude of forces developed in each layer of reinforcement can be discerned for every iteration of the depth of neutral axis. This can be seen in the equation, below.

$$M_{pf,i} = F_{pf,i} (h/2 - d_{pf,i}) \quad (24)$$

Where $(M_{pf,i})$ is the moment from prestressing strands at layer i , and $(d_{pf,i})$ the distance from the outermost compression side to the center of strand at the current layer.

The resultant axial force and bending moment of the pile cross section are simply the summation of forces of the concrete contribution and that of the prestressing CFRP:

$$P = C_c + \sum_{i=1}^n F_{pf,i} \quad (25)$$

and

$$M = C_c \left(\frac{h}{2} - \beta \frac{c}{2} \right) + \sum_{i=1}^n F_{pf,i} \left(\frac{h}{2} - d_{pf,i} \right) \quad (26)$$

From this point, a non-dimensionalized interaction diagram for the ultimate capacity can be generated by graphing pairs of axial and bending capacities as 'c' is iterated along the depth of the cross section. The following Figures 21 and 22 illustrate similar parametric studies as the PC curves have shown previously. The first Figure offers a glimpse of differing f'_c values, and the latter highlights a change of reinforcement ratios.

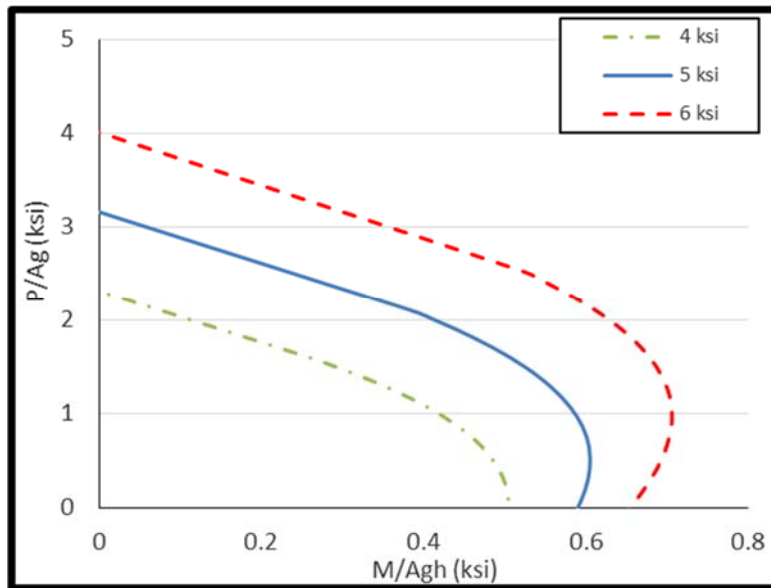


Figure 21. Influence of f'_c iteration on strength interactions; $f_{tu}=360$ ksi, $f_{re}=216$ ksi, $E_{pf}=20,000$ ksi, $A_{pf}=2.26$ in².

As can be seen in the Figure 21, and similar-to the curves generated with PC, at low levels of concrete compressive strength member capacity is eclipsed by the amount of prestressing force present in the CFRP strands. The maximum moment capable lies close to the x-axis, and the 6 ksi curve in its transition from axial and bending influence to pure axial loading appears more developed. As was illustrated in the PC diagrams, the higher the compressive strength of the concrete, the greater capacity the cross section has to withstand the prestressing forces and exhibit a higher overall capacity. The inclusion of greater strength concrete resulted in increase in axial load strength and moment resistance, similar to the behavior that has been observed for prestressed steel tendons.

Typical prestressed steel concrete cross sections with steel strands will deform elastically until cracking, and then the rate of deflection will progressively increase as the reinforcements yield until failure occurs by concrete crushing or strand rupture. FRP prestressed cross sections will deform elastically until cracking, then continue to deform in a linear manner under increasing load until the ruptures or the

ultimate concrete compression strain is exceeded. Parametric reinforcement ratios iterated within the cross section for CFRP strands are shown below in Figure 22.

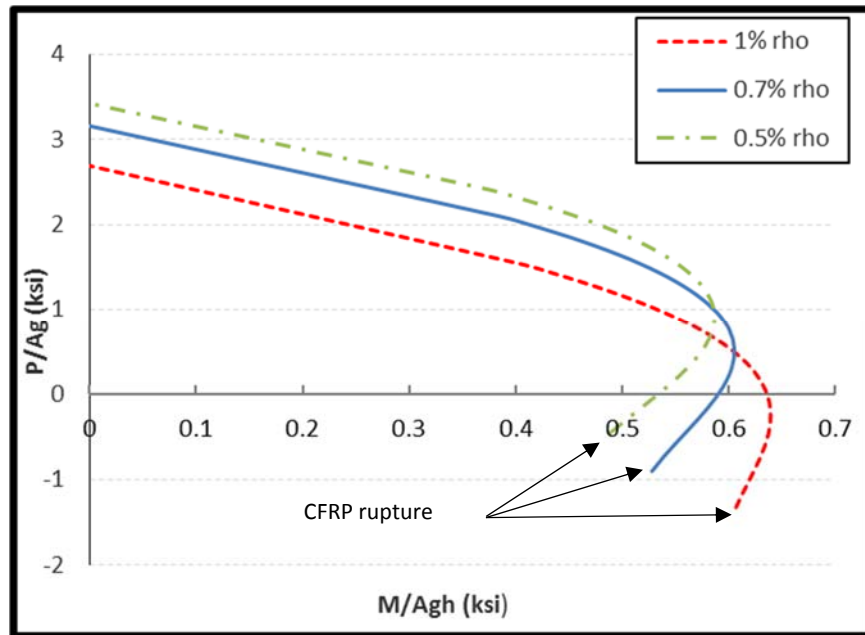


Figure 22. Influence of reinforcement ratio iteration on strength interactions; $f_{fu} = 360$ ksi, $f_{fe} = 216$ ksi, $E_{pf} = 20,000$ ksi.

Figure 22 shows a similar trend as the equivalent figure for PC in that as the reinforcement ratio increases from 0.5% to 0.1%, the axial and bending interaction portion of the diagram is lessened as well as the axial resistance. As CFRP has an even higher tensile capacity than steel, even less reinforcement is needed for an equivalent capacity. This was addressed earlier in the document, stating the need to keep the reinforcing patterns identical so as to compare these materials on a one-to-one basis.

As is evidenced in the Figures above, regardless of the type of strands used, the increase in reinforcement ratio used in concrete cross sections led to an increase in bending moment capacity and a reduction in combined strength interaction. This is consistently true since reinforcements in concrete columns are the primary contributor of tensile strength, and hence the increase in this quantity would lead to increase in bending resistance. Initial prestressing was introduced to concrete columns, and in addition to the gain in bending resistance some amount of axial compression strength was sacrificed. This apparently can be beneficial for columns subjected to bending, but would be restrictive during the service life of piles structures. In some cases, the introduction of prestressing forces may significantly diminish the overall strength.

The following Figure 23 illustrates a comparative ultimate capacity between PC and FRP PC with equivalent capacities, but dissimilar reinforcement ratios.

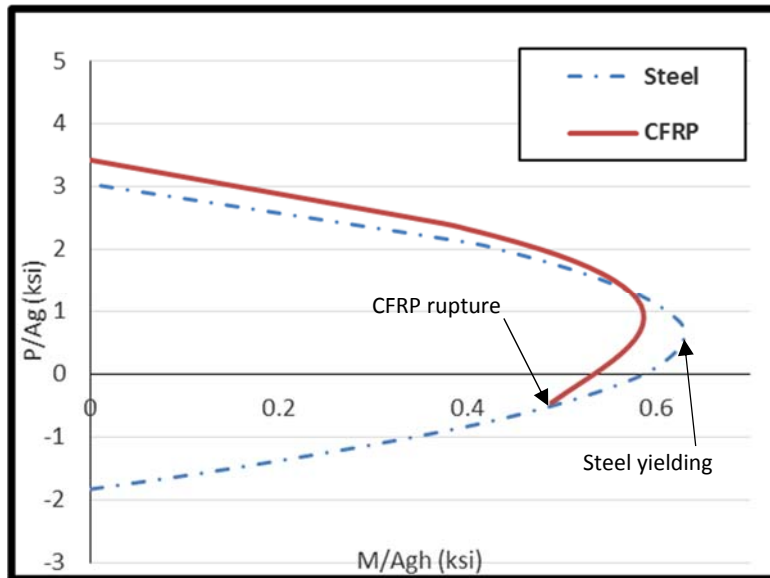


Figure 23. Non-Dimensionalized P-M Diagram of Equivalent PC & FRP PC Section, 5 ksi $f'c$. (Steel: 270 ksi, $f_{fe} = 230$ ksi, $E_{ps} = 29,000$ ksi; CFRP: 360 ksi, $f_{fe} = 216$ ksi, $E_{fs} = 20,000$ ksi).

Due to this diminished rate of returns apparent in both PC and CFRP Figures (due to over-prestressing the section), there appears an idealized P-M diagram curve. A 0.53% reinforcement ratio for prestressed CFRP comes closest in capacity to 0.7% for prestressed steel. As can be seen in Figure 23, for an equivalent display of sectional capacity, design engineers may incorporate more steel to achieve similar behavior in bending moment capacity in CFRP-prestressed piles. Namely, in this configuration, steel expresses greater bending moment while CFRP has a larger axial capacity by 13%. This number, when no longer normalized in the P-M diagram, equates to $\frac{1}{2}$ " diameter steel strand and a 0.41-inch 7-wire CFCC strand. As can be seen in Figure 23, for an equivalent display of sectional capacity, design engineers need to incorporate more steel to achieve similar behavior in axial capacity and slightly increased bending moment capacity compared to CFRP-prestressed piles.

In the analysis of previously published literature, the Florida Department of Transportation led a study that aimed to fabricate several full-scale CFRP-reinforced prestressed piles and drive them with typical hammering forces. FDOT's feasibility study thoroughly outlined the many different stages of construction and special considerations that were made in the implementation of CFRP. One of these considerations was the diminished amount of prestressing force used in the pile, notably changing from 75 to 65% of the ultimate capacity of the reinforcement. This reduction was perhaps due in part to the enormous difference in ultimate strengths of the two materials, a 270 ksi ultimate strength versus a 360 ksi, and to avoid the effects of brittle strand failure. This leads to the argument that in order to achieve equivalent capacities, 25% less CFRP reinforcement need to be used. This was foregone however in favor of one-for-one replacement for a more direct comparison, but ultimately also included in the cost analysis portion at the conclusion of this Chapter. In additional publications, it was found that CFRP and steel RC columns behaved similarly up to their peak loadings, exemplifying their similarities in withstanding loadings before variant failure types (Benmokrane et al. 2015). The interaction diagram of the CFRP RC columns, according to Benmokrane, is similar in shape to their companion steel RC columns until the point of high eccentric loading.

Previously, a large concern regarding the implementation of any kind of FRP reinforcement was its ability to resist mechanical abrasion from repeated driving hammer blows. In FDOT's study, no

significant cracking or witness marks were present upon final driving, suggesting that the reinforcement within did not succumb to any loss of capacity. From these observations, when ACI 440 provisions are met by the design of the member, the concrete cover should be sufficient to withstand any reinforcement damage. Nevertheless, maximum stresses that propagate during handling and driving should at least be considered in the design process.

Effect of Slenderness on PC Piles

In the analysis completed above, the consideration of slenderness in the members was not taken into account, and shall be addressed in this portion. An analysis of the effects of slenderness in the cross sections analyzed in Chapter 3 was forgone as the problem is addressed in two-fold by the lateral soil pressure afforded to piles and the nature of prestressing itself.

In a study of GFRP reinforced slender columns (Deiveegan and Kumaran 2010) observed reduced capacities from 10-20% when compared to steel reinforced concrete columns, noting the effects that a reduced elastic modulus has in slenderness considerations. In regards to prestress elements, as the modulus of elasticity of FRP products can be as low as one-quarter or two thirds that of prestressing steel tendons, the deflection of prestressed concrete using FRP tendons will tend to be larger than that of concrete beams prestressed with steel tendons. However, the low relaxation losses of FRP tendons will tend to reduce deformations due to time-dependent effects.

In conventional RC piles that are driven into weak soils that might be found in the conditions along the Gulf Coast, slender piling would be susceptible to buckling. In a study by (Mirmian et al. 2002) to reduce the tendency of buckling during the driving of concrete-filled FRP tubes, it was advised that driving should commence after filling the tubes with concrete, adding sufficient stiffness to resist these effects. It was found in (Han and Frost 2002), a theoretical study on buckling of FRP composites under driving impacts with anisotropic properties, relatively low moduli of elasticity, relatively high elastic to shear modulus ratios compared to steel, that shear deformation plays important role in determining buckling load of FRP piles. They found that except for very long piles or very soft soils, buckling of FRP was not significant in conventional RC piles. As CFRP has an increased modulus of elasticity as compared to GFRP, and that the cross sections analyzed were prestressed, these effects are further mitigated.

As RC piles are considered fully restrained columns when lateral earth pressures of strong cohesive soils resist deformation of the member, buckling would therefore only occur in weak soils of undrained shear strengths of $c_u < 209$ psf (10 kPa) and only in slender members (Vogt et al 2009; Hayward Baker 2016). For this assumption to be valid the lateral deflection of a pile shaft towards the soil must be met with an equivalent a supporting soil resistance. This resistance cannot exceed the limiting earth pressure of such soils around a pile, and assuming any lateral soil support for the member, it must be ensured that during the lifecycle of the structure, the assumed lateral soil support can be maintained. In addition, in PC piles, the internal axial prestressing force in bonded strands produces no column action, and as a result, buckling would not occur as long as the prestressing strand and the surrounding concrete are in direct contact with one another along the total length of the member (Nawy 2009), and according to the specifications by CSA, a perfect bond shall be considered between FRP and concrete. Therefore the tendency of the pile to bend at mid-length from buckling effects is canceled by the stretching effect of the axially-embedded prestressing strands.

At the very worst conditions, namely during the driving of the prestressed pile, guides and supports should be erected to prevent vibration and buckling or in areas of high seismicity (Gerwick 1968; Mays et al. 2005).

3.3 Comparison of Findings with Previous Literature

To corroborate the current model that is being proposed, a comparison to other contemporary models was conducted. In the following Figure 24, equations used to predict the strength interaction diagram of FRP RC were compared to Benmokrane et al. (2015) publication of similar results. The comparison is shown below. As can be seen by the following results, a very similar interaction diagram is generated to that published by Benmokrane. In fact, locations of maximum axial load and bending moment agree quite closely to the other study, it is only in the combination of these two forces that findings differ slightly.

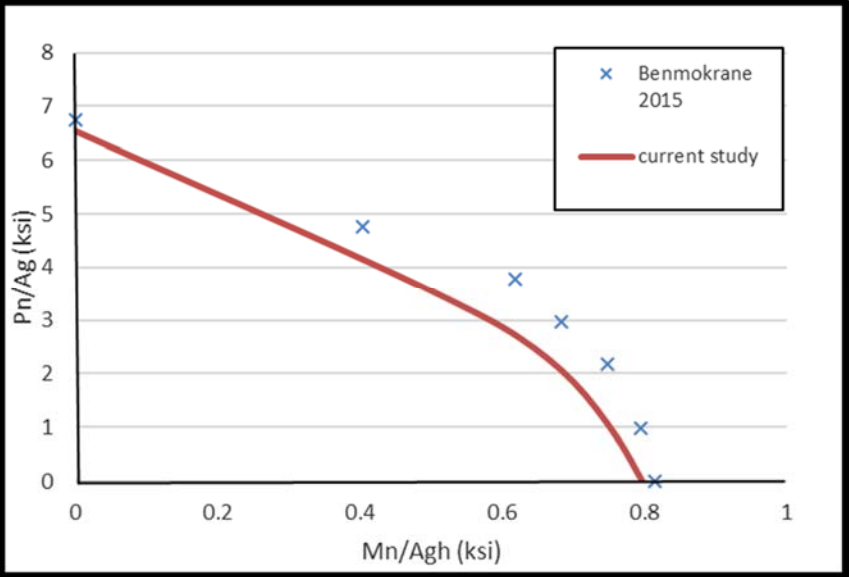


Figure 24. Strength Interaction Diagram of FRP RC; 250 ksi, $f'_c=5\text{ksi}$, $E_{pr}=20,000\text{ksi}$, $\rho=4\%$ (Benmokrane et al. 2015).

As was done in the RC case, a comparative model is provided in the Figure below, illustrating the similarity in the strength interaction diagram between the current study and results published previously in the steel PC case. As can be seen by Figure 25, below, and similar-to the previous comparison, at locations of pure axial load or bending moment, the two models come close in agreement. It is when the two forces combine in interaction that the models differ slightly, indicating relative agreement between the interaction equations set forth in previous studies and the current study.

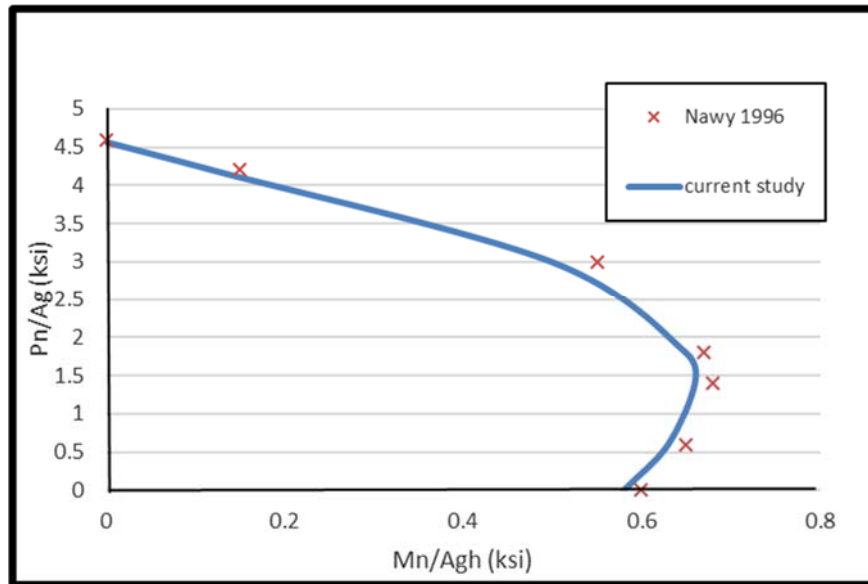


Figure 25. Strength Interaction Diagram, Steel PC; 250 ksi, $f'_c=6$ ksi, $E_{ps} = 29,000$ ksi (Nawy 1998).

3.4 Assessment of Transverse Reinforcement

While the behavior of FRP as primary reinforcement in concrete members has been significantly investigated, the behavior of FRP bars, spirals, and hoops embedded within reinforced concrete compressive members still requires additional information (Afifi et al. 2014). In regards to the use of FRP bars as reinforcement, current design codes and specifications by CSA, ISIS, and ACI 440 have severe limitations for structural use- ignoring the compression strength of the reinforcing bar in the design (Almerich et al. 2012). It is rather apparent in the lack of literature on the subject, and it is therefore necessary to broaden the focus on CFRP tendons to FRP transverse reinforcement in general. Within columns undergoing compression (similar but apart from effects experienced in piles), it was found that CFRP transverse reinforcing (spirals) behaved similarly to steel up until experiencing peak loading (Afifi et al. 2013). CFRP reinforcing tendons have been found to be wholly effective at resisting the loading effects of compression until crushing of concrete substrate occurs. It was found that CFRP spiral spacing was more apparent on confinement efficiency and overall ductility than simple strength capacity, and that CFRP spirals and hoops utilized as transverse reinforcement (and in accordance with CSA S806-12 limitations) effectively confine the concrete core. Based on previous experimental results, GFRP embedded within columns as ties and spiral confinement were similar to steel in their capacity to do so (De Luca et al. 2011, Tobbi et al. 2012). The mechanism of CFRP reinforcement confinement is illustrated in Figure 14 above.

An experiment that did involve the use of CFRP as transverse reinforcement in piles yielded premature failure (in the pilot tests) due to the buckling of longitudinal CFRP reinforcement leading to ultimate failure of the column due to a hoop fracture (Arockiasamy and Amer 1998). This early failure helped in determining testing procedures to avoid such lateral failures, namely by drilling the ends of the CFRP tendons up to 1 inch to avoid directly contacting the loading plates used in the rig. This measure aided in eliminating buckling of longitudinal reinforcement in any of the following specimens and should therefore be considered to be implemented in the field. What was found from this research, however, was apparently less enhancement (due to CFRP confinement) than was reported in the literature at the time for similar steel lateral reinforcements.

In regards to the use of CFRP ties or spirals as transverse reinforcement, numerous studies have been conducted over the last two decades by researchers in the US, Canada, Europe, and Japan. It has been observed that many factors will ultimately affect the efficacy of internal ties and spirals such as the actual reinforcement configuration, longitudinal reinforcement ratio, volumetric ratio, and the size and spacing of hoops or spirals (Afifi et al. 2014). When these parameters are tailored to maximize their efficiency, experimental results (De Luca et al. 2010; Tobbi et al. 2012) have indicated that the overall performance of FRP ties and spirals acting as confinement for a concrete core behave similarly to traditional reinforcing steel. In addition, CFRP circular hoops were found to be as efficient as spirals in confining concrete as reported by Afifi et al. (2014), and according to their experimental results, GFRP and CFRP RC columns behaved similarly to steel RC columns and exhibited linear load-strain behavior up to 85% of their peak loads. These studies, however, did not specifically investigate the confinement effect in pile members, but pure axially loaded columns, a scenario that would realistically be experienced in these structures.

While different in application, these studies still prove useful to understand CFRP's confining effects as these two structural members act quite similarly. Mander et al. (1988) demonstrated that adequate confinement of a column's concrete core through transverse reinforcement enhances both strength and ductility thereby changing the material behavior significantly. As axial concrete strain develops under pure axial loading, the confining stress offered by FRP transverse reinforcement increases with concrete expansion until the FRP ruptures. This is due to the material's brittle characteristics, whereas the lateral confining stress given by conventional steel reinforcement remains virtually unchanged or increases marginally with concrete expansion after the steel has yielded. However, confining concrete cores with transverse CFRP stirrups is a passive approach to increasing overall concrete strength and ductility. It has been observed that at low levels of axial strain, the confinement developed from transverse reinforcement is negligible as the transverse strain is also negligible. For CFRP-confined concrete columns, as axial strain increases under some loading, passive confinement begins to play a significant role because confining stresses continue to increase as concrete expands due to the linear elastic properties of CFRP. And for concrete-filled FRP tubes, addressed previously in Chapter 3, the confinement of rectangular columns with FRP tubes can lead to substantial improvement in the ductility of columns, and may also improve the axial load-carrying capacity of the columns if the confinement effectiveness of the FRP tube is sufficiently high (Ozbakkaloglu 2008).

Afifi et al. (2014) proposed a modified Mander et al. (1988) confinement model for CFRP-RC concrete columns with modifications based on experimental findings and semi-empirical formulations. This equation illustrates the nonlinear relationship between the increase in concrete strength and the confinement ratio f'_l/f'_{co} , where f'_l is the effective lateral confining pressure due to FRP stirrups. Afifi et al. (2014) results indicated that lateral FRP confinement was less effective at higher levels of confining pressure.

In a recently published article, Seliem et al. (2016) investigated the effectiveness of CFRP grid transverse reinforcement using pull-out specimen tests, and flexure testing a full-scale prestressed pile. In this CFRP grid configuration, testing results suggest using an embedment length of twice the grid spacing so that the CFRP can realize its full tensile strength. The same results also suggest that, except for short strands, the presence of transverse strands did not have significant impact on behavior. In Seliem et al. (2016) second test, results indicated that the CFRP grid was able to achieve the required confinement currently provided by steel spirals of equivalent size, and that full use of grid material was observed when inspecting the members upon failure, further illustrating its effectiveness. The capacity of piles reinforced by CFRP grid (and less prestressing force) was larger than that of control pile (reinforced with conventional prestressed steel). This slight increase in capacity can, according to Seliem et al. (2016), be attributed to

enhanced confinement offered by the CFRP grid. Lastly, the use of grid reinforcement slightly increases flexural stiffness of prestressed pile due to presence of these longitudinal strands.

3.5 Mechanical Behavior Summary

This study clearly shows that prestressed CFRP strands can adequately replace conventional prestressed steel both in the longitudinal and transverse directions as published by current TxDOT prestressing specifications. Moreover, CFRP can offer equivalent strength with 25% less reinforcement ratios for equivalent capacities. Within the cross section proposed throughout this section, this translates to a ½-inch diameter steel strand and 0.41-inch CFRP strand for the exact same reinforcement patterns, and does not exemplify that CFRP outperforms prestressed steel at the interaction diagram's extrema as well. For pure axial and bending moments, the prestressed CFRP, for all values of f'_c , expands the capacity of the pile member more than the steel.

While this analysis stayed closely to the 18 x 18-inch pile cross section laid forth by TxDOT's specifications, these results could be extrapolated to various cross sectional configurations and reinforcement patterns. As stated previously, the normalized interaction diagrams are intended to be purely illustrative of the mechanical processes occurring in parametrically generated pile cross sections over many differing loading conditions. While it is useful to understand the limits of these piles in regions not associated with pure axial loading, piles realistically operate in pure axial conditions, experiencing greater bending moments during installation and driving operations. With these considerations in mind, and from the evidence presented, it becomes apparent that prestressed CFRP is a promising alternative for pile reinforcement. The use of CFRP reinforcement in prestressing piles offers an alternative to conventional steel strands due to their strength (typically much greater than conventional reinforcement) and advantageous material properties. CFRP tendons are non-conducting and nonmagnetic, and their non-corrosive nature is of paramount interest in pile configurations subjected to extremely corrosive environments. In this Chapter, prestressed concrete cross sections of prestressed steel and CFRP strands were analyzed using the equal assumptions and principles in the development of interaction diagrams.

3.6 Comparative Cost Analysis

Traditionally, materials such as concrete, steel, and timber were used in bridge piles in the U.S. High repair and replacement costs have urged the highway agencies and researchers to investigate the feasibility of noncorrosive materials such as Fiber Reinforced Polymer-FRPs (Fam et al., 2003). Corrosion of steel strands can cause serious damage to the concrete and the structure resulting in concrete spalling. Repairing these surfaces is time consuming and expensive. According to a study by Zhang and Mailvaganam (2006) the cost of rehabilitating RC structures affected by corrosion is now about 50% of total construction cost. Besides, the cost of maintaining of decks and other parts of bridges is about \$90 billion/year (Dunker and Rabbat 1993). Considering the initial costs of materials is a small portion of the overall cost of the bridges, the higher initial cost of CFCC, as compared to steel strands, can be fairly acceptable. Moreover, in order to better assess the value of using FRP reinforcement, several parameters and their effect on the overall budget should be taken into account via a life-cycle cost analysis (LCCA) (Val and Stewart, 2003, Yang et al., 2006, and Breyse et al., 2009). Life-cycle cost analysis is known to be a powerful tool in making investment decisions and managing resources (NCHRP report, 2003). According to the NCHRP, costs are classified into initial, operation and maintenance, rehabilitation and replacement, salvage value or terminal, energy costs (particularly for equipment), motorist user and associated costs, staffing, downtime, tax implications, and increased service life cost. Some of these costs are not directly associated with the construction of piles, but do reveal themselves in budgets related to the construction

of entire bridges (of which piles are included) and the maintenance of these structures over their respective lifecycles.

Several researchers have been studying the effect of using different alternatives for steel strands mainly in bridge applications (Ehlen 1993, Grace et al. 2012, Rizkalla et al. 2006, Mullard and Mark G. Stewart 2012). These studies have concluded that the initial construction cost of bridges' superstructures and substructures with FRP reinforcement are significantly higher than those with steel reinforcement. This price should be considered alongside the long-term cost, however, in order to fully understand all the potential advantages of FRP materials (Rambo-Rodenberry et al., 2016).

The thought of finding new alternative for existing prestressed concrete piles with steel strands is not a new idea. (Fam et al. 2003) has conducted case-study-based research on Route 40 Bridge Nottoway River, Virginia. The research objective was to find alternatives for two piles, which had become obsolete, of the existing bridge. In this study, they have investigated the behavior of a concrete-filled FRP composite pile. The initial cost comparison indicated about 77 percent higher unit cost for the composite pile. A life cycle cost analysis was not performed for this study due to lack of maintenance cost and frequency information.

Florida Department of Transportation has recently conducted research on using CFRP cables in prestressed concrete PC piles (Rambo-Rodenberry et al., 2016). They have shown the feasibility and excellent behavior of CFRP-PC piles as compared to steel strands. They did not include cost analysis in their study as they have been satisfied with the outstanding structural outputs.

Currently the initial cost of CFCC is higher than steel strands (approximately 320% greater for equal lengths of material); however, the fact that the cost of materials is a small part of the overall cost should be highly considered (Roddenberry et al. 2014). Besides, steel strands are suffering from major problems such as corrosion resulting in tremendous amount of repair and rehabilitation expenditure. Currently, 58,000 bridges were considered structurally deficient in the United States, costing an estimated \$45.5 billion dollars to replace (FHWA National Bridge Inventory 2015). As this number includes all manners of deficiencies, it should be noted that structural deficiency due to substructure corrosion accounts for only a percentage of this number. However, corrosion of steel reinforcement in concrete can cause serious harm to the concrete cover which eventually results in spalling of the concrete surfaces. Repairs of these surfaces are often expensive and disruptive.

According to the 2017 ASCE Report Card for bridges, the United States must increase investment from all levels of government and private sector from 2.5% to 3.5% of U.S. GDP by 2025 in order to reach the \$2 trillion 10-year investment gap deficit to replace or rehabilitate. For more local statistics, according to the National Bridge Inventory, 900 of 53,000 bridges in Texas are structurally deficient, costing an estimated \$390 million dollars to repair or replace. Of that number, 130 of 7,600 bridges in TxDOT coastal Districts are reported to be structurally deficient, needing repair or replacement. As the majority of TxDOT bridges over waterways employ some type of piling (approximately 30% of deep foundations let of which 99% of piling driven is prestressed concrete) there stands a significant opportunity for costs savings to TxDOT and other Agencies across the country to employ corrosion-free materials in infrastructure (McClellan 2005).

In order to better estimate the cost of using CFRP stands in prestressed concrete piles and to compare this alternative to steel strands, a case study was considered that will be addressed at the end of this Chapter. Ehlen (1993) has investigated the life-cycle cost-effectiveness of three FRP bridge decks to evaluate the effect of these new materials in projects expenditure. He has included all advantages and

disadvantages of FRP materials using Monte Carlo simulations to assess the uncertainty of the new materials. According to his research there are specific steps in conducting LCC method as follows:

1. Define the project objective and performance-based requirements.
2. Identify the alternatives that satisfy the project objective and performance requirements.
3. Establish the basic assumptions for the analysis that apply to all alternatives.
4. Identify, classify, and estimate all costs that occur over the life-cycle.
5. Compute the LCC of each alternative.
6. Perform sensitivity analyses.
7. Compare the alternatives' LCCs.
8. Consider other project effects.
9. Select the best alternative.

Grace et al. (2012) have done similar studies on CFRP prestressed concrete bridge girders. They have shown that despite the higher initial construction cost of FRP reinforced bridge girders, they can be cost effective for a 100-year of service life as compared to conventional steel reinforced concrete bridge decks considering factors such as initial construction, maintenance, repair, rehabilitation and demolition activities. The process is shown in the flowchart below, illustrating user costs, which themselves are highly variable from case-to-case (traffic volume, bridge location, etc.)

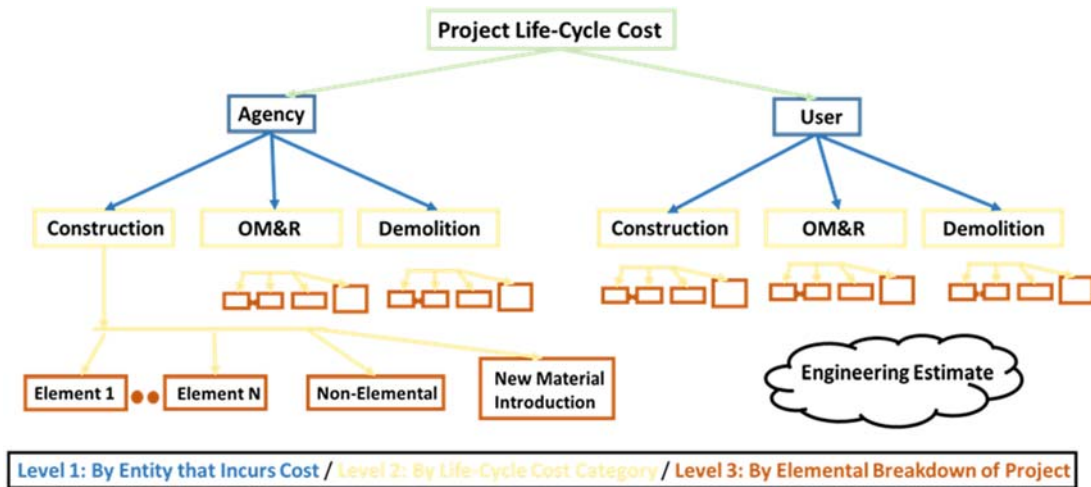


Figure 26. Life-Cycle Cost Analysis Steps, adapted from Grace et al. (2012).

Rizkalla et al. (2006) has conducted cost analysis and value engineering evaluation on various FRP Repair Systems, illustrating that the effectiveness of material is worth the cost of implementation in the long-term.

Using the same methodology, Mullard and Stewart (2012) have shown the effect of repair strategies in using steel strands on factors such as time, cost, and remediation actions via studying the life-cycle cost assessment of maintenance strategies for RC structures in chloride environment. They showed that key parameters in life-cycle cost are inspection intervals, repair thresholds, maintenance strategies, and efficiency of repairs. They conducted a Monte-Carlo event-based simulation analysis to incorporate these parameters. The life-cycle cost (LCC) analysis considers repair and user delay costs. They concluded user delay costs during maintenance actions can be up to ten times higher than the cost of repair itself. Despite the initial increase in construction costs due to the adoption of FRP tendons, it can be an effective tool when considering the entire life-cycle cost of a structure (Burygoyne and Balafas 2007).

In this section, maintenance costs are referred to the costs of inspection as well as repairing and rehabilitation costs. According to the Texas Bridge Inspection Manual, there are five different types of inspections as follows:

1. Initial Inspection. Performed on new bridges or when bridge is first recorded.
2. Routine Inspections. Those regularly scheduled, usually every two years for most normal bridges.
3. Event Driven Inspections also called Emergency Inspections (AASHTO Damage Inspections). Those performed as a result of collision, fire, flood, significant environmental changes, loss of support, etc. and are performed on an as-needed basis.
4. In-Depth Inspections. Performed usually as a follow-up inspection to better identify deficiencies found in any of the above three types of inspection. Detailed underwater or fracture-critical inspections are some of the examples.
5. Special Inspections. Performed to monitor a particular deficiency or changing condition. Unusual bridge designs or features such as external, grouted, post-tensioned tendons, may require a Special Inspection.

According to these definitions, as a regular basis, inspection should be performed every two years, resulting in a considerable effect on the budget. Therefore, inspections play an important role in maintenance costs of bridges during their service life.

3.7 Relevant Costs

In the maintenance of piles, the overall cost is not only the cost for repairing or reconstructing of the structurally deficient piles. There are several other costs related to reconstruction of piles such as delay on the traffic, user cost, etc. which can result in additional costs. Another relevant consideration is that cheaper transportation of the FRP material from factory to site and its installation savings can offset the higher material costs (rarely exceeding 20% of the overall project costs), and when traffic management costs are considered, the use of FRP could potentially provide a cost-savings. The inability for manipulation in the field, as mentioned regarding transverse reinforcement, is in reference to not being able to simply cut and bend CFRP strands as easily as contractors could with steel strands. If the spiral dimensions are incorrect, contractors cannot simply bend the material to shape. CFRP, when prestressed and cast in members, can be cut to size in the same manner as prestressed steel without issue. In addition, as can be seen from the mechanical comparative analysis, fewer prestressing strands are required to achieve equivalent capacities, leading to lower initial material costs.

3.8 Life Cycle Cost Analysis

To attempt to quantify long term costs incurred by the Agency over the design life of their infrastructure, each term included in the LCCA equation, shown below, will be addressed. As mentioned earlier, in order to run life-cycle cost analysis, the following factors with their frequencies should be accessible.

$$CC=DC+CC+MC+RC+UC+SV \quad (27)$$

LCC=life-cycle cost,

DC = design cost,

CC =construction cost,

MC =maintenance cost,

RC =rehabilitation cost,

UC =user cost, and

SV=salvage value.

In conventional cost analyses, such as the return on investment criteria, an initial investment is held over a certain length of time, eventually being recovered by some margin of profit. In the case of infrastructure investment, and in the comparison of reinforcement alternatives specifically, this return on investment will manifest in diminished maintenance and future rehabilitation fees. The effects of owning a bridge e.g. the increase in transportation efficiency, interconnectivity, economic growth opportunity, and improvements in emergency response times would be inherently identical between substructure reinforcement types, and therefore the net value gain of ownership is precluded from further analysis.

3.8.1 Construction and Maintenance Costs

In the determination of the largest factor concerning the LCCA, namely the initial construction cost of building a bridge, all other components of the structure remained equivalent between substructure reinforcement types. The bridge deck and superstructure, abutments and approaches were held equal so that only the differences propagating from the pile reinforcement would become evident.

The dimension of the section used for the piles as well as the amount of reinforcement is derived from TxDOT specification as shown in Figure 27 and will be used to generate the initial construction costs.

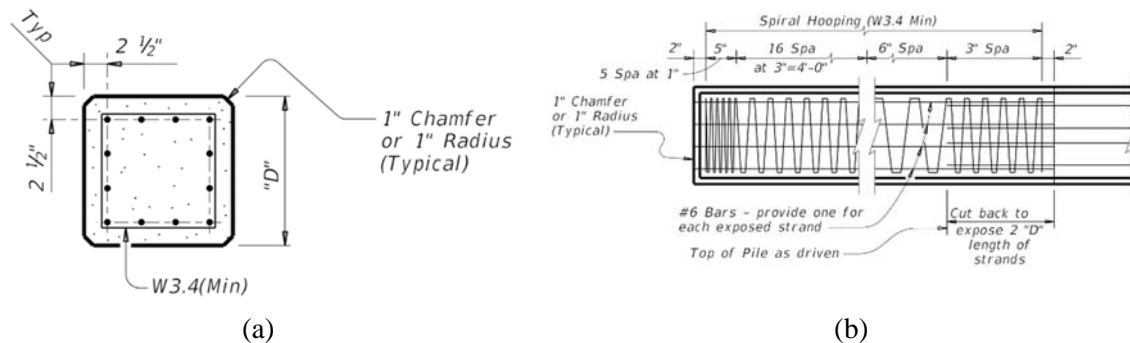


Figure 27. TxDOT Specification for Prestressed Concrete Piles, (a) Typical Section Thru Piles, and (b) Pile Build Up Detail

Since similar studies have been done by Florida Department of Transportation (FDOT), corresponding contractors (Gate Precast Company) in Florida were contacted for the purpose of cost estimation of the case study. The average pile section and length in South Texas are 16-20 inches and 45-65 feet. An 18-inch section with average length of 52-feet is considered in this study, from data acquired by TxDOT low bid prices and paired with the cost of the average bridge replacement according to FHWA NBI. The pile specifications for the case study are as follows:

- 18 inch piling
- 12 strands per pile
- 20 piles
- 52 foot average length

According to quotes of contractors in Florida familiar with the construction process, the cost of using CFRP strands is \$130 per linear-foot (LF) compared to \$40/LF for steel strands. The dimension of both alternatives are exactly the same, the only difference is the type of reinforcement. There is also a delivery cost of about \$900 per truck containing two piles per load which is the same for both options.

Part of the higher cost of CFRP is related to the anchorage system and the prestressing couplers for CFRP cables. According to the manufacturer (Tokyo Rope USA), the cost of CFRP materials plus the anchorage system (including CFRP chucks) is \$66/LF for the desired configuration of the project. This value was calculated by taking a standard 5-strand configuration of 200 LF quoted by Tokyo Rope USA, and applying this to the project’s 12-strand configuration. In order to make sure that the cost estimation in Florida is referable in Southeast Texas, a cost estimation from a local company in Houston Area (Flexicore) was analyzed. They have estimated the project with steel strands for \$43/LF. In addition, a visit to a local prestressing plant (Texas Concrete Partners, TCP) in order to evaluate the possibilities of using the new techniques of using CFRP cables in prestressed concrete piles as well as estimating the relevant costs was undertaken. The local contractor had also confirmed that the cost for steel strands is the same in South Texas area. If we add the \$66/LF and the \$43/LF of contractor fees, then the construction cost will be \$109/LF

Table 7. Cost of pile replacement in coastal regions, State of Texas

Reinforcement Type	Price/LF	Total substructure Cost
Prestressed CFRP	\$ 109.00	\$ 113,360
Prestressed CFRP with 25% less strands	\$92.50	\$96,200.00
Prestressed Steel	\$40.00	\$41,600.00

What can be seen from the above Table 7 is the stark contrast between initial construction costs between prestressed CFRP and steel strands. There is a 273% difference between the one-for-one strand replacement, and a reduced 231% difference in cost between the equivalent capacity piles. This solution brings the initial construction costs of only the piling of a bridge closer together, without the consideration of any additional maintenance and additional service life. Furthermore, while the focus is on cost of substructure only, if we look at the cost of the entire bridge and assume that 20% of the total cost is dedicated to the substructure, then the overall increase in cost will be about 46% as compared to the 231% cost associated with piles.

According to the FHWA NBI, the average cost to replace a bridge structure lies around \$550 thousand/replacement (combing larger spans over channels with smaller spans that traverse drainage systems). Therefore, the difference in costs between conventional prestressed steel bridge piles and prestressed CFRP represents 2.6% of the total cost of new bridge construction, and when accounting for a reduction of 25% in the amount of necessary CFRP strands to attain equivalent capacity, this difference accounts for only 2%. In significantly more expensive capital projects with larger superstructures, the overall cost of the substructure compared to the entire project is diminished even more so. This value illustrates that the remarkable difference in material costs between steel and CFRP can be significantly mitigated when considering the price of the bridge structure in its entirety.

On the other hand, as discussed in Chapter 2 and based on several interviews conducted during research of TxDOT correspondents as well as local consultants, the costs of repairing and rehabilitating existing structurally-deficient prestressed concrete piles is significant. According to a TxDOT database (correspondent Andrew Lee from TxDOT at Beaumont), the average maintenance cost of repairing and

rehabilitation of prestressed concrete piles for low-bid unit price state-wide for May-July 2016, was reported as \$116.00/LF. In addition, the average maintenance cost for prestressed concrete piles in 2014, was reported \$137.50/LF with several dozen feet of work required per repair. These values were in reference to several cases of maintenance available in the low-bid unit spreadsheet including spalling repair, implementing epoxy mortar, and minor repairs of concrete foundations. This limited snapshot of typical repairs does not represent the average costs of maintenance for all prestressed concrete piles in the state, but offers some insight into typical costs incurred by TxDOT.

The value used for annual maintenance cost was generated by calculating the depreciation of value of the initial structure, an imprecise metric, and coupled with typical repair costs. What should be understood in this Table, however, is that maintenance costs do not occur over the entire length of a pile when being repaired, only at the specific location of cracking, and therefore this cost represents the total amount of repair work performed on the substructure divided by the lifespan of the structure. Initially, repair costs would be non-existent, and towards the end of the structure’s lifespan, would become quite costly. In the case for prestressed CFRP strands, there is no assumed maintenance cost for the substructure. With this in mind, a conservative value of maintenance costs accrued per year ranges anywhere from \$350-700 per year of the structure’s lifespan. While not every year during the lifespan of the bridge is associated with an incurred cost to the Agency, biannual diving inspections performed towards the end of the structure’s use play a significant role. This accounts for the aforementioned low-bid unit costs, depreciating value of the bridge structure, and factors the numerous inspections performed by TxDOT and shown in Table 8, below.

Table 8. Initial Construction Costs to Annual Maintenance.

Reinforcement Type	Total substructure Cost	Total Annual Maintenance Cost
Prestressed CFRP with 25% less strands	\$96,200.00	\$-
Prestressed Steel	\$41,600.00	\$610.00

With an initial construction cost difference of \$54,600 between the equivalent capacity reinforcement types, again only attributed to 2% of the total construction cost of a standard bridge as reported by the FHWA NBI, the discounted payback period is used in evaluation. As opposed to the discounted payback period equation, one serious limitation of the conventional payback period formula is that the time value of money is not considered. Therefore in this analysis the payback period method is used, which is the period of time required to reach the break-even point based on the net present value (NPV) of the cash flow. The cash flow in this scenario, refers to the negative cash flow of bridge maintenance and how much the DOT (on average) must spend to keep the structure functioning. The formula of payback period is presented below:

$$PP = I/C \tag{28}$$

Where, (PP) is discounted payback period, (I) represents the initial investment amount, (C) is the cash flow per year. The initial investment, namely, the difference in construction costs between reinforcement types that the DOT would thereby incur is a negative value, and the payback period represents how many years of chronic maintenance costs are accumulated by the steel bridge. By TxDOT standards, the discount rate is fixed at 5% annually, accounting for the time value of money. The payback period formulation is widely used, however, does not account for systemic risk, opportunity cost, etc., which are also very important considerations in investment. By this metric, a period of 90 years of

continued expenditure of maintenance costs and bridge inspections would be required to recoup the additional increased construction costs, indicating that the difference in initial construction costs can be regained by a savings in maintenance over the expected lifespan of the prestressed CFRP bridge. This 90 years that is necessary to recoup the additional initial cost is valid only if we look at the substructure by itself. In reality inspection and maintenance is performed to the entire bridge and if the overall bridge is considered in this cost assessment and again considering that the cost of the substructure count for only 20% of the overall bridge, then the required time to recoup the initial cost could be as low as 18 years.

The costs associated with this idealized bridge were taken directly from TxDOT unit specifications and local contractor’s quotes with no assumed maintenance cost due to the environmental resilience of CFRP. This formulation accounted for all material quantities, transportation, and fabrication costs, and was taken from TxDOT spec pile annual maintenance pricings. The quantities of structurally deficient bridges in the State and within the Coastal counties of Texas were taken from the NHTWA bridge inventory.

3.8.2 Increased Service Life

In addition to the variables set forth previously, an increased service life brought about by the increase in corrosion resistance by CFRP’s could factor into the equation. When considering an increased service life, hesitant parties need only look at the amount of bridge rehabilitations and replacements that were conducted by TxDOT within previous years. In 2010, according to TxDOT yearly bridge facts, 430 such instances were observed (this year being an outlier due to the lasting effects of American Recovery and Reinvestment Act of 2009). Five years later in 2015, a total of 684 instances of bridge repair and replacements were conducted, leading to the general trend of increasing demands to TxDOT in terms of economic costs and man-hours required.

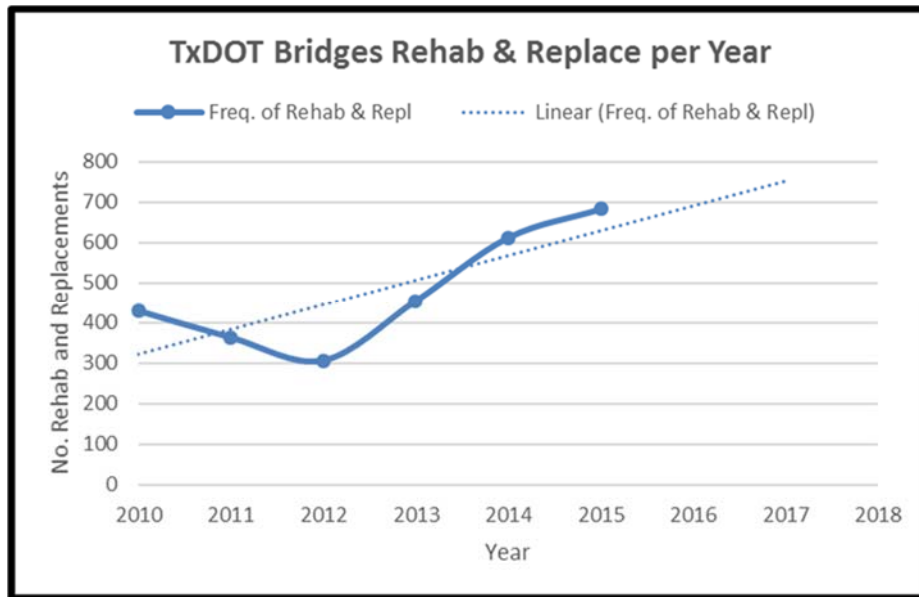


Figure 28. Yearly Increase of TxDOT Repair and Replacements; TxDOT Yearly Bridge Facts)

According to TxDOT yearly bridge facts publications, of all replace and rehabilitation works undertaken by the Agency, 90% of are to rehabilitate and the remaining 10% are for complete replacement. According to the FHWA NBI, the average cost to replace a bridge structure lies around \$550 thousand/replacement (combing larger spans over channels with smaller spans that traverse drainage systems). It is also calculated that retrofitting an existing bridge can typically cost 68% of the cost of total replacement, allowing us to begin quantifying any potential extensions in service life. In addition to this,

the NBI ranks structural evaluations of these bridges on a 1-10 scale where the smaller figures correlate to extensive repairs and retrofitting required, and the larger values to more limited repair works. In fact, of the 90% of rehabilitated TxDOT bridges, according to the NBI, 10% will be extensive in scope with the remaining 90% to be of smaller significance.

In this light, if any increase in service life were to be expected by corrosion-proofing prestressed piling, it would shift the amount of rehabilitation and replacement works performed by TxDOT. If those structures requiring complete replacement would now instead fall into the 90% category of rehabilitation due to their extended service life, this could save a significant amount of cost to the department. In addition to shifting more bridges into the rehabilitation category, of the work performed, there could be cases in which what was once considered an extensive job (according to the NBI) could fall into the limited scope category due to an increased service life.

3.8.3 Design Costs

Unaffected by material type, the design costs incurred by TxDOT when engineering a substructure would remain the same. There exist numerous governing codes published to aid in the design of prestressed FRP-reinforced piles, and over the long term, engineers can become more familiar with this type of construction. Design costs might increase marginally, however, if design professionals remain hesitant to adoption, and similar to increased construction costs associated with prestressed CFRP piles compared to those of steel, engineers would charge for uncertainties.

As can be seen over the cash flow diagram representing the LCCA (where greyed terms are removed from analysis due to their equivalence), conventional prestressed steel accrues numerous costs over the course of its design life. In addition the initial design costs associated with the initial construction, shared with the prestressed CFRP scenario, upon the rehabilitation of the prestressed steel structure at year 75, there is an additional design cost incurred in the design of a rehabilitation scheme. In conventional practice, the fee charged by design professionals varies with the experience of the team and the scope of the project. Such values are very closely guarded by the engineering firm, but according to sources contacted during the literature synthesis portion of research, owners can expect to be charged anywhere from 7-10% of the total cost of the project (Cowart, D. (2016, May 2). If the original price of construction for the average bridge of \$550,000 as referenced by the NBI, the cost of rehabilitation is around \$375,000, and by extension, engineering service fees could account for an additional \$30,000. A cash flow diagram shown in Figure 30 illustrates when such costs are expected to manifest over the course of the 100 year analysis.

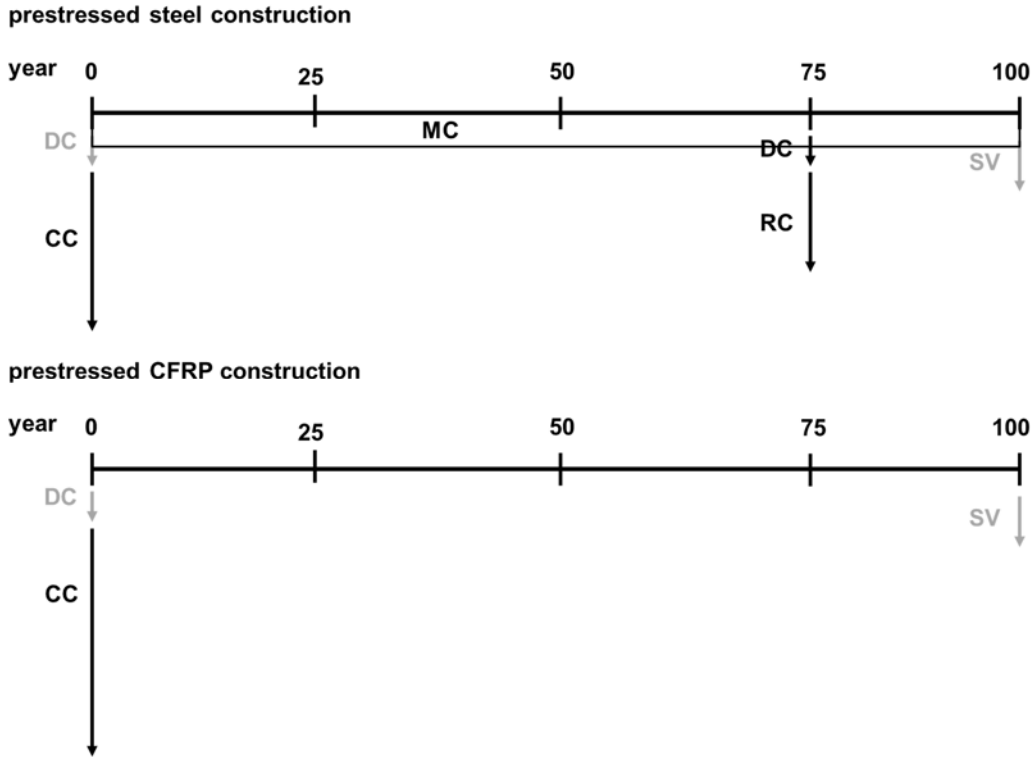


Figure 29. Cash Flow Diagram Illustrating Costs Occurred per Reinforcement Type.

As was evidenced in the initial construction costs segment, the added material costs of implementing CFRP's in the design amounting to around 13% of the total bridge construction costs, are only realized at year 1. With the initial design costs removed at this time due to their equivalence to steel construction, the remaining incurred costs can be seen propagating after this time.

3.8.4 User Cost Savings

User costs are defined as costs that are incurred by motorists, namely the beneficiaries of the bridge, due to a deficiency in the structure deviating from the desired or ideal conditions, or in other word, are a denial of use cost. These costs manifest in the form of vehicle operating costs and costs from delays and accidents initiated by traffic control devices and operators as well as detours due to bridge construction and maintenance from lane closings. Indirect user costs from delay and detours can in part be caused by inadequate traffic clearances, less than desired load capacity, environmental damage, traffic congestion, or construction impacts during maintenance.

From this aspect, it was difficult to quantitatively ascertain a designated user cost for maintenance work done to bridge piles as too little information was available in the field. Not all lane closures and maintenance projects are equal, however, and it is difficult to state that a given closure due to pile repair is equivalent to that of deck repair. While motorists can still use a thoroughfare while the substructure of a bridge is being painted, vehicle operating costs increase significantly if lane closures occur due to replacement of the deck. These values are epistemic in nature and fluctuate significantly between various traffic volumes, lengths of available detours, and the overall length of construction time. Because of the resilient properties of CFRP, it would logically conclude that fewer works of maintenance need be performed to achieve equivalent results utilizing corrodible steel reinforcement. It therefore follows that, at least due to the pile-component of the bridge, a significantly smaller margin of user costs will be

incurred over the life-cycle of the bridge at the time of rehabilitation to the prestressed steel bridge than to the CFRP alternative.

During the replacement or rehabilitation of a bridge, motorists’s incurred user costs can be given by Daniels, et al. (1999):

$$RUC = VOC + AC + VOT \quad (29)$$

Where (RU) represents the total road user costs, (VOC), vehicle operational costs, (AC), accident costs generated by the replacement or rehabilitation, and (VOT) user delay-time costs.

As these variables encompass many highly variable factors prone to change from one district to the next, the generated user costs become difficult to quantify. Walls et al. (1998) asserts that the user delay-time costs (VOT) typically represents 95% of the total road user costs (RUC), thereby making the calculation of this quantity less challenging. From this simplification, DOT’s have tabulated expected values of VOT for regular vehicles and trucks for use in this calculation. The recommended values from TxDOT, circa 1998 as offered by Daniels, are \$11.97/car-hr and \$21.87/truck-hr. Dollar values were adjusted for inflation according to information published by the Bureau of Labor Statistics. The combined traffic values was formulated from the annual-daily-traffic (ADT) and annual-daily-truck-traffic (ADTT) values from the NBI database. The value of VOT is therefore the total user delay-time costs per rehabilitation, shown below:

$$VOT = \frac{\text{Detour Length}}{\text{Velocity}} \times \text{Delay} \times (\text{VOT, vehicle} \times \text{ADT} + \text{VOT, truck} \times \text{ADTT}) \quad (30)$$

From this equation, several assumptions were made to quantify the effect of rehabilitation that a prestressed steel bridge would realize. Namely, that in the case of the typical NBI bridge, it happens to be located within some radius of traffic congestion significance in a system, and that the rehabilitation delay lasting approximately 3 months will cause motorists to choose an alternate route, adding an average detour of 5 miles. This can be visualized in Table 9, below.

Table 9. User Delay Assumptions for Bridge Rehabilitation.

Average Detour Length (miles)	Average Velocity (MPH)	AHVEHT	Delay Cost Veh (\$/Veh-hr)	AHTT	Delay Cost Truck (\$/Truck-hr)	Average Delay Duration (hr)	Average Delay Cost (MM USD)
5	65	350	17.69	20	32.32	2160	1.1
5	65	500	17.69	70	32.32	3600	3.1

Where (AHVEHT) is the average hourly vehicle traffic and (AHTT) is the average hourly truck traffic. As can be seen in this idealized calculation, a user cost of \$1.1 million dollars is generated during a 3 month period in relatively low-traffic conditions. Parameters can be easily manipulated to show just how quickly user costs can accumulate, and increasing the amount of motorists using the structure and delaying rehabilitation efforts by an additional 2 months, an additional \$2 million dollars is added to the price.

It would therefore be within reason to label this projected average of \$2 million dollars in user cost savings over the course of bridge rehabilitation as realistic. However, the calculation of user cost is not realized by TxDOT, but the motorists themselves. As the Agency does not formally recognize user costs in the analysis of new bridge construction, this number is precluded from direct analysis, but nevertheless remains an important factor in design considerations.

3.8.5 Rehabilitation Cost

Employing concrete patches for spalling repair, periodic reseals, or general repairs associated with the concrete foundation are all costs previously associated with maintenance costs. When analyzing the costs incurred by TxDOT in rehabilitation costs such as new structural overlays or additional shoring piles, a representative figure of 68% of the total initial construction costs as provided by the FHWA is used (equating to an additional \$375,000 for a typical bridge according to the NBI). In the idealized LCCA, as seen in the cash flow diagram, whereas prestressed CFRP construction continues functioning at capacity through the design life of 100 years, after 75 years of use in prestressed steel, an unavoidable rehabilitation costs is incurred (assuming the Agency opts to forego complete replacement).

The advantage given to CFRP here is the ability to significantly delay or avoid rehabilitation costs before total replacement is required, prolonging any incurred costs to the Agency. Such rehabilitation costs function only to prolong the service life of the structure, and are not assumed to prolong this beyond an additional 25 years of design life. At this time in the lifecycle of the prestressed steel structure, significant user costs are again realized by motorists as extensive retrofits are applied to the bridge.

3.8.6 Salvage Value

Because of the relatively recent emergence of CFRP materials, there does not exist any literature regarding the salvage value of the material, let alone any precedential dealings by DOT's. It is this lack of precedent that hinders the quantification of the LCCA term, but an educated guess can be made. While reinforcing steel can offer some return on material costs when a retired structure is salvaged for scrap, CFRP will not be able to be extracted for this purpose. While there is no historic basis for this salvage value, it can be inferred that the reinforcing material will not hold any monetary value upon termination. The ability for the material to withstand structural loads deteriorates as the reinforcement is subject to blunt forces as the carbon fiber bonds are damaged, ruling-out any reuse.

Realistically, DOT's do not recoup any initial costs of construction when salvaging bridges through the sale of their constituent materials. In either reinforcement scenario, DOT's would contract-out the demolition of the bridge to the lowest bidder, again incurring a cost rather than realizing any gain. With this assumption, it is not out of the realm of reason to offer no salvage value to the material. The demolition costs of the structure, going hand-in-hand with the salvage costs of the bridge, would remain unchanged if all things remain equal between steel-reinforced and CFRP-reinforced bridges. The mobilization and operation costs of demolition crews remain unchanged as the nature of the salvage remains the same.

3.8.7 Comparative Cost Summary

The feasibility and cost analysis of prestressed concrete piles with CFRP cables is investigated along with a side by side comparison with steel strands in this Chapter. The initial cost of a prestressed concrete pile using CFRP reinforcement is more than three times that of the same section using steel strands. According to the literature review and recent research in different DOT's, it is generally believed that the long term resilient behavior of CFRP reinforcement will results in improved performance during the 100-year service life. Analyzing the various components of each term in the LCCA, the following can be stated.

- Implementing prestressed CFRP within piles in a typical NBI bridge construction project accounts for an increase of 2% of total budget as compared to using conventional prestressed steel strands if substructure cost is estimated at 20% of the total cost of a bridge.

- An increased service life, as assumed by the design of the CFRP structure, can delay or eliminate any rehabilitation and maintenance costs incurred by steel (calculated to be \$610/year, with a payback period of 90 years if the focus is only on substructure but could be as low as 18 years, again if the cost of the substructure is considered as 20% of the total cost of a bridge)
- The additional cost incurred by including rehabilitation and design costs in prestressed steel can be expected to account for 68% of initial construction costs
- By far the largest costs generated would be the user costs resulting from putting the structure out of service during rehabilitation and extensive maintenance, and for a 3 month period of moderate traffic needs, could account to \$2 million

It is important to consider that part of the higher construction of CFRP reinforcement - as compared to steel strands - can be due to the fact that prestressed concrete piles with CFRP are not currently manufactured on a large-scale basis. Lack of experienced contractors in constructing PC-CFRP piles can also be considered as another reason for higher initial cost of CFRPs. It is hoped that by increasing the use of this new generation of noncorrosive piles in the near future, the related costs reduce significantly. In this light, the implementation of prestressed CFRP in bridge piles can be considered as an effective alternative to prestressed steel, when considering the entire lifecycle of the bridge structure.

Items that were not addressed in the LCCA that can marginally affect the payback period of CFRP-reinforced piles were the consideration of a non-linear increase in maintenance costs over the bridge's lifespan (which was assumed constant). As time increases, repairs become more frequent and more expensive. In addition, the research did not address potential decreases in CFRP material and construction costs over time as the technology may become more prevalent in the market.

Chapter 4: Additional Gaps in Knowledge

4.1 Introduction

Upon study of the available literature and ongoing studies associated with prestressed CFRP piles, the following topics were identified as critical gaps in the existing body of knowledge related to the use of CFRP prestressed piles:

- Drivability Concerns and a Reduction of Concrete Cover
- Deterioration of CFRP in Saltwater
- Embedment Lengths and Splicing Configurations for CFRP Piles and Tendons
- Prestress Loss Effects for CFRP Strands
- Circular, Octagonal, and Square-Reinforcement Patterns in Piles

While much research has been done concerning CFRP used to reinforce beams and columns, far fewer studies were conducted relating to piling. It is in this study of gaps in knowledge that the Research Team will identify whether implementation of CFRP-prestressed piles would likely result in any benefits to the Department and State and what additional steps must be taken.

4.2 Further Drivability Concerns & Reduction of Concrete Cover

A point of concern associated with embedding prestressed CFRP cables that was raised at the outset of this project was the ability for the reinforcing material to withstand significant abrasive pile-driving blows when being driven into soils. As FRP's are known for their susceptibility to mechanical abrasion unlike their steel counterparts, this was investigated during the course of the Report. This concern about abrasion to the CFRP piles is focused mostly to the portion of the pile being repeatedly struck by a pile driver and less so to the abrasion from frictional forces developed along the sides of the pile during driving. What was found by full-scale tests performed by FDOT and VDOT was CFRP's resilience to damage from hammer blows when embedded in concrete was as significant as its steel counterpart (Sen and Issa 1992; Arockiasamy and Amer 1998; Roddenberry 2014). If damage was present at all upon completion of the pile driving, there was only minor surface damage to the concrete substrate and the internal reinforcement was able to withstand expected loadings. The successfully driven prestressed-CFRP pile designed and fabricated for the VDOT its investigation can be seen below in Figure 27. Success in this application was the evidence of little to no external damage to the pile by concrete spalling. Additional research to quantify reinforcement capacity loss could be undertaken by testing piles to ultimate failure upon being successfully driven.



Figure 30. Successfully Driven Prestressed-CFRP Piles, Ozyildirim and Sharp (2013).

It was not reported in any previous literature whether the overall concrete cover normally protecting the prestressed steel can be reduced in the case of CFRP reinforcement. While the concrete cover does protect the internal reinforcement from mechanical abrasion, it also protects the steel prestressing strands from corrosion. A significant advantage of FRP's, as stated numerous times in the previous portions of this Report, is its natural resilience to electrochemical degradation. Because of this material property, CFRP's can be exposed to harsh chemical environments for prolonged amounts of time without significant loss in capacities (Rizkalla et al. 2003; El-Salakawy 2003; Afifi et al. 2014). This should be paired with CFRP transverse reinforcement in order to eliminate any corrosion all together (longitudinal and transverse reinforcement). In addition, any transverse reinforcement that acts to confine the member (not embedded within the concrete) would give rise to new frictional driving issues that would not have been addressed by previous pile driving research. This would therefore be a gap in existing knowledge and would need to be addressed before implementation. In the comparative parametric studies done in early reports, the Research Team acknowledged the increases in ultimate capacities offered by CFRP strands, but opted for a one-for-one replacement of conventional prestressed steel reinforcement to more closely adhere to TxDOT specifications. While fewer strands could be used to achieve equivalent steel capacities, roughly 30% less, the overall concrete cover used in TxDOT standards (as seen in Figure 28) could be reduced.

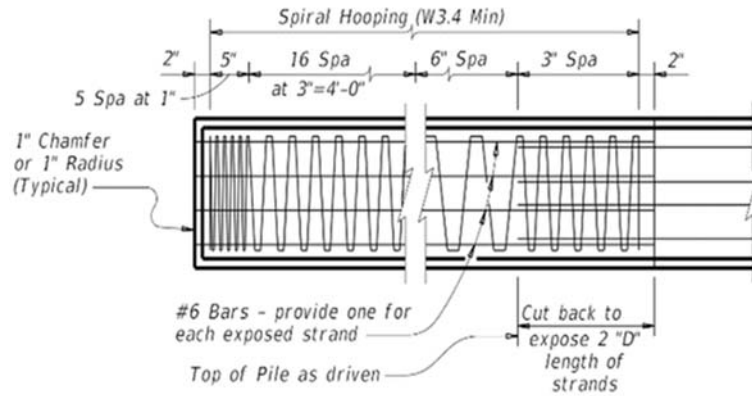


Figure 31. Current TxDOT Transverse Reinforcement Spec. for Prestressed Piling

Researching possible reduction of concrete cover would also be a straight-forward endeavor, as the only metric that would alter from conventional capacity tests would be the fabrication of the member. Numerous tests have been performed at the University of Houston concerning ultimate capacities of bridge girders prestressed with CFRP, as well as tests performed by FDOT on prestressed piles reinforced with CFRP (Roddenberry et al. 2014, 2016). To this end, if it can be determined that the clear cover can be reduced for piles reinforced with CFRP's, a not insignificant amount of concrete material can be saved, bringing fabrication costs closer to steel reinforced piles.

4.3 Deterioration of CFRP in Saltwater and Ultra Violet Light

In addition to the gaps in knowledge stated previously, there is a lack of understanding of the deterioration of CFRP's exposed to ultra violet (UV) light. From experimentation, it has been observed that UV light causes extensive erosion of the epoxy matrix within CFRP's, resulting in a non-negligible reduction in mechanical properties. While there exists a significant amount of literature that can attest to this difficult material property as well as some manufacturer's guidance, there are no quantitative studies focusing on the prestressed-CFRP strand's susceptibility to UV light.

With CFRP strands, manufacturers wind their strands with a protective layer of synthetic yarn, seen in Figure 29, to resist deterioration, also having the benefit of improving its bond characteristics to concrete.



Figure 32. Spool of CFCC Transverse Reinforcement with Yarn Covering

Research Agencies that have utilized CFRP products nominally address this deficiency in their publications, but offer no quantitative reduction in capacity (as it assumes relatively minor losses due to the protective coat of yarn). While this might suffice for smaller, more manageable testing environments, it is to be hoped that prestressed-CFRP can be utilized extensively in the field, an arena notorious for uncertainty and accidents during fabrication and construction. Typically, reinforcing steel is stored on construction sites exposed to the elements, and is incorporated into the structure over time, unlike the recommendations specified by the manufacturer. If contractors needed to find a special facility in which to store coils of CFRP reinforcement, storage would become a more significant cost than with conventional prestressing steel strands. It would therefore be prudent to study the effects of prolonged UV exposure and how this might be further mitigated by design professionals and contractors to make CFRP's easier to work with.

It should be noted that studies have been conducted in the chemical and UV degradation of carbon fiber-reinforced epoxy composites and FRP wraps, but there is a significant lack of information regarding prestressing CFRP strands (Chin et al. 1997; Roddenberry et al. 2014). There has been much interest in the study of harsh environmental degradation associated with CFCC in accelerated chemical baths, but the gap in understanding persists with UV degradation and long-term studies of environmental deterioration. As the Research Team has recommended the use of CFRP's in coastal regions (specifically to resist corrosive saline environments), the need to more precisely measure deterioration apart from accelerated chemical conditions should also be studied in more detail.

Experimental studies that could quantify these deteriorating effects could be conducted by exposing certain spools to varying intensities of UV, and subsequently test the strands in tension. . These scenarios would lead researchers to better understand what could happen to the material on a typical jobsite during construction, and might lead to certain recommendations concerning capacity loss. While this information might help reduce some uncertainties associated with CFRP's, as stated previously, DOT's across the country are currently implementing the technology in structures. Capacities calculated by researchers with FDOT and VDOT were corroborated with experimental values, thereby eliminating the need to factor further UV damage during fabrication. It is the opinion of the Research Team that CFRP-prestressed piles could be implemented by TxDOT without the need to further develop UV degradation quantities that would result from further research, but in the interests of constructability, some measure

should be taken to fully quantify UV effects other than a blanket advisory. For CFRP's to be employed more frequently, the materials should be easy for the contractor to handle and store as well.

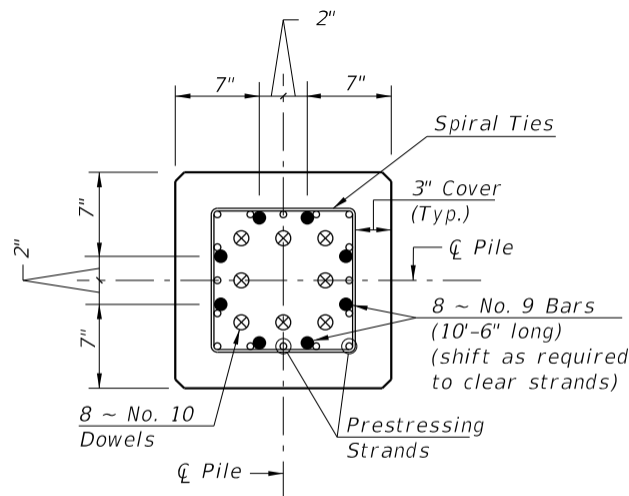
4.4 Embedment Length and Splicing Configurations

Another important quantity that requires further study is a more accurate measure of the embedment length of CFRP's in piling. Guidance has been provided by ACI and AASHTO in the form of design equations that attempt to predict the embedment length relating the development length to prestress in the reinforcement can be seen in the following equation, below.

$$L_d = \frac{1}{3} f_{se} d_b + (f_{ps} - f_{se}) d_b \quad (31)$$

While this equation can accurately predict the development in steel-reinforced members, numerous studies have resulted in additional design equations to better predict the development length of CFRP members. While some equations published on the matter involve relationships between initial prestress and ultimate tensile stress (Mahmoud and Rizkalla 1996), the cross-sectional area of reinforcement and concrete compressive strength (Domenico 1995), and the initial prestress force and characteristic properties of CFCC (Lu et al. 2000), such equations fall short of experimental values. This issue was addressed in Rodenberry et al. (2014) publication, highlighting the discrepancy in predicted values and experimental ones, citing the need for further research into the quantification of accurate embedment lengths for CFRP.

In addition to the unquantified embedment length of CFRP prestressing strands, specific splicing configuration design guidelines are significantly lacking in substance to be able to design efficiently beyond the design aids published by FDOT, an example of which can be seen in Figure 31, below. This figure is one of numerous design aids published by FDOT in 2016 as part of their "Invitation to Innovation", a program by where the Department seeks to publish all CFRP-related findings in the public domain to offer more opportunities to study the gaps in knowledge associated with the material.



(See Drivable Preplanned Predresses Precast Splice Detail)

SS PILE SPLICE REINFORCEMENT DETAILS
Figure 33. FDOT Design Aid for Prestressed Concrete Pile Splices.

Previous studies conducted by Benmokrane (2015) have specified lap splice configurations for CFRP's in tensile uses, illustrating their proportionality to the splice length up to the rupture of the

reinforcing bars, a quantity can therefore be predicted from the CFRP bar mechanical properties according to the author. Yet for the purposes of pile reinforcement, a comprehensive study or set of published guidelines does not yet exist.

To summarize, much research has been conducted on the development length of CFRP beams, leading to the introduction of design equations that refine those specified by ACI and AASHTO, but very little information is available relating to development lengths for purposes splicing piles. These previously published do not account for the different anchorage types associated with substructure members and therefore more research is required to accurately quantify this.

4.5 Prestress Loss Effects for CFRP Strands

Several DOT's across the country including FDOT and VDOT have committed resources to fabricate and test full-scale CFRP-reinforced piles for feasibility and proof of concept. Not only were ultimate strengths and validation of design parameters inspected, many small issues of constructability were discovered through the fabrication of the piles. From the literature synthesis performed at the outset of this project, and from additional research gained throughout, the Research Team was able to find some equations laid forth by ACI 440 based on previous studies and some information from ongoing NCHRP tests, but there is a lack of a comprehensive study.

What design professionals and technical documents use to quantify these values to make engineering judgements are, at best, extrapolations of steel prestress losses with empirically-derived coefficients to more accurately model CFRP. The material properties of CFRP and steel differ significantly, and while coefficients used in design parameters laid forth by ACI 440 and FDOT can make approximations, experimental values in this field would do much to address such deficiencies. Experimental values of prestress losses gathered in several studies differed a substantial amount from predicted values that employed equations published by ACI, leading many researchers to cite the need for more accurate design equations (Domenico 1995; Issa 1999). This value is actually an aggregate of several losses, namely from elastic shortening, the eventual shrinkage of concrete upon hardening, short and long-term concrete creep, frictional losses between the prestressing cable and concrete, minor relaxation in the prestressed steel, and anchorage seating. As most of these effects rely on the material properties of the reinforcement, each will differ significantly when CFRP's are introduced as the prestressing agent. In addition to this, the anchorage system employed in the prestressing of CFRP strands adds an additional discrepancy in prestress losses that has been remarked in several studies, a quantity that could be more refined by additional experimentation and incorporated into design equations.

This prestress loss has been the topic of research in recent ACI publications as well as theses published as early as 1990's (Domenico 1995, Roddenberry et al. 2016). While this value remains an important metric, studies published by FDOT and VDOT have fabricated CFRP piles without this exact knowledge and have begun to incorporate these piles into their current infrastructure. It is therefore the recommendation of the Research Team that while some entities have begun implementing CFRP piles with the design equations laid forth by ACI and the technical specifications published by FDOT, there is a lack of compelling evidence to disregard such prestressing losses and research should therefore be undertaken to quantify this. If this quantity is desired to be known through experimental values, the following can be undertaken. Figure 32 illustrates the casting bed used by FDOT researchers in the fabrication of their prestressed CFRP piles used in their inconclusive study of prestress losses.

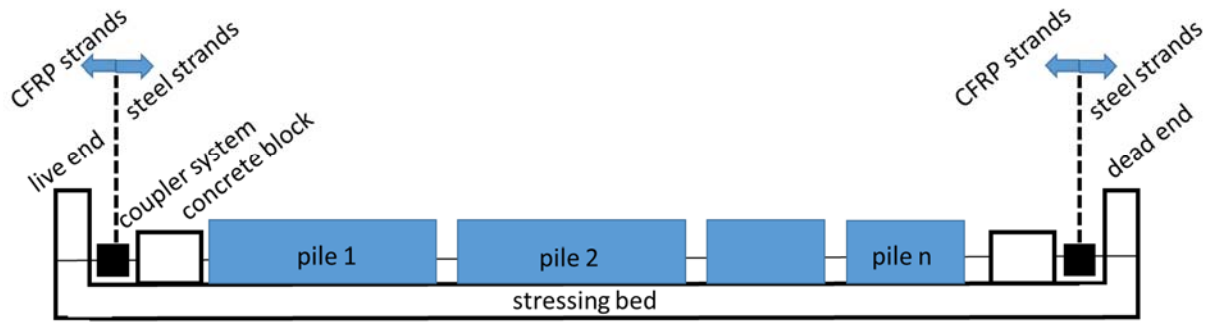


Figure 34. FDOT Prestressing Casting Bed (Roddenberry et al. 2016).

Any potential benefits that stem from this knowledge would reveal themselves in the greater accuracy of design calculations, which might lead to reduced labor costs or less material waste. As prestressing CFRP cables currently requires greater initial material costs and more manual labor than conventional prestressed steel, improving the accuracy of determining prestress losses might help deflate these costs, providing an additional economic incentive to more accurately quantify prestressing losses.

4.6 Statistical Reliability Analyses of CFRP's

Unlike conventional construction materials like steel and concrete, FRP's are still relatively new to the market and are therefore inherently less well-understood. It is in this light that FRP materials are prescribed additional safety coefficients by ACI to account for brittle failure and the unfamiliarity associated with the material. While there exists a significant body of knowledge in regards to the structural reliability of more conventional building materials, there is a lack of this information for FRP's and their associated fabrication products (Melchers, R. 2011). This deficiency simply stems from the relatively little available long-term data DOT's have concerning structures reinforced with FRP's, and will almost certainly be improved upon the longer the market matures.

In order to perform more rigorous probabilistic analysis, simply put, more data is required. While fatigue analysis can be performed by many research institutions, this can only offer an approximation of what really happens in structures in service today. Test piles can be exposed to rigorous cyclic loadings scenarios in a lab environment, but there exists no data regarding the long-term condition of CFRP reinforcing material to use in reliability studies. Long-term fatigue performance, particularly the effects of cracks on bond characteristics could be determined from a more complete historical data set, relying in part from fatigue testing in a lab environment and structures in the field. Further, as the mechanical properties of CFRP's differ significantly from conventional steel reinforcement, experimentally-derived factors associated with the reliability of steel are not equivalent to these new structures. Due to the differing natures of failure inherent with these two materials, there exists a discrepancy that does not address FRP failure mechanisms.

The availability and reliability of bridge operations in terms of a closed-form expression to quantify overall use and downtime systems is an interesting reliability analysis that could be conferred to CFRP-reinforced systems (Der Kiureghian et al. 2005). Downtime refers to the amount of time a bridge will be taken out of service for repairs and maintenance as well as the amount of time required to plan for this. In their reliability study, component failures are assumed to be homogenous Poisson events and their subsequent repair durations are assumed to be exponentially distributed as illustrated in Figure 33, below. Such closed-form expressions are based on the steady-state availability of materials, the mean rate of component failure, and the mean duration of downtime and lower bound reliability of a system with

randomly and independently failing repairable components. These conditions all differ significantly between conventional prestressed-steel and prestressed-CFRP, no longer allowing for the basic probabilistic distributions assumed by the researchers, and therefore requires additional study.

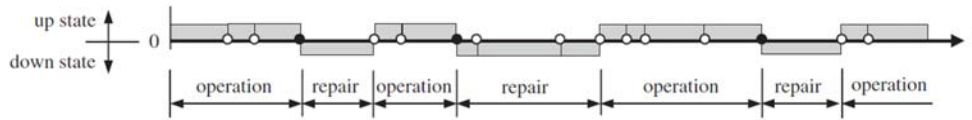


Figure 35. A Realization of Underlying Poisson Process (Der Kiureghian et al. 2005).

While the basis for many reliability studies made for steel-reinforced components may still hold true for newer CFRP-reinforced structures, their inherent values and relative probabilities can only be more accurately quantified with further fatigue testing coupled with long-term study of existing structures. It is the recommendation of the Research Team, however, that such extensive reliability analyses need not be conducted before the technology can be adopted. From specifications laid forth by ACI 440, guidance provided by the manufacturer, numerous studies conducted by FDOT and VDOT, and the careful adherence to these guidelines, CFRP's can be effectively employed and understood utilizing methods associated with reliability methods available to design professionals today.

4.7 Circular, Octagonal, and Square-Reinforcement Patterns in Piles

Yet another gap in knowledge associated with prestressed-CFRP piles lies in the design specifications provided by TxDOT prestressing guidelines. As these specifications are meant to address steel prestressing, there could be more precise or more efficient patterns of reinforcement utilized by other DOT's that could be of benefit when paired with CFRP's. In the current specifications, FDOT and TxDOT both call for square reinforcement patterns within square cross sections for bridge piles. There is a lack of research that can address the differences in axial and bending moment capacities between square, octagonal, and circular-reinforced pile members with respect to FRP reinforcement, some of which are depicted in Figure 34, below.

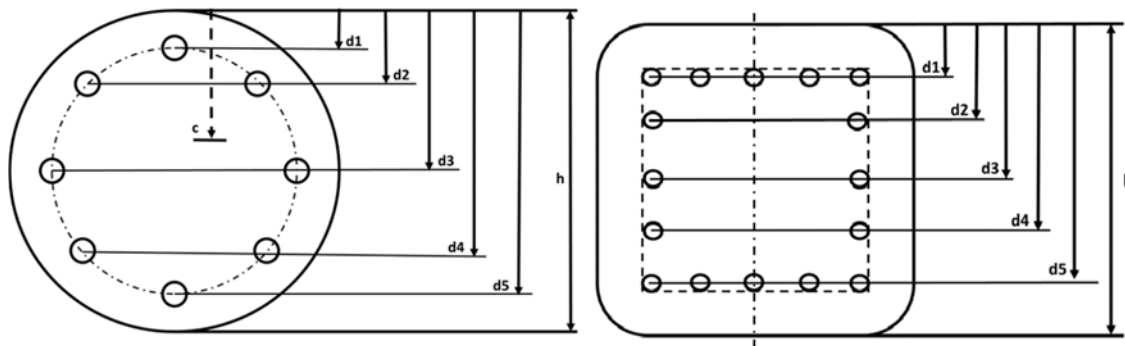


Figure 36. Circular and Rectangular Cross Sections for Prestressed Concrete.

While the frictional forces that develop along the lengths of these driven piles is derived from the geometries of the cross section and therefore offer varying amounts transference and support to a structure, there is an apparent lack of literature concerning this topic for prestressed-CFRP. Experimental studies that could corroborate or disagree with current standards could be executed relatively simply, varying the reinforcement pattern while keeping the reinforcement ratio consistent across each iteration. Such studies could help improve understanding nuanced confinement effects that correlate directly with

the reinforcing pattern, aid in discovering the locking and unlocking effects of spiral reinforcement in CFRP strands and how, if at all, this could differ from steel reinforcement, a factor important for seismic considerations. While such research would not directly affect TxDOT specifications and therefore the implementation of prestressed-CFRP piles, the knowledge gained from such an endeavor might lead to less required internal reinforcement by finding a more suitable reinforcement pattern thereby potentially reducing material costs.

Chapter 5: Summary and Recommendations for Further Study

5.1 Summary

The mechanical and material behavior of CFRP strands, with their environmental durability, superior axial strength has been very well documented in previous literature. The results obtained from the Research Team's preliminary interaction diagrams have illustrated equivalent axial and flexural (P-M) behavior to conventional prestressed steel strands with fewer CFRP members. While FRP's do exhibit undesirable brittle failure modes, when designed to its strengths, this behavior can be avoided entirely. The cross sections used to obtain the P-M diagrams were modeled very closely to standard TxDOT prestressing specifications as well as new literature put forth by FDOT, adhering to spacing requirements, reinforcement ratios, and strand staggering.

To conduct a more realistic analysis, the Research Team forewent one-for-one strand replacement and instead focused on equivalent design capacities, highlighting the axial strength of CFRP. It was found that 25% less reinforcement could be used in the prestressed-CFRP to achieve similar capacities in prestressed-steel. When this reduction in reinforcement is considered, the initial cost of implementation is also significantly reduced. When comparing the two materials, Agencies would need to spend 46% more in initial construction costs to adopt the newer material. This is assuming that the cost of the substructure count to 20% of the total cost of the bridge. In fact if estimate that the bridge will be replaced once in its lifetime at a cost of \$550,000, then the additional cost of the CFRP will be estimated at only 2% and it could be recouped in about 18 to 20 years of the life of the structure. When accounting for increased lifespans in CFRP members (an estimated 25% increase), significantly reduced life-cycle maintenance costs, and reduced initial construction costs, prestressed-CFRP will become definitely a long-term solution and will benefit the Agency in the long-run.

With literature synthesis, mechanical behavior comparison, and economic comparison completed, the following conclusions were made:

- From parametric studies and the LCCA, CFRP's become closer in life-cycle cost to conventional steel PC for new construction, taking full advantage of CFRP's environmental durability over entire lifespan.
- CFRP ties/spirals performed equivalently to steel counterparts in strength demands.
- Analyzing piles of equal capacity (25% fewer CFRP strands), initial costs may be an additional 230% for piles only but could be less than 45% of the overall cost of the bridge. This development not only brings economic equivalence closer in the first 20 years of the life of the structure but will also bring significant resilience to environmental degradation, reducing need for maintenance; Increases expected lifespan of substructure by design life of at least 25% and CFRP will bring major savings after 20 years of the life of the piles.
- Based on interviews with TxDOT engineers, prestressed reinforcement corrosion in piles not the most pressing issue for TxDOT engineers, but with CFRP's, the problem can completely go away
- Research Team's final recommendation is that there exist some minor gaps in knowledge regarding CFRP-prestressed piles that should be addressed with additional research before full implementation is recommended.
- While life cost analysis shows that the use of CFRP in piles could increase the initial cost of the substructure, it also indicates that there will be great saving over the life of the bridge. This is not

very conclusive since the study focused on pile construction and maintenance only. Degradation and deterioration occurs in the superstructure as well and that was not included in this study.

- Research Team highly recommends to the Agency to join other DOTs and lead the effort in adopting this technology in their bridges. The use of CFRP strands for piles may be beneficial in the construction of signature structures that are exposed to salt-water and a detailed economic analysis should be considered for those types of structures given the implications and consequences of strand corrosion in those types of structures. While other DOTs have developed in-house design specifications for use of CFRP in Piles, AASHTO is also developing design specifications for use of CFRP in bridge girders. Most of the research leading to these AASHTO specifications is carried out at the University of Houston and at the end of this research project most of the research gaps would have been resolved.

5.2 Recommendations for Further Study and Implementation

Of the various recommendations for further research offered in this document, from further investigating prestress losses, potentially reducing concrete cover, additional saltwater deterioration studies, more rigorous structural reliability considerations, or an analysis of various reinforcement patterns with CFRP's, some require the Agency's immediate attention or funding to implement prestressed-CFRP piles in new construction. While these suggest there is room for additional research as evidenced in the gap of knowledge from the Research Team's literature synthesis, most are auxiliary and non-critical, offering only minor improvements to existing methods and design guidelines. This is evidenced through the technology's adoption and implementation by various other DOT's across the country with little apparent reticence.

From the preliminary literature synthesis performed at the beginning of this project and various materials gathered in the completion of its subsequent tasks, CFRP outperforms its steel counterpart in corrosion resistance, axial and limited bending moment capacity, and its overall viability as a suitable structural reinforcement alternative to prestressed-steel. This has been well-validated in numerous peer-reviewed journal articles and DOT publications with reproducible values and full-scale prestressed-CFRP piles being employed in public works projects in both Florida and Virginia. Numerous technical aids have been published for limited design purposes of bridge piles by FDOT and VDOT, and CFRP's economic viability has been reviewed by several literature sources (Rizkalla et al. 2006; Grace et al. 2012). While important in establishing some guidance in design, these specifications do not address splicing in between individual piles, drivability concerns, or any guidance on transverse reinforcement.

In the assessment of the condition of piles within the state as reviewed in earlier reports from numerous site visits, interviews of design professionals and contractors in the state, the Research Team had determined that prestressed-CFRP must be considered for new construction purposes over maintenance and repair ends. It was determined that the issue of deteriorated bridge piles due to internal steel corrosion was of minor significance to Agency budgets, in the proportion to the overall number of repairs made, and from the experience of those intimately involved in such repairs. This change in the concentration of benefit area led the Research Team to adopt a new approach.

The implementation of CFRP-prestressed piles, when restricted to new construction endeavors, would likely result in substantial net benefits to the Agency and State and it is therefore the opinion of the Research Team that the implementation of this technology cannot be delayed by the gaps of knowledge presented in this report, and could be implemented in some signature structures.

References

- ACI Committee (2002). Corrosion of Metals in Concrete, Manual of Concrete Practice. 222R-01. American Concrete Institute, Farmington Hills, MI, USA.
- ACI Committee 440 Report (2002). Guide for the Design and Construction of Externally Bonded FRP Systems for Strengthening Concrete Structures. ACI Committee 440, Technical Committee Document 440.2R-02.
- Afifi, M., Mohamed, H., and Benmokrane, B. (2013). "Strength and Axial Behavior of Circular Concrete Columns Reinforced with CFRP Bars and Spirals." *J. Compos. Constr.*, 10.1061/(ASCE)CC.1943-5614.0000430, 04013035.
- Afifi, M., Mohamed, H., Chaallal, O., and Benmokrane, B. (2014). "Confinement Model for Concrete Columns Internally Confined with Carbon FRP Spirals and Hoops." *J. Struct. Eng.*, 10.1061/(ASCE)ST.1943-541X.0001197, 04014219.
- Almerich, A., Martin, P., Molines, J., and Roviera, J. (2012). "RTHP Rebar: New Internal Reinforcement of Reinforced Concrete Elements." 6th Int'l. Conference on FRP Composites in Civil Engineering (CICE 2012), Rome 2012.
- American Concrete Institute (ACI). (2006). Guide for the design and construction of concrete reinforced with FRP bars. ACI 440.1R-06, Detroit.
- ASCE. 2017 Infrastructure Report Card. Extracted from: <http://www.infrastructurereportcard.org>
- Arockiasamy, M., and Amer, A. (1998). "Studies on Carbon FRP (CFRP) Prestressed Concrete Bridge Columns and Piles in Marine Environment." Report B-9076, Florida Department of Transportation.
- Arockiasamy, M., and Sandepudi, K. (1994). "Active Deformation Control on Bridges Prestressed with Aramid Fiber Reinforced Plastics (AFRP) Cables", Final Report submitted to US and Florida Department of Transportation.
- Atadero, R. (2011). "Areas of Uncertainty in the Use of Fiber Reinforced Polymer (FRP) Composites in the Rehabilitation of Civil Engineering Structures." *Service Life Estimation and Extension of Civil Engineering Structures*: 96-116. Print.
- Bakis, C., Bank, L., Brown, V., Cosenza, E., Davalos, J., Lesko, J., Machida, A., Rizkalla, S., and Triantafillou, T. (2002). "Fiber-Reinforced Polymer Composites for Construction—State-of-the-Art Review." *J. Compos. Constr.*, 10.1061/(ASCE)1090-0268(2002)6:2(73), 73-87.
- Balazs, G. L., and Borosnyoi, A. (2001). "Long-term behavior of FRP." *In: Proceedings of the International Workshop on Composites in Construction: A reality*. American Society of Civil Engineers, VA.
- Benmokrane, B., Ali, A. H., Mohamed, H. M., Robert, M., and ElSafty, A. (2015). Durability performance and service life of CFCC tendons exposed to elevated temperature and alkaline environment. *Journal of Composites for Construction*, 20(1), 04015043
- Bentur, S., Diamond, S., and Berke, N. (1997). "Steel Corrosion in Concrete: Fundamental and Civil Engineering Practice." E & FN Spon, London.

- Benzaid, R., and Mesbah, H. (2013). "Circular and Square Concrete Columns Externally Confined by CFRP Composite: Experimental Investigation and Effective Strength Models, Fiber Reinforced Polymers" - The Technology Applied for Concrete Repair, Dr. Martin Masuelli (Ed.), InTech, DOI: 10.5772/51589.
- Breysse, D., Elachachi, S. M., Sheils, E., Schoefs, F., and O'Connor, A. (2009). "Life cycle cost analysis of ageing structural components based on non-destructive condition assessment." *Australian journal of structural engineering* 9.1: 55-66.
- Bruce Jr, R. N., and Hebert, D. C. (1974). "Splicing of Precast Prestressed Concrete Piles: Part 1—Review and Performance of Splices". *PCI JOURNAL*, 19(5), 70-97.
- Burgoyne, C., and Balafas, I. (2007). "Why is FRP not a financial success?" Proc. FRPRCS-8th Int. Symp. On FRPs for Reinforced Concrete Structures, T. Triantafillou, ed., Univ. of Patras, Greece, 1-10.
- Canadian Standards Association (CSA). (2012). "Design and Construction of Building Components with Fiber Reinforced Polymers." CAN/CSA806-12, Mississauga, ON, Canada.
- Chin, J. W., Nguyen, T., and Aouadi, K. (1997). "Effects of environmental exposure on fiber-reinforced plastic (FRP) materials used in construction." *Journal of Composites, Technology and Research*, 19(4), 205-213.
- Clarke, J.L., Darby, A., and Ibell, T. (2004). "Strengthening concrete structures with fibre composite materials: Updating Technical Report 55", *Proceedings of the Conference 'Advanced Polymer Composites for Structural Applications in Construction'* (AISC 2004). Edited L. C. Hollaway, M. K. Chryssanthopoulos and S. S. J. Moy. Woodhead Publishing Ltd, Cambridge, UK.
- Cook, R., McVay, M., and Britt, K. (2003). "Alternatives for Precast Pile Splices- Part 1." Report BC354 RPWO#80- Part 1, Florida Department of Transportation.
- Cusson, D., and Paultre, P. (1995). "Stress-strain model for confined high strength concrete" *Journal of Structural Engineering*, ASCE, Vol. 121, No. 3.
- Deiveegan, A., and Kumaran, G. (2010). "Reliability Study of Concrete Columns Internally Reinforced with Non-Metallic Reinforcements." *International J. Civil and Structural Engineering*, Vol 1, No 3.
- De Luca, A., Nardone, F., Matta, F., Nanni, A., Lignola, G., and Prota, A. (2011). "Structural Evaluation of Full-Scale FRP-Confined Reinforced Concrete Columns." *Journal of Composites and Construction* 1061/(ASCE)CC.1943-5614.0000152.
- Dimitriou, A. D. (2004). "*Rehabilitation of damaged reinforced concrete beams using FRP materials.*" Msc dissertation, University of Surrey Guildford, Surrey, UK.
- Dong, Y., and F. Ansari. (2011). "Non-destructive Testing and Evaluation (NDT/NDE) of Civil Structures Rehabilitated Using Fiber Reinforced Polymer (FRP) Composites." *Service Life Estimation and Extension of Civil Engineering Structures*: 193-222. Print.
- Dunker, Kenneth F., and Basile G. Rabbat. (1993). "Why America's bridges are crumbling." *Scientific American*: 66-72.
- Ehlen, Mark A. (1999). "Life-cycle costs of fiber-reinforced-polymer bridge decks." *Journal of Materials in Civil Engineering* 11.3: 224-230.

- El-Hacha, R., Wright, R., and Green, M. (2003). "Prestressed fibre-reinforced polymer laminates for strengthening structures.", *Progress in Structural Engineering*, Vol. 3, Issue 2.
- El-Salakawy, E., Benmokrane, B., and Desgagné, G. (2003). "FRP composite bars for the concrete deck slab of Wotton Bridge." *Canadian Journal of Civil Engineering*, 30(5).
- Enomoto, T., Grace, N., and Harada, T. (2011). "Life Extension of Prestressed Concrete Bridges Using CFCC Tendon and Reinforcements." Tokyo Rope Manufacturing.
- Enomoto, T., Harada, T., Ushijima, K., and Khin, M. (2009). "Long Term Relaxation Characteristics of CFRP Cables." Tokyo Rope Manufacturing.
- Fam, A., Pando, M., Filz, G., and Rizkalla, S. (2003). Precast piles for Route 40 bridge in Virginia using concrete filled FRP tubes. *PCI journal*, 48(3), 32-45.
- Federal Highway Administration. (1998). Design and Construction of Driven Pile Foundations. Publication No. FHWA-HI-97-013, Washington, DC.
- Federal Highway Administration, NBI (2015). National Bridge Inventory. Federal Highway Administration. Extracted from: www.fhwa.dot.gov/bridge/nbi
- Fleming, W., Weltman, A., Randolph, M., and Elson, W. (1992) "Piling Engineering", Second Edition, John Wiley & Sons, Inc., New York.
- Frangopol, D.M., and S. Kim. (2011). "Service Life, Reliability and Maintenance of Civil Structures." *Service Life Estimation and Extension of Civil Engineering Structures*: 145-78. Print.
- Gerwick, B. (1968). "Prestressed Concrete Piles". General Report to FIP Symposium on Mass-Produced Prestressed Precast Elements. Madrid. 1968.
- Grace, N. F., Jensen, E. A., Eamon, C. D., and Shi, X. (2012). "Life-cycle cost analysis of carbon fiber-reinforced polymer reinforced concrete bridges". *ACI Structural Journal*: 109(5), 697.
- Guades, E.J., Aravinthan, T., and Islam, M.M. (2010). "An Overview on the Application of FRP Composites in Piling System." Southern Region Engineering Conference, University of Southern Queensland.
- Gulikers, J. (2005). "Numerical Modeling of Reinforcement Corrosion in Concrete." In Böhni, H. *Corrosion in Reinforced Concrete Structures*; Boca Raton, FL, USA; CRC Press, pp 1-45.
- Hamilton, H. R., and Dolan, C. W. (2000). "Durability of FRP reinforcements for concrete". *Progress in structural engineering and materials*, 2(2), 139-145.
- Han, J., Frost, J., and Brown, V. (2002). "Design of Reinforced Polymer Composite Piles under Vertical and Lateral Loads." *FRP Composite Piling: Instrumentation, Monitoring, & Performance Assessment*, TRB2003 Session A2K00. 2003.
- Hayward Baker LLC (2016). *Product Data Sheet, Micropile Brochure*. Retrieved from <http://www.haywardbaker.com/uploads/solutions-techniques/micropiles/Hayward-Baker-Micropile-Brochure.pdf>
- Hollaway, L.C. (2011). "Key Issues in the Use of Fibre Reinforced Polymer (FRP) Composites in the Rehabilitation and Retrofitting of Concrete Structures." *Service Life Estimation and Extension of Civil Engineering Structures*: 3-74. Print.

- Issa, M. (1999). "Experimental Investigation of Pipe-Pile Splices For 30" Hollow Core Prestressed Concrete Piles." Report 98-8.
- Issa, M., Alrousan, R., and Issa, M. (2009). "Experimental and Parametric Study of Circular Short Columns Confined with CFRP Composites." *J. Compos. Constr.*, 10.1061/(ASCE)1090-0268(2009)13:2(135), 135-147.
- Juran, G., and Komornik, U. (2006). "Behavior of Fiber-Reinforced Polymer Composite Piles Under Vertical Loads" FHWA-HRT-04-107, Federal Highway Administration.
- Kandola, B. K., and Horrocks, A. R. (1998). "Flame retardant composites, a review: The potential for use of intumescent." *In Fire Retardancy Polymers- The Use of Intumesence*, ed. R. Delobel, The Royal Society of Chemistry, London.
- Karbhari, Vistasp M., and Luke Lee S. (2011). "Service Life Estimation and Extension of Civil Engineering Structures". Oxford: Woodhead, 2011. Print.
- Katsuki, F., and Umoto, T. (1995). "Prediction of Deterioration of FRP Rods Due to Alkali Attack." *Proceedings of the International RILEM Symposium (FRPRCS-2)*, Ghent, 82-89.
- Kobayahsi, K., and Fujisaki, T. (1995). "Compressive behavior of FRP reinforcement in non-prestressed concrete members." *Proc. 2nd Int. RI-LEM Symp. On Non-Metallic (FRP) Reinforcement for Concrete Structures*, E & FN Spon, London.
- Lignola, G., Prota, A., Manfredi, G., and Cosenza, E. (2007). "Experimental Performance of RC Hollow Columns Confined with CFRP." *J. Compos. Constr.*, 10.1061/(ASCE)1090-0268(2007)11:1(42), 42-49.
- Lu, Z., Boothby, T., Bakis, C., and Nanni, A. (2000). "Transfer and Development Lengths of FRP Prestressing Tendons." FHWA project, *PCI Journal*, vol. 45.
- Mahmoud, Z. I., and Rizkalla, S. H. (1996). Bond of CFRP prestressing reinforcement. *Advanced Composite Materials in Bridges and Structures (ACMBS-II)*, Montreal, Quebec, Canada, 877-884.
- Marco, I., Travesa, A., Llinas, L., and Muñoz, M. (2012). "Numerical Simulation of the Mechanical Behaviour of FRP RC Tensioned Elements." 6th Int'l. Conference on FRP Composites in Civil Engineering (CICE 2012), Rome 2012.
- Mays, T., Black, J., and Foltz, R. (2005). "A Simplified Design Procedure for Precast Prestressed Concrete Piling in Areas of High Seismicity to Include the Effects of Pile Buckling."
- Melchers, R.E. (2011). "Probabilistic Methods for Service Life Estimation of Civil Engineering Structures." *Service Life Estimation and Extension of Civil Engineering Structures.* 179-92. Print.
- Meyerhoff, G., (1976). "Bearing Capacity and Settlement of Pile Foundations." *Journal of the Geotechnical Engineering Division, American Society of Civil Engineers (ASCE)*, pg. 195-228
- McClelland, M. (2005). "Deep Foundations for Transportation Facilities." CIGMAT-2005 Conference & Exhibition, Houston 2005.
- Mirmiran, A., Shao ,Y., and Shahawy, M., 2002. Analysis and field tests on the performance of composite tubes under pile driving impact, *Composite Structures, Building And Construction Materials*; 55, 127-135

- Mohamed, H., Afifi, M., and Benmokrane, B. (2014). "Performance Evaluation of Concrete Columns Reinforced Longitudinally with FRP Bars and Confined with FRP Hoops and Spirals under Axial Load." *J. Bridge Eng.*, 10.1061/(ASCE)BE.1943-5592.0000590, 04014020.
- Mullard, J., and Stewart M. (2012). "Life-Cycle Cost Assessment of Maintenance Strategies for RC Structures in Chloride Environments", *JOURNAL OF BRIDGE ENGINEERING* © ASCE, (2012): 17(2): 353-362
- Mullins, G., and Sen, R. (2005). "Use of FRP for Corrosion Mitigation Applications in a Marine Environment". *Florida Department of Transportation*.
- Nawy. E.G. Reinforced Concrete – A Fundamental Approach. 5th Ed. Prentice Hall, Upper Saddle River, New Jersey, N.J., 2009.
- NCHRP Report 483. "Bridge life-cycle cost analysis". Transportation research board. (2003) Washington, DC.
- Ozyildirim, H., and Sharp, S. (2013). "Carbon Fiber Strands for Prestressed Concrete Piles." Virginia Concrete Conference, March 8 2013.
- Ozbakkaloglu, T., and Oehlers, D. J. (2008). "Manufacture and testing of novel FRP tube confinement system", *Engineering Structures*; 30, 2448-2459
- Prakash, Suriya, Qian Li, and Abdeldjelil Belarbi. (2012). "Behavior of Circular and Square Reinforced Concrete Bridge Columns under Combined Loading Including Torsion." *Structural Journal* 109.3 (2012): 317-28. Web.
- Quayyum, S., and Rteil, A. (2012). "A Proposed Design Equation for the Development Length of FRP Rebars in Concrete." 6th International Conference on Advanced Composite Materials in Bridges and Structures, Kingston Ontario 2012.
- Rezazadeh, M., Ramezansafat, H., and Barros, J. (2016). "NSM CFRP Prestressing Techniques with Strengthening Potential for Simultaneously Enhancing Load Capacity and Ductility Performance." *J. Compos. Constr.*, 10.1061/(ASCE)CC.1943-5614.0000679 , 04016029
- Richart, F., Bertin, R., and Lyse, I., 1933, "Reinforced Concrete Column Investigation – Tentative Final Report of Committee 105, and Minority Recommendations for Design Formula of Reinforced Concrete Columns," *ACI Journal, Proceedings* V. 29, No. 6, Feb. 1933, pp. 275-284.
- Rizkalla, S., Hassan, T., and Hassan, N. (2003). "Design Recommendations for the use of FRP for reinforcement and strengthening of concrete structures." *J. Progress in Struc. Eng. Mater.*, 5(1).
- Rizkalla, S., Rosenboom, O., Miller, A., and Walter, C. (2006). "Value Engineering and Cost Effectiveness of Various Fiber Reinforced Polymer (FRP) Repair Systems, Phase II." FHWA/NC/2006-39, North Carolina Department of Transportation.
- Roddenberry, M., Joshi, K., Fallaha, S., Herrera, R., Kampmann, R., Chipperfield, J., and Mtenga, P. (2016). Construction, strength, and driving performance of carbon-fiber-reinforced polymer prestressed concrete piles. *PCI Journal*.

- Roddenberry, M., Mtenga, P., and Joshi, K. (2014). *Investigation of carbon fiber composite cables (CFCC) in prestressed concrete piles* (No. 031045).
- Seliem, H., Ding, L., Rizkalla, S.H., and Gleich, H. (2016). "Use of a Carbon-Fiber-Reinforced Polymer Grid for Precast Concrete Piles." *PCI Journal* 61.5 (2016): 37-47. Print.
- Sen, R., Issa, M., and Mariscal, D. (1992). "Feasibility of Fiberglass Pretensioned Piles in a Marine Environment Final Report" CEM/ST/92/1, contract c-3321, Florida Department of Transportation.
- Sharp, S., Tanks, J., Bradshaw, E., and Ozyildirim, H. (2014). "Monitoring and Inspecting Precast Piles with Carbon-Fiber Reinforced Polymer (CFRP) Prestressing Cables during Cold-weather Casting." NDE/NDT for Highways & Bridges: Structural Materials Technology (SMT) Conference 2014.
- SimTREC Design Manual No. 3, (2001). "Reinforcing Concrete Structures with Fiber Reinforced Polymers (FRPs).", *Intelligent Sensing for Innovative Structures Canada Corporation (ISIS)*, Winnipeg, Manitoba, Canada, 147 pp.
- Sikorsky, C., and V.m. Karbhari. (2011). "Structural Health Monitoring and Field Validation of Civil Engineering Structures." *Service Life Estimation and Extension of Civil Engineering Structures*: 223-43. Print.
- Soudki, K. (2011). "Using Fibre Reinforced Polymer (FRP) Composites to Extend the Service Life of Corroded Concrete Structures." *Service Life Estimation and Extension of Civil Engineering Structures*: 75-95. Print.
- Thoft-Christensen, P. (2003). "Corrosion and Cracking of Reinforced Concrete". Aalborg: Dept. of Building Technology and Structural Engineering. (Structural Reliability Theory; No. 228, Vol. R0313).
- Tobbi, H., Farghaly, A.S., and Benmokrane, B. (2012). "Concrete Columns Reinforced Longitudinally and Transversely with Glass Fiber-Reinforced Polymer Bars." *ACI Structural Journal*, 109(4).
- Toumpanaki, E., Lees, J., and Terrasi, G. (2014). "Shear Modulus of Cylindrical CFRP Tendons Exposed to Moisture." *J. Compos. Constr.*, 10.1061/(ASCE)CC.1943-5614.0000521, 04014059.
- Triantafillou, T., and Deskovic, N. (1991). "Innovative Prestressing with FRP Sheets: Mechanics of Short-Term Behavior." *J. Eng. Mech.*, 10.1061/(ASCE)0733-9399(1991)117:7(1652).
- TxDOT. Bridge Division. Concrete Repair Manual. By Gregg A. Freeby. Austin: TxDOT, 2015. Web. 15 June 2015.
- Val, D. V., and Stewart. M. G. (2007). "Life cycle cost analysis of reinforced concrete structures in marine environments." *Structural Safety*, 25(4), 343–362.
- Vogt, N., Vogt, S., and Kellner, C. (2009). "Buckling of slender piles in soft soils." *Bautechnik* 86(S1):98-112, August 2009. Web.
- Wu, W. (1990). "Thermomechanical Properties of Fiber Reinforced Plastic (FRP) bars." Ph.D dissertation, West Virginia Univ., Morgantown, WV.
- Yang, S. I., Frangopol, D. M., and Neves, L. C. (2006). "Optimum maintenance strategy for deteriorating bridge structures based on lifetime functions". *Engineering structures*, 28(2), 196-206.

- Zhang, J., and Mailvaganam, N. P. (2006). Corrosion of concrete reinforcement and electrochemical factors in concrete patch repair. *Canadian Journal of Civil Engineering*, 33(6), 785-793.
- Zhang, K., Fang, Z., Nanni, A., Hu, J., and Chen, G. (2014). "Experimental Study of a Large-Scale Ground Anchor System with FRP Tendon and RPC Grout Medium." *J. Compos. Constr.*, 10.1061/(ASCE)CC.1943-5614.0000537, 04014073.
- Zhu, H., Muliana, A., and Rajagopal, K. (2015). "Effect of Prestress on the Mechanical Performance of Composites." *J. Eng. Mech.*, 10.1061/(ASCE)EM.1943-7889.0000902, 04015011.